2015

Therapeutic Uses of Broadly Neutralizing Anti-HIV-1 Antibodies in Humanized Mice

Ariel Halper-Stromberg

THERAPEUTIC USES OF BROADLY NEUTRALIZING ANTI-HIV-1 ANTIBODIES IN HUMANIZED MICE

A Thesis Presented to the Faculty of

The Rockefeller University

in Partial Fulfillment of the Requirements for

the degree of Doctor of Philosophy

by

Ariel Halper-Stromberg

June 2015

THERAPEUTIC USES OF BROADLY NEUTRALIZING ANTI-HIV-1 ANTIBODIES IN HUMANIZED MICE

Ariel Halper-Stromberg, Ph.D.

The Rockefeller University 2015

Combination anti-retroviral drug therapy (ART) significantly suppresses HIV-1 viremia in most infected individuals, but is incapable of curing disease. The major barrier to HIV-1 cure is a population of long-lived cells that harbor replication-competent provirus and are refractory to current therapies—termed the latent reservoir. New therapeutic approaches to clear latent HIV-1-infected cells are necessary to achieve cure. In the first part of this thesis, I show that HIV-1 mutates and diversifies at the expected rate within humanized mice (hu-mice) and that hu-mice can sustain HIV-1 viremia for up to 4 months, thus allowing hu-mice to be used as a small animal model to study HIV-1 therapeutics. Using hu-mice, I show that when administered as single agents, recently discovered broadly neutralizing monoclonal antibodies (bNAbs) induce selective pressure at restricted viral epitopes. This causes a transient drop in viremia and the rapid emergence of viral escape mutants. When bNAbs are administered in combinations that target at least three independent epitopes, the emergence of viral escape variants is prevented.

In the second part of this thesis, I show that viremia returns in hu-mice when antibody concentrations drop beneath their therapeutic thresholds. But the rebounding viruses do not carry signature escape mutations and are still

sensitive to antibody neutralization. This suggests silently infected cells persist in hu-mice. I use hu-mice to assess viral eradication regimens that combine antibody therapy with latency reversal agents (LRAs). I show that a combination of bNAbs plus a combination of LRAs prevent viral rebound in humanized mice. To determine if antibodies play a unique role in clearing latently infected cells, I compared antibodies to ART for their efficacy in preventing viral rebound. I found that antibodies were more effective than ART at preventing viral rebound, and that this effect depended on intact Fc-FcR interactions. Within the limitations of the model, these studies provide proof of principle that antibodies combined with LRAs can be used to clear the latent reservoir in humanized mice and should be explored in other models.

To my Eitan, Seth, and my parents, thank you for all the support.

ACKNOWLEDGEMENTS

First and foremost I would like to thank my advisor, Michel. You taught me to focus my experiments to get definitive results, yet pushed me to go after the most important questions. You provided tremendous resources and gave me personal guidance to support me through difficult projects. Overall, my experience in your lab has helped me grow and I am truly grateful for your mentorship.

Thanks to all the members of the Nussenzweig lab for helpful advice, scientific contributions, and support. Special thanks to Josh Horwitz and Alex Gitlin for intellectual and experimental help, and continued friendship; to Ching-Lan Lu for help; to Anna Gazumyan, Cassie Liu, Caroline Eden and Alexander Abadir for making my experiments possible by producing incredible amounts of antibodies; to Tom Eisenreich for teaching me how to handle mice, managing the mouse colonies, and bleeding mice; to Davide Robbiani for sharing his Swiss chocolates and providing expertise; to Zoran Jankovic for outstanding support as lab manager and relentless effort to keep the lab coffee machine stocked and operating; to Jennifer Mcquillan for support as the lab's executive assistant; to Virginia Mendendez for support with grant writing; to Philipp Rommel for humoring me on all my stupid jokes; to Natalie Freund for support and friendship; to Hugo Mouquet and Johannes Scheid for scientific expertise and countless lunch discussions at the Abbey Dining Hall; to Florian Klein and Thiago Oliveira for scientific support.

Thanks to the Rockefeller Dean's office and the Tri-Institutional MD-PhD Program Office for their administrative support. I cannot overstate how impressed I am that you made my experience as a graduate student so bureaucracy-free. Special thanks to Ruth Gotian and Olaf Anderson. You continue to give me valuable advice and encouragement and keep the Tri-I MD-PhD program running extremely well.

Thank you to those who have served on my faculty advisory committee: Charlie Rice, David Ho, and Eric Pamer. Charlie also led an amazing Virology course at Rockefeller University that stoked my interest in the entire field. Thanks to my external examiner, Malcolm Martin. I would also like to thank the collaborators who contributed to this work, most notably Mike Seaman of Beth Israel Deaconess who performed all of the TZM.bl assays.

These projects were made possible through excellent fellowship support from the NIH (MSTP grant GM07739 and F30 fellowship AI109830), as well as the Center for HIV/AIDS Vaccine Immunology and Immunogen Discovery grant AI100663 and National Institute Of Allergy and Infectious Diseases of the NIH Grants AI100148 and AI081677. This work was also supported by the Bill and Melinda Gates Foundation through the Collaboration for AIDS Vaccine Discovery Grant OPP1033115, and the Howard Hughes Medical Institute.

Finally, I'd like to thank my classmates, friends, and family. To Andrew Levine

and Zander Nguyen for being awesome roommates. To Lizzy Hubin, you have made my time at Rockefeller infinitely more enjoyable; thank you for your companionship, support, and love. To my parents, you have always been there for me and encouraged me. To my brothers, Seth and Eitan, you have shown genuine interest in my work throughout and kept me motivated. I dedicate this work to you.

TABLE OF CONTENTS

LIST OF FIGURES

LIST OF TABLES

CHAPTER 1:

INTRODUCTION

Human Immunodeficiency Virus (HIV) infection is incurable and requires lifelong combination antiretroviral therapy (ART) to keep viral replication in check. In the absence of therapy, infection leads to high viral loads and gradual loss of target $CD4^+$ T cells that culminates in Acquired Immunodeficiency Syndrome (AIDS). While ART can significantly suppress viremia and slow the progression of disease, ART cessation leads to rapid virological relapse. The major obstacle to a cure is a population of infected cells that harbor replication-competent, integrated provirus—termed the latent reservoir. The latent reservoir forms very early after infection, remains stable in size over time, and is refractory to both ART and HIV-1 specific immune responses. Despite its success, ART requires daily dosing, has adverse side effects, is susceptible to viral resistance, and is not universally accessible, making curative therapies highly desirable. A single case of an HIV-1 cure has been reported, but it involved a treatment regimen that carries a high risk of mortality and is impossible to implement on a broader scale. While the single reported cure case provides proof of concept that reservoir eradication is possible, there are still significant gaps in our molecular understanding of the viral reservoir and how to target it to achieve prolonged viral remission and cure. These problems are exacerbated by the lack of small animal models to facilitate latency studies and potential therapeutic interventions. My work demonstrates that humanized mice can be used as a model to study HIV-1

therapy and I use this model to evaluate the effects of broadly neutralizing antibodies (bNAbs) against HIV-1. I extend this analysis to investigate bNAbs' ability to impact the establishment, and maintenance of the latent reservoir within humanized mice.

1.1 Course of HIV Infection

HIV can be transmitted through sexual contact at mucosal interfaces, blood, or mother-to-child. Regardless of transmission route, the virus infects target $CD4^+$ T cells, rapidly expands within lymph nodes, and disseminates into the periphery within days. Viremia usually peaks 3-4 weeks following transmission, reaching viral loads up to 10^7 copies per ml. During the early phase of infection, individuals typically experience an acute HIV syndrome, characterized by flu-like symptoms, fever, and lymphadenopathy(Moir et al., 2011; Pantaleo et al., 1993). Following peak viremia, viral loads decrease with the onset of the cytotoxic $CD8^+$ T lymphocyte (CTL) response. The onset of a CTL response induces rapid selection of viral escape mutants—identified by amino acid changes clustered within $CD8^+$ T cell recognition epitopes(Goonetilleke et al., 2009; Turnbull et al., 2009). Neutralizing antibodies against the viral envelope glycoprotein (*Env*) emerge ~12 weeks after infection and impose immune pressure selecting for viral variants with mutations in *Env* that mediate antibody-escape(Gray et al., 2007; Richman et al., 2003; Wei et al., 2003). The antibody response evolves to bind and neutralize the newly escaped

virus, but new escape variants quickly emerge and completely replace the antibody-sensitive strains in circulation, leading to successive rounds of antibody neutralization and viral escape(Richman et al., 2003; Wei et al., 2003).

Eventually an equilibrium between immune pressure and viral turnover is reached ~3-6 months after infection and viremia settles at a stable level known as the viral set point. Set point viral loads are typically between 10^3 and 10^5 copies/ml. However there is wide variation, and higher set points are predictive for faster disease progression(Fauci and Lane, 2012; Mellors et al., 1996). By the time viral set point is reached, the infection has progressed to the chronic phase, where symptoms typically subside in what is called clinical latency. Despite the absence of symptoms, viral replication and turnover remain high, causing continued depletion of $CD4^+$ T cells and immune dysreglulation(Lane et al., 1983; Moir et al., 2011).

Homeostatic mechanisms to maintain adequate immune cell populations cannot keep pace with virally-mediated cell death and chronic infection leads to progressive immunological decline. This decline is characterized by increasing susceptibility to infection-related cancers and pathogens normally cleared by an immune-competent adult. Contraction of these diseases indicates the end of clinical latency, and untreated individuals usually die within 1 year of contracting an opportunistic infection. Overall, patients left untreated typically develop stage 3 AIDS within 8-10 years of HIV infection, and the median time to death following seroconversion is ~11 years, but it is clade dependent(Markowitz et al., 2003; Otten et al., 2000; Todd et al., 2007; UNAIDS, 2007).

1.2 Therapy Against HIV-1

Current therapy for HIV-1 is combination antiretroviral therapy (ART), which consists of three different drugs that target various stages of the viral life cycle. The major stages targeted are viral entry, reverse transcription, integration, viral packaging and budding. The necessity for drug cocktails was suggested by the rapid emergence of drug-resistant virus in patients who received azidothymidine (AZT), the first approved anti-HIV-1 drug(Boucher et al., 1990). Even dual therapy with AZT and the second approved anti-HIV-1 drug, didanosine (DDI), was shown to be no more effective than AZT alone(Saravolatz et al., 1996). However, triple therapy that included a protease inhibitor drug was shown to block viral replication and suppress viral loads to undetectable levels within weeks of therapy initiation(Hammer et al., 1997; Ho et al., 1995). Blocking viral replication dramatically slows the course of disease and restores $CD4^+$ T cell levels. Most patients with access to ART can manage HIV as a chronic disease and expect a near-normal lifespan. They even have extremely low probabilities of transmitting disease as long as their viral load is suppressed(Cohen et al., 2011).

However, despite the success of ART, there are major shortcomings that make new therapies highly desirable. Firstly, ART requires daily dosing and has adverse side effects, such as impaired lipid metabolism and psychiatric events. In addition to being inconvenient, this causes poor adherence, which can lead to

drug resistance. Secondly, ART is expensive and not accessible in many resource-poor countries despite extensive international efforts to make ART more available. This is underscored by the fact that for every 10 individuals started on ART in the developing world, 16 are newly infected(Ruelas and Greene, 2013).

While daily dosing and adverse side effects create adherence challenges, ART's biggest shortcoming from a therapeutic perspective is its inability to directly clear infected cells—it can only block new rounds of replication. While productively infected $CD4^+$ T cells die very quickly *in vivo* (half-life estimated to be ~1.6 days(Perelson et al., 1997)), there also exists a latent reservoir of extremely long-lived $CD4^+$ T cells that harbor replication-competent integrated provirus(Chun et al., 1997b; Finzi et al., 1997; Wong et al., 1997). Even after years of viral suppression with ART, this population of cells is capable of producing rebound viremia when ART is stopped(Davey et al., 1999). This makes ART a lifelong therapy and necessitates alternative therapies that can directly kill infected cells and accelerate the clearance of the latent reservoir.

1.3 The Latent Reservoir

The latent reservoir is the largest barrier to HIV cure and the success of eradication strategies is likely to hinge on their abilities to sufficiently clear this reservoir.

1.3.1 Dynamics and Kinetics of the Latent Reservoir

While the precise timing of reservoir establishment is unknown in humans, studies from non-human primates (NHPs) suggest the reservoir is established as early as 24-72 hours after intravenous (i.v.) infection(Tsai et al., 1998; 1995), and 36-72 hours after vaginal or rectal infection(Otten et al., 2000; Whitney et al.). The timing of reservoir establishment has been determined by administering ART to macaques at variable times after viral exposure and monitoring for viral acquisition upon ART cessation. ART as post-exposure prophylaxis (PEP) is fully protective in macaques when administered within 24 hours of i.v. exposure for at least 4 weeks, but only partially effective when initiated 48 hours after exposure. Even when ART is maintained for 6 months after initiation 72 hours following rectal transmission, 4 of 4 monkeys have rebound viremia(Whitney et al., 2014). Because the complete viral generation time is estimated to be ~2 days *in vivo*(Markowitz et al., 2003) and ART can block new rounds of replication, these experiments suggest HIV latency is established in some of the earliest infected cells.

While NHP models suggest $CD4^+$ T cells found in Gut Associated Lymphoid Tissue (GALT) are critical for early viral spread and latency establishment(Haase, 2010), the full cellular composition of the latent reservoir during both acute and chronic phases of infection remains an ongoing debate. While macrophages and follicular dendritic cells have been implicated as long-term cellular depots of virus, most cell types tested for longevity following HIV-infection have half-lives less than 2-6 weeks *in vivo*—making them unlikely to contribute to the clinically relevant reservoir(Ruelas and Greene, 2013)—there . Resting memory $CD4^+$ T cells containing integrated, replication-competent provirus are the best-established source of a stable reservoir. It is estimated that ~$1/10^6$ resting memory $CD4^+$ T cells are latently infected, yielding a total of ~10^5-10^7 latently infected $CD4^+$ T cells in an individual(Chun et al., 1997a; Finzi et al., 1997). The estimated half-life of these latently infected cells varies widely from 6 months to 10+ years depending on the patient, ART regimen, and the quantitation assay(Finzi et al., 1999; Ramratnam et al., 2000; 2004; Siliciano et al., 2003). Regardless of the precise half-life, it is agreed that cells composing the latent reservoir are very stable, and using an estimated half-life of ~44 months, current models estimate eradication of this reservoir solely with ART will require >60 years of continuous therapy(Siliciano et al., 2003). However, there is still no rapid, precise assay to measure the size of the latent reservoir—making it very difficult to evaluate clinical interventions. Furthermore, the rarity of latent cells makes them very difficult to study *in vivo* and there is no established small animal model system to facilitate this.

In addition to the sheer size and longevity of the reservoir, additional hurdles to reservoir eradication include: (1) the possibility of viral spread in the presence of ART due to cell-cell viral infection that is more efficient than cell-free virus(Sigal et al., 2011), (2) drug-free or "immunologically privileged" sanctuaries in the body that allow viral spread
(Fukazawa et al., 2015; Sigal and Baltimore, 2012), (3) homeostatic proliferation of $CD4^+$ T cells containing HIV provirus(Chomont et al., 2009) and (4) underestimation of the true reservoir size due to inaccurate reservoir measurement assays(Ho et al., 2013).

The dynamic interaction between latently infected cells and ongoing immune responses further complicates efforts to clear it. Despite the early establishment of the reservoir and predominant belief that resting cells harbor provirus, recent studies show the reservoir's composition is far less static than previously recognized. It has been shown that patients who begin ART during acute infection (<3 months after transmission) have a reservoir composed of wild-type *Gag* sequences at epitopes targeted by CTLs(Deng et al., 2015). Whereas patients that start ART in the chronic phase of infection (>3 months after transmission) have a reservoir composed of mutated/escaped sequences within CTL-targeted *Gag* epitopes. The findings show that although the reservoir is established within days of infection, the viral sequences archived in the viral reservoir reflect the ongoing dynamics between viral replication and immune responses.

In total, it is clear that existing ART is not enough to eliminate the latent reservoir in a clinically meaningful time period. In fact, ART intensification studies that include additional ART drugs on top of the conventional triple therapy fail to affect reservoir size(Dinoso et al., 2009; Gandhi et al., 2010). From a therapeutic perspective, strategies to accelerate the reduction of the latent reservoir are required to have a clinical impact and *in vivo* model systems are needed to facilitate their discovery.

1.3.2 The only known cure

While the dynamics and kinetics of the latent reservoir make eradication a daunting task, a single reported case of HIV cure provides proof of concept(Hütter et al., 2009). Timothy Brown, also known as the Berlin Patient, was diagnosed with HIV in 1995 and began ART ~6 years later. He received two doses of total body irradiation and two stem cell transplants from a human leukocyte antigen (HLA)-identical donor who was homozygous for the CCR5Δ32 mutation that prevents viral entry from R5 tropic HIV strains. ART was stopped just prior to the first transplant, and viremia has remained undetectable for over 5 years. Despite the fear that X4 tropic strains would emerge, it has not occurred.

While the extent of reservoir reduction attributable to the total body irradiation (TBI) alone was initially unknown, subsequent case studies reveal TBI alone is insufficient for eradication. Two patients who received stem cell transplant from a non-CCR5Δ32 donor experienced viral rebound 12 and 32 weeks, respectively, after ART treatment interruption(Henrich et al., 2014). In

total, the Berlin patient demonstrates that eradication is possible, but both irradiation and bone marrow transplant from an HIV-resistant donor is necessary. These procedures are risky and non-scalable. Bone marrow transplant alone carries a 7-30% mortality risk and only ~1% of the Caucasian population has the CCR5Δ32 mutation. A different approach is needed to eradicate the latent reservoir for more patients, yet an efficient way to target HIV latency remains unknown. A better understanding of latency on the molecular level is necessary for improved targeting.

1.3.3 Molecular Understanding of HIV Latency

Postintegration HIV latency refers to the proviral reservoir formed within resting memory $CD4^+$ T cells, as opposed to pre-integration latency that exists in the form of cytoplasmic linear viral cDNA or nuclear episomal viral DNA. Pre-integration latent virus is significantly more labile than the post-integration form and usually degrades within days to weeks(Pierson et al., 2002; Sharkey et al., 2005), making it unlikely to contribute to virological relapse after long-term ART. The predominant model for post-integration latency establishment is a three-step process: (1) Naïve $CD4^+$ T cells become activated in response to antigen. (2) As they revert to a resting, memory state, they become infected by rare chance, and (3) due to the reduced permissiveness of HIV-1 gene expression in a resting state, integrated provirus persists for a very long time(Eisele and Siliciano, 2012; Siliciano and Greene, 2011). This model is supported by the finding that latent

HIV is found in memory $CD4^+$ T cells, but to a much lesser extent in naïve $CD4^+$ T cells(Brenchley et al., 2004; Eisele and Siliciano, 2012).

However, the model has never been empirically verified and cannot completely account for all experimental observations. For instance, the NHP model shows that resting $CD4^+$ T cells are some of the first cells infected and can potentially seed the reservoir(Zhang et al., 1999b). There is no evidence for a transition from an activated to a resting state in these cells. Furthermore, the model implies that cellular activation should reverse latency, yet the vast majority of proviruses do not become transcriptionally active in response to cellular activation(Cillo et al., 2014; Ho et al., 2013).

An alternative model of latency has been proposed that attempts to reconcile these issues. The alternative model argues that intrinsic properties of the virus—namely viral transactivator (Tat) protein—determine latency fates, as opposed to cell activation state(Razooky et al., 2015). However, the evidence for this model is limited to *in vitro* systems and computational modeling, making it difficult to evaluate its relevance. In short, it is clear that our molecular understanding of the reservoir is significantly lacking and we do not know all the factors governing viral silencing and viral activation. This significantly hampers our ability to manipulate virus expression and access the latent reservoir for eradication strategies.

However, some host-cell factors and pharmacological compounds that influence viral expression are known, which provides leads for potential ways to reverse latency. The best understood block on viral transcription is epigenetic

silencing. Nucleosomes 1 and 2 (nuc-1 and nuc-2) consistently form within the 5' LTR of integrated provirus(Shirakawa et al., 2013) and suppress transcription. Additionally, several transcription factors have been shown to recruit histone deacetylases (HDACs) to the HIV promoter. The importance of HDAC activity is highlighted by the ability of HDAC inhibitors to reverse HIV latency by stimulating viral transcription both *in vitro* and *in vivo*(Archin et al., 2012; Wei et al., 2014).

Host-cell factors nuclear factor of activated T cells (NFAT) and nuclear factor kappa-light-chain-enhancer of activated B cells (NF-κB) have been shown to be positive regulators of viral transcription. At rest, NF-κB exists as a p50/RelA heterodimer in the cytoplasm, while p50/p50 homodimers bind to the LTR in the nucleus and prevent transcription. The p50/RelA heterodimers are required to move to the nucleus to recruit histone acetyl-transferases (HATs) to promote transcription. Once in the nucleus, RelA initiates transcription by interacting with the Cdk7 kinase subunit of Transcription Factor II Human (TFIIH) and with positive transcription elongation factor b (P-TEFb) to phosphorylate RNA Pol II and mediate transcriptional elongation.

The role of NFAT in viral transcription is driven through the protein kinase C (PKC) pathway, in which Ca^{2+} release stimulates calcineurin to dephosphorylate NFAT, leading to NFAT nuclear localization and binding to the 5' LTR. Phorbol esters such as prostratin are some of the most potent inducers of HIV viral transcription by PKC-mediated activation. Because PKC activation is a downstream consequence of T cell activation through the antigen receptor, CD3/CD28 cross-linking also stimulates viral transcription through this pathway.

However, only a small fraction of full-length provirus is activated from resting $CD4^+$ T cells despite uniform cellular activation with PHA and CD3/CD28 cross-linking(Cillo et al., 2014; Ho et al., 2013), indicating either general stochasticity of viral reactivation or other missing factors besides cellular activation.

In addition to host-cell factors, the viral protein Tat plays a role in regulating viral transcription. In the absence of Tat, most transcripts terminate prematurely. Whereas in the presence of Tat, 99% of transcripts reach full-length(Kao et al., 1987). This is because Tat binds the transactivation-responsive element (TAR) within the 5' end of HIV transcripts and recruits the P-TEFb complex to remove the blocking effect of negative elongation factor (NELF). The importance of Tat and the P-TEFb complex is highlighted by compounds that disrupt their interactions. Bromodomain containing protein 4 (Brd4) can bind P-TEFb and prevent its interaction with Tat, thus blocking transcription(Zhu et al., 2012). Brd4 inhibitors such as JQ1 and I-BET that remove this block have been shown to stimulate viral transcription from latent cells(Boehm et al., 2013; Li et al., 2012; Zhu et al., 2012).

While the agents that reverse latency mentioned above show promise, our understanding of HIV integration and latency maintenance is mostly derived from transformed cell lines, so its translation to latency *in vivo* remains unclear. This is highlighted by our inability to come up with a comprehensive paradigm for HIV latency. Our limited understanding of reservoir eradication and latency reversal strategies *in vivo* comes from clinical trials that used pharmacologic agents in attempts to reduce the size of the latent reservoir.

1.4 Shock and Kill Approach

Considering the stability, size, and rapid establishment of the latent reservoir, it is commonly believed a strategy that accelerates reservoir reduction is required to achieve a functional cure. Because latently infected cells do not express viral antigen, they are invisible to the immune system. And although productively infected cells die rapidly, the natural rate of activation of latently infected cells is too low to meaningfully reduce reservoir size. The “shock and kill” approach aims to solve these problems by stimulating latently infected cells to express viral antigen so that they either die by cytopathic effects or are killed by the immune system. Infection spread is prevented by maintaining antiretroviral therapy(Deeks, 2012).

The strategy has been tested clinically a number of ways (Table 1). The first trials used IL-2, which has been shown to activate T-cells and stimulate HIV-1 production *in vitro*. Although IL-2 stimulated $CD4^+$ T cell proliferation, it did not reduce proviral DNA or infectious units per million (IUPM) (Dybul et al., 2002; Stellbrink et al., 2002). Patients who received anti-CD3 antibody plus IL-2 showed activation and proliferation of T cells along with transient increases in HIV RNA levels. However, there was no reduction in reservoir size and the therapy resulted in long-lasting depletion of $CD4^+$ T cells as well as other toxic side effects(C et al., 2000; Van Praag et al., 2001). Together, these results led

investigators to shift to latency reversal agents that did not induce global cellular activation.

HDAC inhibitors were the first class of non-global T-cell activator LRAs to be tested. In the first test, ART intensification using enfuvirtide plus valproic acid was shown to reduce infection units per billion resting $CD4^+$ T cells by a mean of 63% in four patients and the study claimed that reservoir half-life decreased from ~44 months to 10 months(Lehrman et al., 2005). However, follow up studies that analyzed larger numbers of patients who had been receiving ART plus long-term valproic acid for neurologic or psychiatric conditions could not detect differences in the sizes of the latent reservoirs compared to controls(Sagot-Lerolle et al., 2008; Siliciano et al., 2007).

Another more potent class I HDAC inhibitor suberoylanilide hydroxamic acid (SAHA, also known as vorinostat) was also tested in human patients. Although short-course treatment was shown to boost viral transcription in patients as measured by increases in cell-associated unspliced *Gag* RNA transcripts(Archin et al., 2012; Elliott et al., 2014), prolonged administration did not impact the size of the latent reservoir as measured by quantitative viral outgrowth assays(Archin et al., 2014).

Panobinostat, a pan HDAC inhibitor, recently completed phase 1/2 clinical testing and demonstrated similar results. There were increases in cell-associated unspliced HIV RNA, but no decreases in reservoir sizes as measured by integrated HIV DNA and IUPM. Furthermore, the median time to viral rebound following ART interruption in 9 patients who had received panobinostat was 17

days—no different from historical controls(MD et al., 2014). Romidepsin, an HDAC inhibitor estimated to be 2-3 logs more potent than vorinostat(Wei et al., 2014) is currently completing clinical testing (ClinicalTrials.gov NCT02092116), but the results are still pending. Additional candidate LRAs that work by alternative mechanisms, such as disulfiram (unknown mechanism) and GS-9620 (TLR7 agonist), are also being investigated either in humans(Spivak et al., 2014), or primary cell models(Sloan et al., 2015).

While the use of LRAs that do not induce global T cell activation are necessary for toxicity issues, they present fundamental problems for the shock and kill approach: Firstly, no reactivation regimen tested *in vivo* to date has shown efficient latency reversal that could significantly affect the latent reservoir. Modeling of infection dynamics suggest that a 3 to 4 log reduction in reservoir size is required to prevent viral rebound for at least 1 year after ART interruption(Hill et al., 2014). Vorinostat was shown to reactivate just 0.079% of proviruses from ART-suppressed patient cells following 7 days of culture(Cillo et al., 2014). It is clear that more efficient reactivation regimens are required to have a clinical impact.

The second problem is how to kill reactivated cells. It is generally assumed that reactivated cells will die by cytopathic effects because productively infected cells have very short half-lives. However, this short half-life is determined from infected cells with the assumption of T cell activation. Although one school of thought is that reactivated cells will die as long as ART is on board, it is not clear if a latent cell reactivated by a non-global T cell activator will induce

Table 1. Shock and kill trials in humans

Authors	Journal	Publication Year	Patients	Intervention	Readout	Result
Chun *et al*	Nature Medicine	1999	26 patients; 14 treated, 12 controls	intervals of 3-18 megaunits IL-2 for 5 days	VOA with resting CD4+ T cells	replication competent virus was isolated from all 12 patients receiving HAART alone, but only 6 of 14 patients receiving IL-2 plus HAART (3 of these 6 patients had culturable virus with larger numbers of input resting CD4+ T cells); both patietns who discontuned HAART had rapid viral rebound in follow-up study
Prins *et al*	AIDS	1999	3 patients	5 mg OKT3 (days 1-5) and 2-9 megaunits rhIL-2 (days 2-6)	plasma viremia, lymph node (LN) viremia, and T-cell activation; viral outgrowth assay (VOA)	no consistent changes in plasma HIV-1 RNA; no differences in infectious units per million (IUPM) resting CD4+ T cells; severe side effects due to OKT3 and rhIL-2
Lafeuillade *et al*	Journal of Acquired Immune Deficiency Syndromes	2001	10 patients	5-drug HAART plus 3 courses of IL-2, 7.5 megaunits twice a day for 5 days and 2 courses of γ-interferon 100 µg every other day for 2 weeks	treatment interruption, LN viral RNA, PBMC DNA, cellular activation	minimal changes in plasma viremia; 4 log drop in LN HIV-1 RNA; 0.8 log drop in PBMC proviral DNA; presence of virus upon CD4+ T cell co-culture; viral rebound within weeks in 2 patients who underwent treatment interruption
Stellbrink *et al*	AIDS	2002	42 patients; 21 treated, 21 controls	8 cycles of 9 megaunits IL-2 daily for 5 days, 6 wks apart, beginning 4 wks after initiating HAART	viremia in peripheral blood (PB), lymphoid tissue, CSF; proviral DNA; treatment interruption	no effect on proviral DNA in PB or on rebound viremia; IL-2 significantly increased CD4+ T cell counts
Kulkosky *et al*	Journal of Infectious Diseases	2002	3 patients	didanosine, hydroxyurea for 1 month, then 400 µg OKT3, and IL-2 during HAART	plasma viremia; 2-LTR DNA circles; treatment interruption	no significant changes in plasma viremia; no effect on viral rebound after HAART interruption; one patient had increase in 2-LTR HIV DNA circles after OKT3/IL-2 administration
Lehrman *et al*	Lancet	2005	4 patients	HAART plus 500-750 mg oral valproic acid, twice daily for 3 months	quantitative VOA (qVOA)	reduction in Infectious Units Per Billion in 3 of 4 patients
Sagot-Lerolle *et al*	AIDS	2008	24 patients; 11 experimental, 13 controls	HAART plus valproic acid for >2 years for seizures	total and integrated HIV-1 DNA; qVOA; treatment interruption for 3 patients	no significant difference between experimental group and controls for any paramter measured
Archin *et al*	Nature	2012	8 patients pre-selected for response to vorinostat in vitro	HAART plus a single dose of 400 mg oral vorinostat	cell-associated viral RNA in resting CD4+ T cells	all 8 patients had increase (mean 4.8) in cell-associated unspliced *Gag* transcripts
Elliott *et al*	PLoS Pathogens	2014	20 patients	HAART plus 400 mg oral vorinostat daily for 14 days	cell-associated viral RNA in total CD4+ T cells at day 14	increase of CA-unspliced RNA in 18 of 20 patients, median 7.4 fold; no changes in HIV DNA, plasma viremia or IUPM
Archin *et al*	Journal of Infectious Diseases	2014	5 patients	HAART plus 8 weekly cycles of vorinostat (Monday to Wednesday)	plasma HIV-1 RNA; cell-associated viral RNA; total cellular DNA; qVOA	no significant changes in frequency of resting CD4+ T cells harboring virus; small increases in cell-associated RNA in 3 of 5 patients
Rasmussen *et al*	Lancet	2014	15 patients	HAART plus 3 doses (20 mg) oral panobinostat per week, every other week for 8 weeks	cell-associated viral RNA, plasma viremia, total and integrated HIV DNA; qVOA	transient increases in cell-associated HIV RNA corresponding to panobinostat administration; no changes in HIV DNA or IUPM; 9 patients who underwent treatment interruption showed rapid viral rebound
Spivak *et al*	Clinical Infectious Diseases	2014	16 patients	HAART plus 4 daily doses of 500 mg disulfiram	plasma HIV-1 RNA and qVOA	transient increases in plasma HIV-1 RNA in 6 patients; no consistent changes in latent reservoir size

cell death with the same kinetics as productively infected cells. To this point, it has been shown that $CD4^+$ T cells from ART-suppressed patients did not die following vorinostat reactivation alone(Shan et al., 2012). Rather, $CD8^+$ T cells had to be stimulated with Gag peptides to induce killing of cells whose latent state was reversed with vorinostat. This requirement for robust, functional CTL responses to kill reactivated cells is problematic in HIV-infected patients. For one, CTL activity declines over time as part of the general immune dysregulation of HIV infection, and the latent reservoir often harbors provirus that has already escaped a patient's CTL responses(Deng et al., 2015). Secondly, it has been shown that HDAC inhibitors interfere with CTL responses by reducing their interferon-γ production, proliferation, and ability to kill HIV-infected primary $CD4^+$ T cells(Jones et al., 2014). In all, both the "shock" and "kill" arms of the "shock and kill" approach require major advances for clinical impact, highlighting the two most important questions for HIV eradication research: (1) how can we improve latency reversal efficiency? And (2) how do we kill latent cells?

This thesis explores the use of broadly neutralizing antibodies as a novel anti-HIV-1 therapeutic that can suppress viremia and kill HIV-infected cells. We show that combinations of latency reversal agents are significantly more effective than single LRAs and when combined with bNAbs in a shock and kill approach *in vivo*, viral rebound from the reservoir in hu-mice is significantly reduced.

CHAPTER 2:

RESULTS

2.1 Humanized Mice

To test the efficacy of bNAbs *in vivo*, we utilized a humanized mouse system that has been reported previously(Brehm et al., 2010; Henrich et al., 2014; Traggiai et al., 2004). Briefly, NOD/Rag1$^{-/-}$IL2rg$^{-/-}$ mice irradiated at birth and reconstituted with 2×10^5 CD34$^+$ fetal liver hematopoietic stem cells (HSCs) were screened for the presence of human CD4$^+$ T cells 8-12 weeks later (Fig. 1) Mice with detectable human CD4$^+$ T cells were infected with ~60ng p24 HIV-1_{YU2} by intraperitoneal (i.p.) injection and allowed 2-3 weeks for viremia to spread and diversify. Prior to antibody administration, mice developed stable plasma viral loads between 10^3 and 10^7 copies/ml (geometric mean 1.06×10^5).

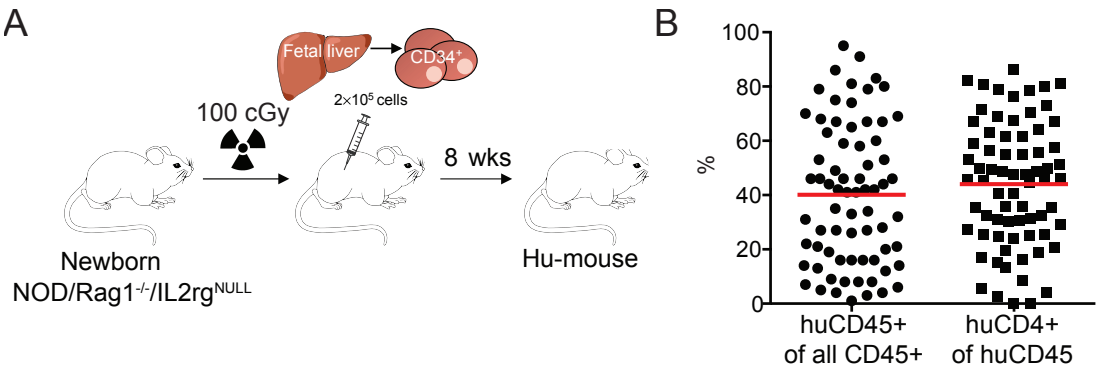

Figure 1. Generation of humanized mice (A) Schematic of hu-mouse generation (B) Human reconstitution of mice. Percentage of human $CD45^+$ cells among mouse and human $CD45^+$ cells in the peripheral blood prior to HIV infection (*Left*) and percentage of human $CD4^+$ T cells among the human $CD45^+$ cells (*Right*).

2.2 Viral diversification

To determine the rate of viral diversification, I cloned and sequenced gp120 within the mice when there was no selection pressure. I found an average of 2.9 mutations per 1400 base pairs sequenced attributable to viral mutation at 28 days following infection (Fig. 2). Assuming the HIV-1 generation time *in vivo* is 2 days(Markowitz et al., 2003), I calculate the mutation rate to be 1.5×10^{-4} in this system, consistent with diversification rates reported previously(Ince et al., 2010; Mansky and Temin, 1995).

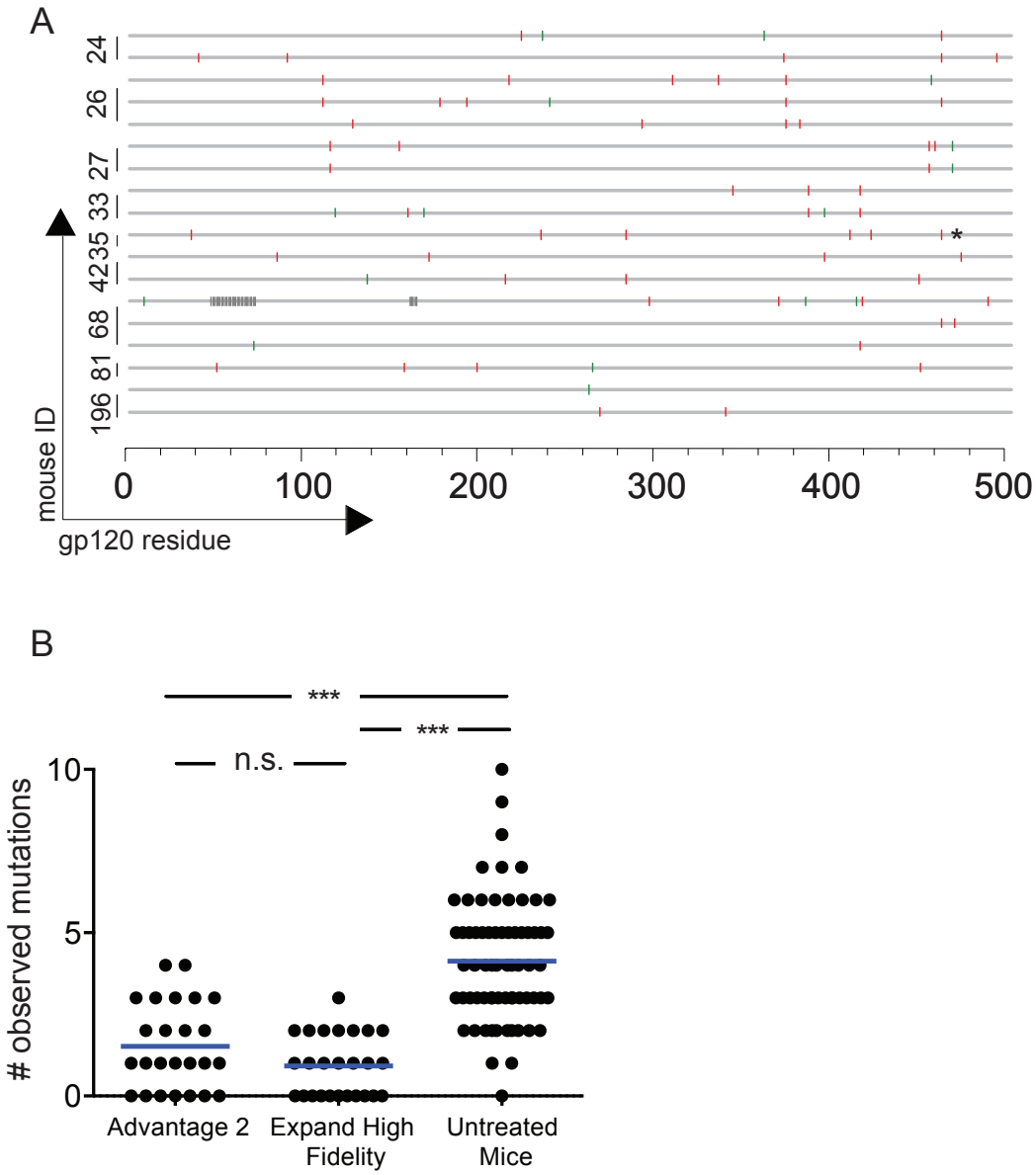

Figure 2. Viral diversification in untreated mice. (A) gp120 clones from untreated mice are shown by horizontal gray bars. Red ticks indicate non-synonymous mutations relative to wild-type HIV-1_{YU2}. Green ticks indicate synonymous mutations. Sequences obtained from 9 different mice, indicated on the left. Gp120 residue numbering according to HXB2 strain. (B) Number of mutations observed in gp120 due to polymerase error during PCR amplification compared to number of mutations observed in clones obtained from mouse plasma. Two different polymerases were used for testing polymerase error. HIV-1_{YU2} plasmid was used as the amplification template.

2.3 Antibody escapes *in vivo*

It was previously reported that rapid escape to single antibodies quickly emerges in humanized mice(Poignard et al., 1999). To see if this held true for newly identified bNAbs, viremic hu-mice were administered one of five different bNAbs: 45-46^{G54W}, PG16, 3BC176, PGT128, and 10-1074(Diskin et al., 2011; Klein et al., 2012; Mouquet et al., 2012; Walker et al., 2011; 2009). The five bNAbs were chosen based on their extensive breadth and potency in *in vitro* assays, and because they were reported to target different epitopes based on biochemical and structural analyses. However, it was unknown how the virus would respond *in vivo* considering fitness costs and the number of mutations required to reach certain amino acids.

For 4 of the 5 bNAbs, there was a transient decline in viremia followed by rebound within 7 days (Fig. 3), suggesting viral escape. To identify the escape routes selected by certain bNAbs, I cloned and sequenced gp120 from the rebound viremia. I found that the viral quasi-species within each mouse was rapidly replaced with clonal escape variants that had amino acid substitutions at 1-3 residues within gp120 (Fig. 4). Most strikingly, the escape sites detected for each effective bNAb were shared across identically treated mice—indicating a strong selection pressure for those escape routes, as opposed to a wide range of chance mutations and the emergence of founder clones following population bottlenecks. I defined recurrent mutation sites as occurring within at least 50% of the gp120 clones sequenced within 2 or more mice. In contrast, passenger

mutation sites were defined as occurring in multiple clones within a single mouse, but not shared

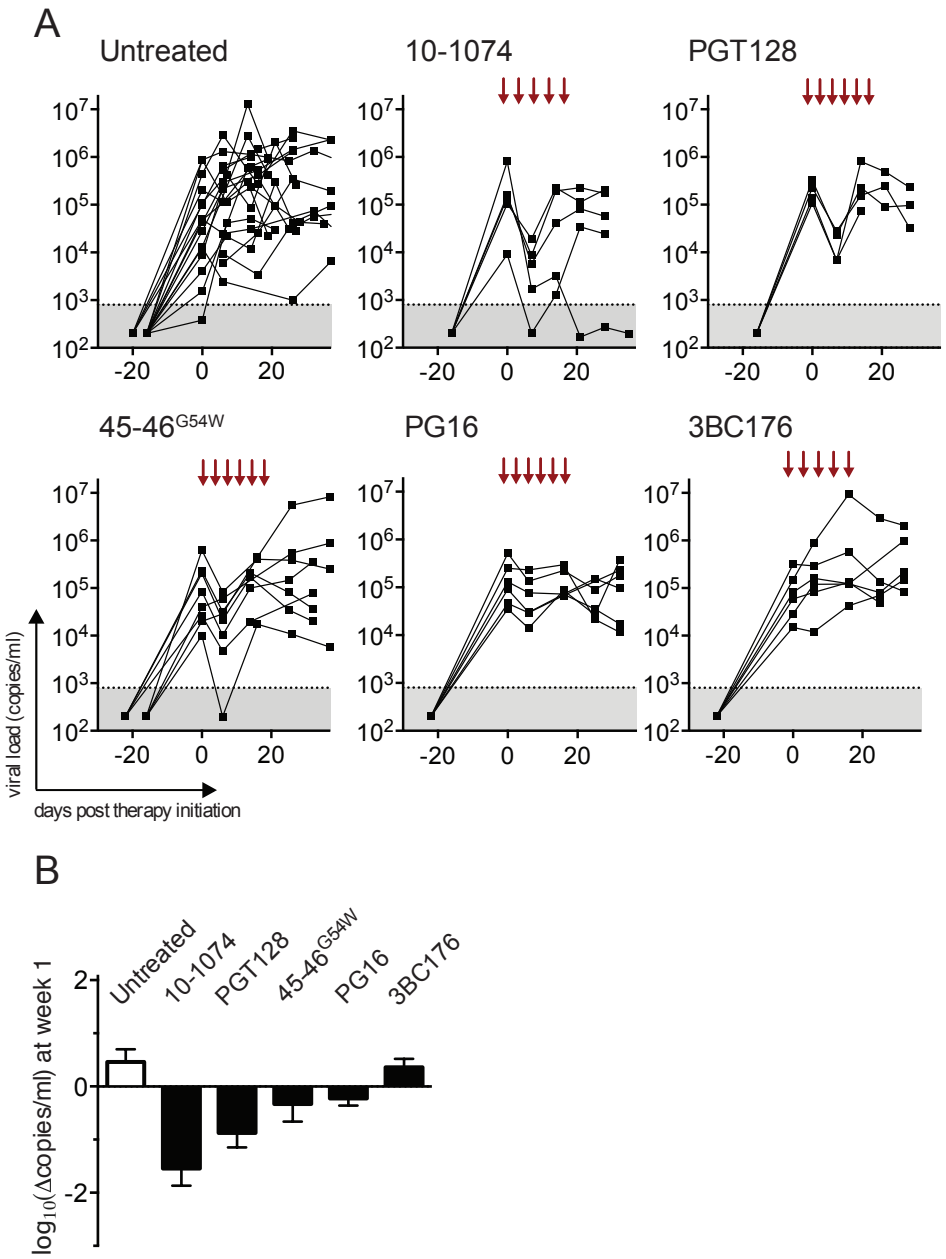

Figure 3. Transient viremia decline in monotherapy treated mice. (A) Plasma viremias for untreated mice and monotherapy treated mice. Lines represent individual mice, red arrows indicate antibody injections of 0.5 mg. Gray shading indicates the quantitation limit for HIV-1 RNA by qRT-PCR. (B) Quantification of drop in viral load seen in first week of antibody injections.

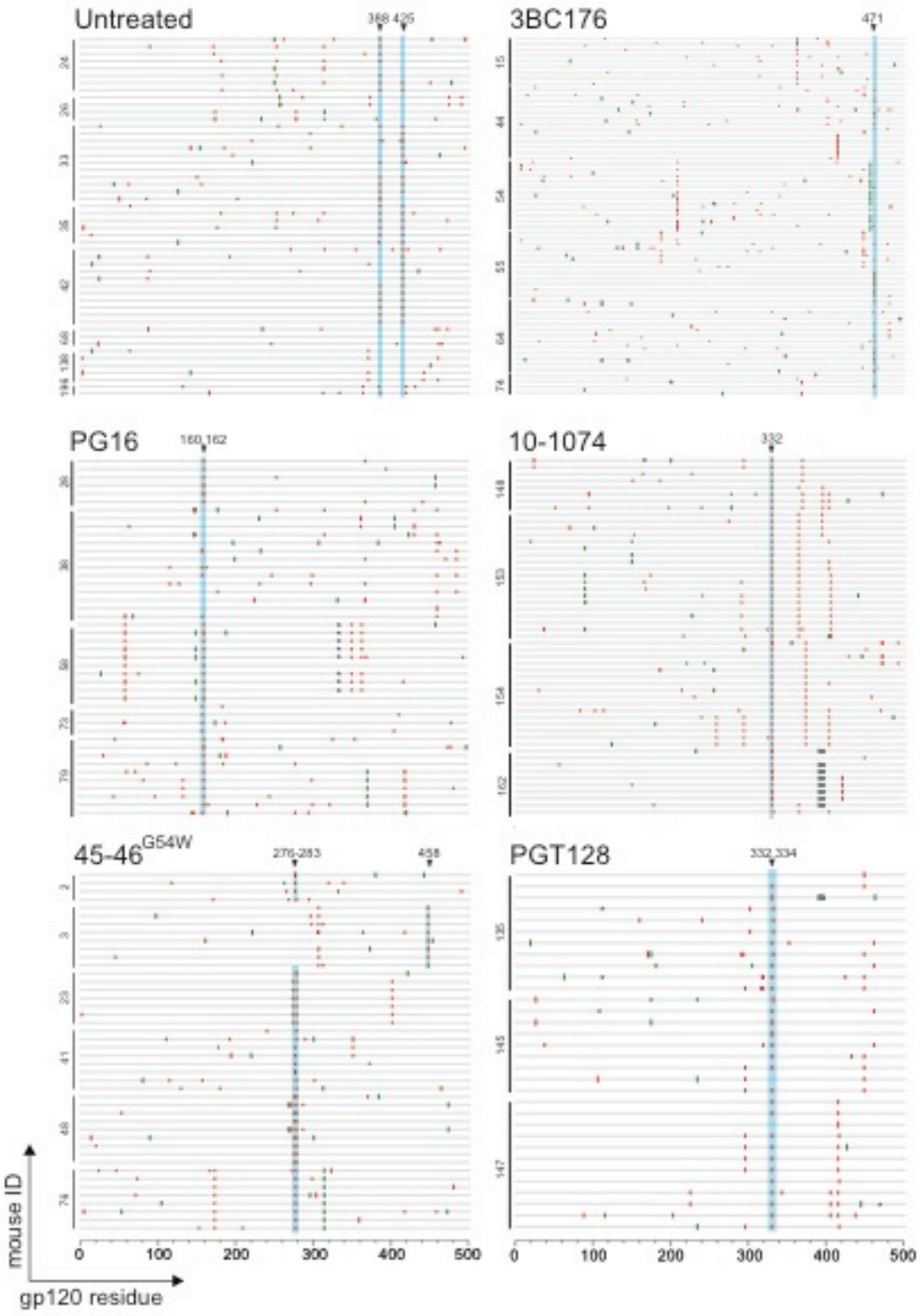

Figure 4. Monotherapy selects for recurrent escape variants across multiple mice. Gp120 sequences shown as in Figure 2a. Blue shading highlights recurrent mutations observed in at least 50% of clones from 2 or more mice. The mouse from which the sequence was obtained is indicated on the y-axis.

across multiple mice, or as being shared across multiple mice, but occurring in fewer than 50% of the gp120 clones. For the four effective bNAbs, 92% of gp120 clones contained a recurrent mutation.

For 45-46^{G54W}, escape clones had recurrent mutations at residues 279, 280, or 458 (HXB2 numbering). For PG16, escape clones had mutations at residues 160 or 162, both of which form the potential N-linked glycosylation site (PNGS) at site 160. PGT128 and 10-1074 both had mutations at residues 332 or 334, corresponding to the PNGS at site 332 (Table 2). There was only one recurrent mutation for 3BC176-treated mice (G471R), however only 31% of gp120 clones from these mice had this mutation and 2 of 6 mice did not exhibit this mutation or any other recurrent mutation—indicating significantly less selection pressure. 3BC176 also was the lone antibody tested not to produce a transient drop in viremia. From this, I conclude that there is a narrow range of preferred escape sites for the effective antibodies.

Table 2. Recurrent mutations in monotherapy treated mice. Gp120 domains and residue sites of recurrent mutations observed *in vivo* for each of the 5 bNAbs tested as monotherapy.

Antibody Monotherapy	gp120 domain	Recurrent Mutations
45-46^{G54W}	CD4bs	276, 278, 279, 280, 281, 458
PG16	V1/V2 loop	160, 162
10-1074	glycans in base of V3 loop	332
PGT128	V3-loop glycans	332, 334
3BC176	conformational/undetermined	471

To verify that the recurrent mutations at a single residue detected in the plasma actually conferred resistance as opposed to either passenger substitutions or a combination of many mutations, I cloned the putative escape mutations into an otherwise wild-type HIV-1_{YU2} pseudovirus and tested these pseudoviruses for sensitivity to their respective antibodies in TZM.bl assays. As predicted, the single residues were sufficient to confer resistance (Table 3). The lone exception was G471R, which did not confer resistance to 3BC176, consistent with 3BC176's inability to reduce viremia. In contrast, passenger mutations did not confer resistance to any of the antibodies. I conclude that point mutations at selected residues are sufficient to confer escape, and I term these signature escapes.

Table 3. Recurrent mutation pseudovirus sensitivities in TZM.bl. IC_{50} values of pseudovirus variants containing recurrent mutations or passenger mutations.

		IC_{50} (µg/ml) in TZM.bl neutralization assay				
	Observed in (Mouse ID)	3BC176	PG16	45-46^{G54W}	PGT128	10-1074
WT	-	0.319	0.612	0.024	0.169	0.312
Recurrent mutation in 3BC176-treated mice						
G471R	44, 55, 64, 74	0.159	0.154	0.008	0.02	0.091
Recurrent mutation in PG16-treated mice						
N160K	22, 25, 38, 43, 49, 56, 73	0.145	>50	0.007	0.086	0.155
T162N	22, 25, 56, 79	0.154	>50	0.013	0.166	0.175
Recurrent mutation in 45-46^{G54W}-treated mice						
N279H	2	0.209	0.294	>50	0.064	0.177
N280Y	25, 49, 76	0.276	0.145	>50	0.031	0.126
Recurrent mutation in PGT128 or 10-1074-treated mice						
N332K	135, 147, 148, 153, 154, 162	0.232	0.988	0.017	>50	>50
N332Y	135, 145, 162	0.269	0.632	0.01	>50	13.6
S334N	135, 145	0.218	0.615	0.02	>50	7.308
Recurrent mutations in tri-mix treated mice						
T162I-G458D	16	0.275	>50	14.33	0.012	0.047
T162N-N280Y	25	0.138	>50	>50	0.027	0.079
Theoretical penta-mix mutations						
N160K-N280Y-N332K	-	0.146	>50	>50	>50	>50
N160K-A281T-N332K	-	0.1	>50	>50	>50	>50
T162I-N280Y-N332K	-	0.13	>50	>50	>50	>50
T162I-N279K-N332K	-	0.149	>50	>50	>50	>50

		KEY				
		< 0.1	>0.1 - 1	>1-10	>10-50	>50
Recurrent mutations in tri-mix treated mice						
T162I-G458D	16	0.275	>50	14.33	0.012	0.047
T162N-N280Y	25	0.138	>50	>50	0.027	0.079
Theoretical penta-mix mutations						
N160K-N280Y-N332K	-	0.146	>50	>50	>50	>50
N160K-A281T-N332K	-	0.1	>50	>50	>50	>50
T162I-N280Y-N332K	-	0.13	>50	>50	>50	>50
T162I-N279K-N332K	-	0.149	>50	>50	>50	>50
Passenger mutations						
Y61H	58	0.243	0.285	0.015	0.098	0.26
E102K	43, 64, 154	0.173	0.341	0.023	0.11	0.207
N295S	148, 154	0.347	0.5	0.017	0.145	0.159
I311M	3	0.23	2.67	0.013	0.248	0.253
S365L	15, 74	0.26	0.273	0.009	0.045	0.153
G366E	38, 44, 148, 153, 162	0.187	0.167	0.001	0.021	0.074
I371M	28, 38, 74, 148, 161	0.2	0.303	0.013	0.064	0.164
N413K	148, 154, 162	0.188	0.557	0.014	0.032	0.109
E429K	16, 33, 65	0.146	0.503	0.017	0.082	0.167
N295S-G366E-N413K	-	0.222	0.131	0.001	0.012	0.021
Recurrent mutatuions + passenger mutations						
T162I-Y61H	58	0.156	>50	0.014	0.088	0.115
T162N-V430E	79	1.67	>50	0.003	0.037	0.106
N280Y-A174T	76	0.064	0.138	>50	0.01	0.021
N332S-N413K	-	0.181	0.526	0.017	>50	>50

Although the residue locations were restricted, I extended the analysis to determine how restricted the amino acids at each of these locations were. I detected multiple amino acids at each site for 3 of the 4 effective bNAbs. For PG16 and PGT128, there was remarkable tolerance of amino acid and nucleotide substitutions. Of the 27 possible single nucleotide changes that would eliminate the PNGS at the bNAb's corresponding epitope, I detected 13 of them in at least one clone. Overall, there were 7 different amino acids detected at sites 160 and 162 for PG16, and 5 different amino acids detected at sites 332 and 334 for PGT128 (Fig. 5). Considering the short time frame for escape in this experiment, and the limited number of mice tested, the virus appears to have sampled a large part of its mutational space at the escape residues. Thus, there appears little restriction for which nucleotide change is selected—as long as it eliminates the PNGS.

Similarly, despite the limited residue sites conferring escape to 45-46^{G54W}, there were 8 different amino acids resulting from single nucleotide changes detected, underscoring the flexibility allowed at those residues. In contrast, the escapes detected for 10-1074 were impressively narrow. Fifty-one of 53 clones across four different mice all had identical N332K substitutions (Table 2 and Fig. 5). The N332K mutation conferred complete resistance to 10-1074 in TZM.bl (IC_{50} > 50 μg/ml). Meanwhile, HIV-1_{YU2}^{N332Y} and HIV-1_{YU2}^{S334N}, both of which occurred in just 1 of 53 clones, had IC_{50}'s of 13.6 and 7.3 μg/ml, respectively. While the N332Y and S334N escapes are approximately ~30x less sensitive to 10-1074 than wild-type HIV-1_{YU2}, they are not completely resistant, suggesting

the frequency of observed escapes is directly related to the sensitivity to the corresponding antibody in this system.

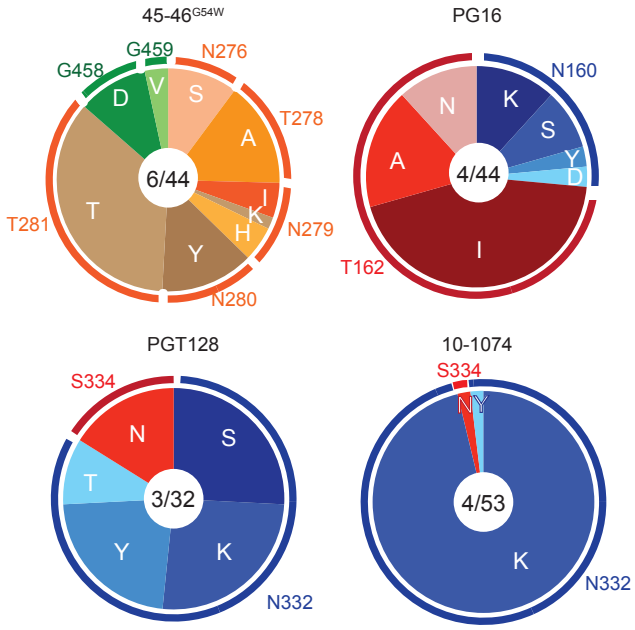

Figure 5. Amino acids detected at escape sites in monotherapy. Each pie chart represents all the escape clones detected within monotherapy treated mice. Different colors of the pie represent the proportion of sequences that contain a particular amino acid at the escape site. The escape sites and the wild-type amino acids are shown on the outside of each pie slice. The numbers inside the centers of the pies represent the number of mice that escape clones were obtained from, and the total number of escape clones sequenced, respectively.

2.4 Antibody combinations

Because the selected bNAbs target distinct epitopes on the HIV-1 glycoprotein and have limited escape routes, we investigated whether treatment with antibody combinations could prevent the emergence of escape. A tri-mix of antibodies that targets two identifiable epitopes (PG16, and 45-46^{G54W}, 3BC176) was able to sustainably suppress viremia in 3 of 11 treated mice, but rapid escape emerged in 8 of 11 mice (Fig. 6). To determine if there was a synergistic or additive effect on allowed escape routes with combination therapy, I cloned and sequenced gp120 from the 8 mice that escaped. All 88 sequences simultaneously contained the signature escapes observed for PG16 and 45-46^{G54W} in monotherapy (Fig. 7). Additionally, nearly all the same amino acid substitutions seen in monotherapy were observed during combination therapy (Fig. 8). Testing the observed mutations in TZM.bl confirmed two signature mutations were sufficient to confer resistance to PG16 and 45-46^{G54W}. In contrast, gp120 clones obtained after antibody levels decayed beneath their therapeutic thresholds from the 3 mice that did not escape during therapy showed mutations at either the PG16 epitope (N162P) or in the vicinity of the confirmed 45-46^{G54W} epitope (K282R), but never both simultaneously. From this, I conclud that escape from bNAbs is additive.

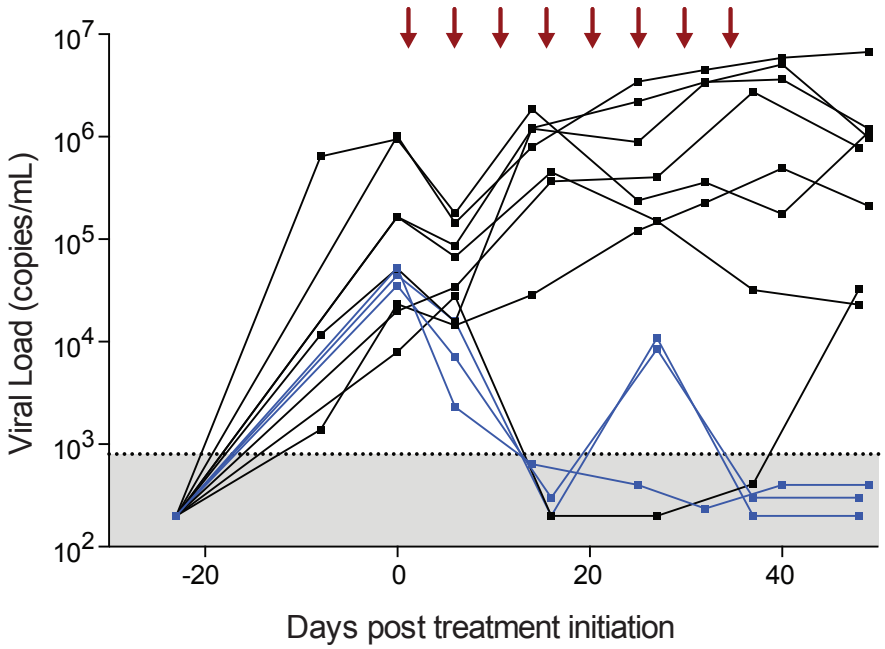

Figure 6. Viremias in tri-mix treated mice. Plasma viremia from 11 mice treated with a tri-mix of bNAbs (45-46^{G54W}, PG16, 3BC176). Antibody injections indicated with red arrows. Lines indicate individual mice. Black indicates mice that escaped during therapy. Blue indicates mice that did not escape.

Because ~72% of mice treated with an antibody combination that targets two independent epitopes still show viral escape, we tested if an antibody combination that targets three independent epitopes is sufficient to completely prevent escape. We included 10-1074 and PGT128 into the combination antibody mix, both of which target the N-linked glycan at position 332 according to the monotherapy experiments. All 13 mice treated with this antibody combination had viral loads suppressed beneath the limit of quantitation for 3 weeks (Fig. 9). However, ~21 days following antibody therapy initiation, 3 of the 13 mice had detectable viremia return even though antibodies were still being administered. I cloned gp120 from the plasma of each of these three mice (10

clones, 7 clones, 6 clones obtained from each mouse, respectively) and found that all 23 clones sequenced had evidence of APOBEC3G/F mediated G to A hypermutation that resulted in premature stop codons (Fig. 10). I found no signature escape mutations to any of the antibodies. Although it remains unanswered how the cells producing these viral particles persisted such that I could repeatedly detect virus, it appears the detectable viremia does not represent actively spreading virus, but rather infected cells producing defective virus. From this, I conclude that a combination of antibodies that targets three independent epitopes prevents emergence of escape variants in humanized mice.

To determine if virus was completely cleared in mice that did not show viral escape, we discontinued antibody therapy after 31-60 days and monitored the mice for an additional 100 days. In 7 out of 8 mice that survived, viremia returned. I obtained 28 gp120 clones from 5 of the rebounding mice. Three clones showed signature escape mutations to 10-1074 and PGT128, but not to PG16 or 45-46^{G54W}, while the remaining clones did not show signature escape mutations to any of the antibodies (Fig. 10). Only 1 of 28 clones showed a stop codon likely resulting from G to A hypermutation. From this, I conclud that replication-competent, antibody-sensitive virus persisted throughout the treatment period and was capable of producing viral rebound.

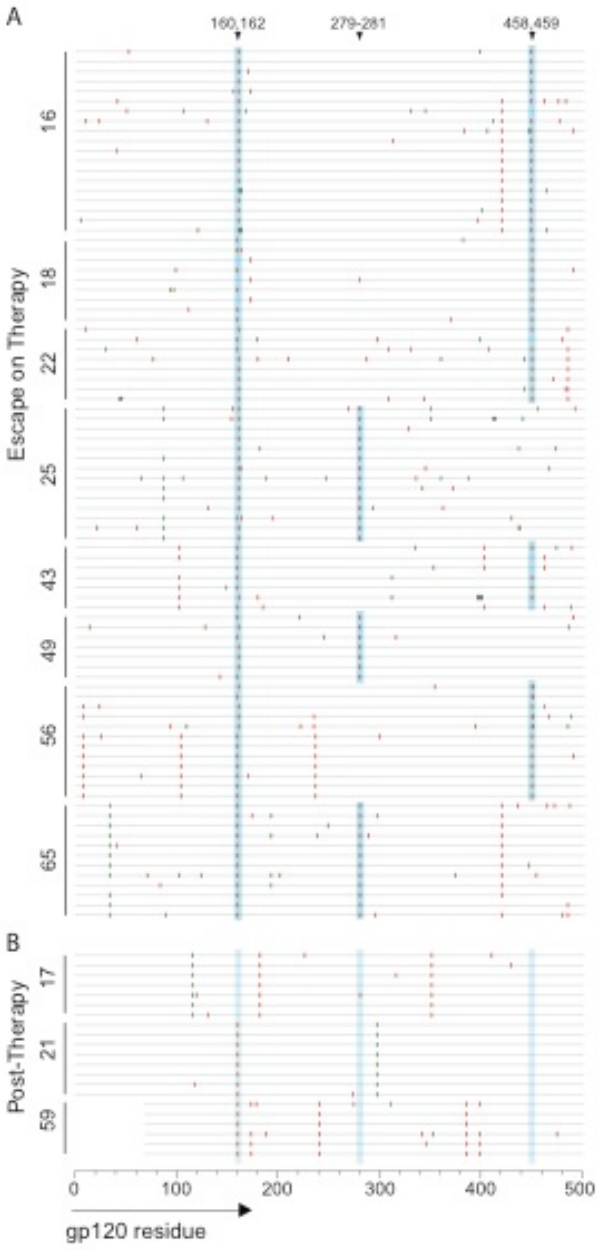

Figure 7. Gp120 sequences from tri-mix treated mice. Gp120 sequences shown as in figure 4. (A) Sequences obtained from mice that escaped during tri-mix therapy, showing simultaneous escape to PG16 and 45-46^{G54W}. (B) Sequences obtained from mice that did not escape therapy, after therapy was discontinued and mice showed rebound viremia.

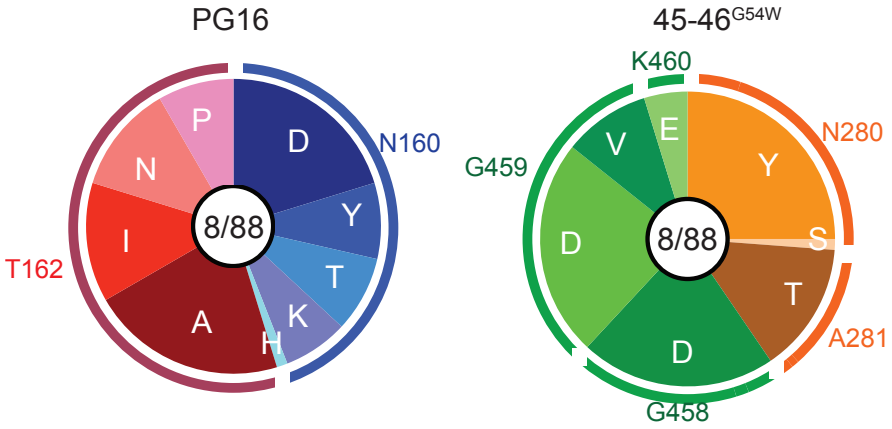

Figure 8. Amino acids detected at escape sites in tri-mix treated mice. Pie charts as in figure 5. All 88 clones obtained from the 8 escaped mice simultaneously contained escape to both PG16 and 45-46^{G54W}.

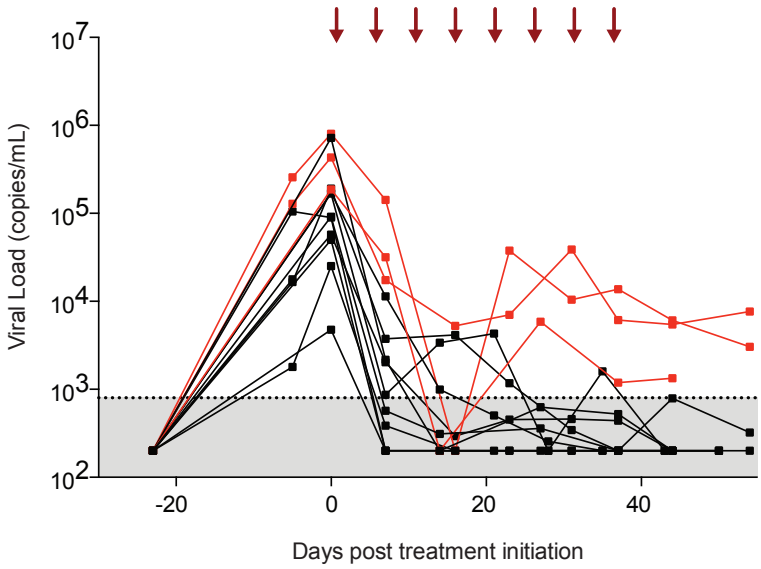

Figure 9. Plasma viremias from penta-mix treated mice. Viremias shown for 13 mice treated with penta-mix antibodies. Injections shown with red arrows. Black lines indicated individual mice that were suppressed beneath the quantitation limit during therapy. Red lines indicate mice that had detectable viremia during therapy, from which I obtained gp120 clones.

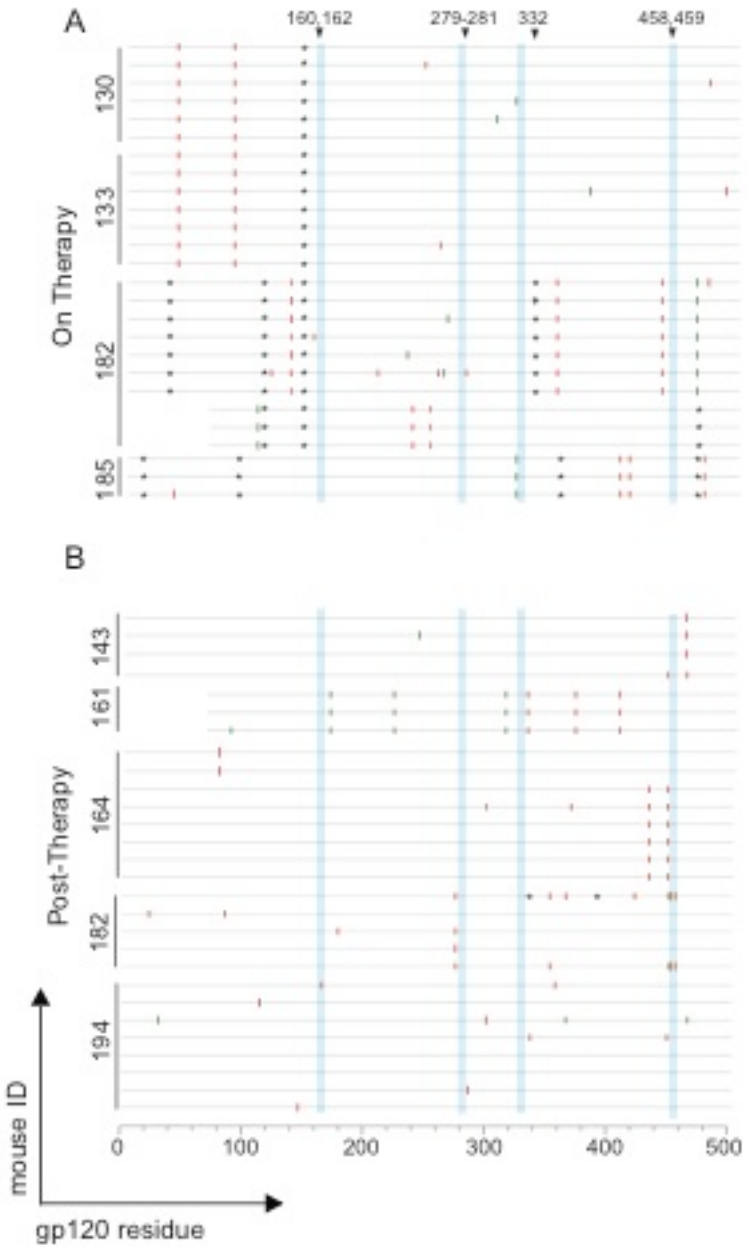

Figure 10. Hypermutation within penta-mix treated mice. Gp120 sequences shown as in figure 4. Asterisks indicate in-frame stop codons as a result of G to A hypermutation. (A) gp120 clones obtained from mice during penta-mix therapy (indicated by red viremia lines in figure 9). (B) gp120 clones obtained from mice after therapy discontinuation when mice exhibited rebound viremia.

2.5 Humanized mice as a model to study HIV latency

The emergence of rebound viremia after sustained suppression mimics the clinical scenario for patients treated with ART. However, ART can only block new rounds of viral replication, whereas bNAbs can bind and clear viral particles directly(Chun et al., 2014; Igarashi et al., 1999). Therefore undetectable plasma viremia in ART-suppressed patients implies there are no productively infected cells releasing virions into the blood, whereas this possibility cannot be excluded in bNAb-suppressed mice. To test if there are productively infected cells during bNAb-mediated suppression, I measured cell-associated viral RNA from bNAb-treated-humanized mice with undetectable plasma viral loads. Twenty-nine of 35 samples measured across different time points from 23 suppressed mice had undetectable cell-associated viral RNA, with the 6 detectable samples averaging 0.03 copies per cell (range 0.007 to 0.2) (Fig. 11). In contrast, untreated mice had detectable cell-associated RNA in 12 of 15 samples, with an average of 0.7 copies per cell (range 0.1 to 5). From this, I conclude that bNAbs are not just clearing cell-free virus, but also eliminating productively infected cells or arresting viral production from cells.

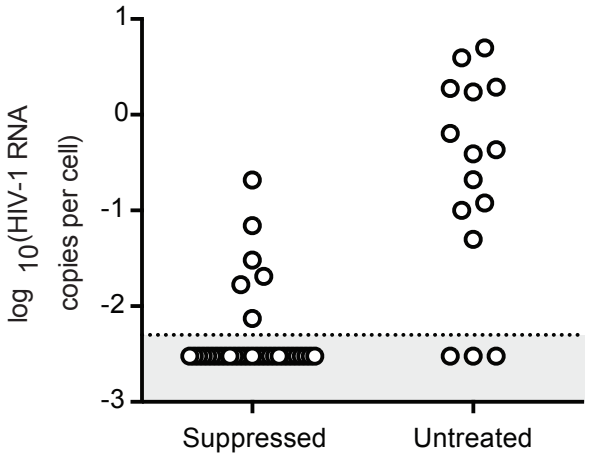

Figure 11. Cell-associated viral RNA mostly undetectable in antibody suppressed mice. Cell associated viral RNA isolated from PBMCs in antibody-treated mice with undetectable plasma viremias (left) and untreated, viremic mice (right). Viral RNA expressed per cell equivalent, as determined by CCR5 DNA copies.

For ART-suppressed patients, it is believed that resting memory $CD4^+$ T cells comprise the primary long-lived reservoir of infected cells capable of producing rebound viremia upon ART discontinuation(Chun et al., 1997b; Eisele and Siliciano, 2012; Finzi et al., 1997; Wong et al., 1997). To determine if resting $CD4^+$ T cells capable of producing viremia exist in humanized NRG mice suppressed with bNAb combinations, I isolated resting $CD4^+$ T cells from 6 HIV-infected humanized mice that were suppressed with bNAb combinations and cultured the cells using a standardized viral outgrowth assay (VOA)(Laird et al., 2013). Six of 16 culture wells became p24+, an indicator of robust viral production (Fig. 12). Based on the number of resting $CD4^+$ T cells and number of culture wells tested, I calculate ~2.2 IUPM cells(Laird et al.), a frequency

consistent with that obtained from ART-suppressed bone-marrow, liver, thymus (BLT) humanized mice(Denton et al., 2012) and human patients(Chun et al., 1997a; Siliciano et al., 2003). From this, I conclude that humanized NRG mice harbor replication-competent virus within resting $CD4^+$ T cells in the presence of bNAbs.

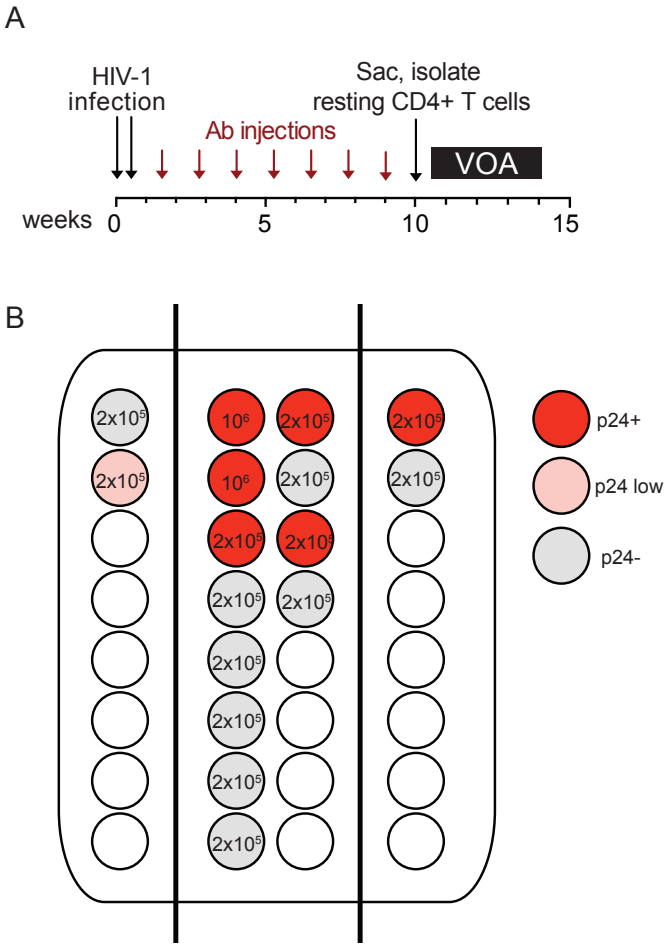

Figure 12. Resting $CD4^+$ T cell isolation and VOA from antibody suppressed mice. Resting $CD4^+$ T cells were isolated from antibody-treated humanized mice with undetectable plasma viral loads. Mouse cells were depleted, and human $CD4^+$ T cells were purified by negative isolation, followed by depletion of activated cells. Resting $CD4^+$ T cells from identical fetal liver donors were pooled together and cultured by VOA protocol. Cells from three different donors were obtained and cultured separately, as indicated by vertical black lines. Individual culture wells were tested for p24 in the supernatant by ELISA. Number inside each well represents number of resting $CD4^+$ T cells started in the culture.

Because antibody-sensitive virus capable of producing rebound viremia upon therapy cessation persists in the presence of bNAbs and humanized mice harbor resting $CD4^+$ T cells containing replication-competent virus, I decided to test strategies that could prevent viral rebound by eliminating persistent viral reservoirs.

2.6 Combination Therapy with bNAbs and Inducers

I employed a “shock and kill” approach, in which viral transcription is induced within $CD4^+$ T cells harboring integrated provirus. Since $CD4^+$ T cells harboring non-expressed provirus have very long half-lives and are unrecognizable to immune surveillance, the goal is to induce viral transcription to enable viral cytopathic effects or immune-mediated killing(Deeks, 2012). Humanized mice with established HIV-1_{YU2} infections (viremia ranging from 4.70×10^3-7.96×10^5 copies/ml at 2-3 weeks after infection) were treated with a tri-mix of bNAbs (10-1074, PG16, 3BNC117) that could prevent escape and suppress viremia. When plasma viremia and cell-associated HIV RNA dropped below detection, mice were co-administered a viral inducer for 5-14 days, and monitored for viral rebound for an additional 47-85 days (Fig. 13).

I tested three inducers: vorinostat, an HDAC inhibitor(Archin et al., 2012; 2009; Contreras et al., 2009), I-BET151, a BET protein inhibitor(Boehm et al., 2013), and αCTLA4, a T-cell inhibitor pathway blocker. These inducers were

selected based on their differing mechanisms of action, established safety and pharmacokinetics in mice, and abilities to induce HIV-1 transcription *in vitro*.

Mice receiving antibodies plus vorinostat showed no significant differences in viral rebound compared to mice receiving antibody alone (Fig. 13). The same result was seen for hu-mice treated with antibodies plus I-BET151 or αCTLA4 (Fig. 13). All 10 mice that received antibody therapy plus vorinostat showed viral rebound when the antibody dropped below therapeutic levels. Of 12 mice that received antibody therapy plus I-BET151, 11 had viral rebound, and 10 of 11 mice that received antibody plus αCTLA4 showed viral rebound. In total, of 33 mice that received antibody plus a single inducer, 31 showed viral rebound. In comparison, of 25 mice that received antibody therapy alone, 22 rebounded after the level of passively administered antibody decayed below the therapeutic threshold ($p = 0.64$, Fisher's Exact Test).

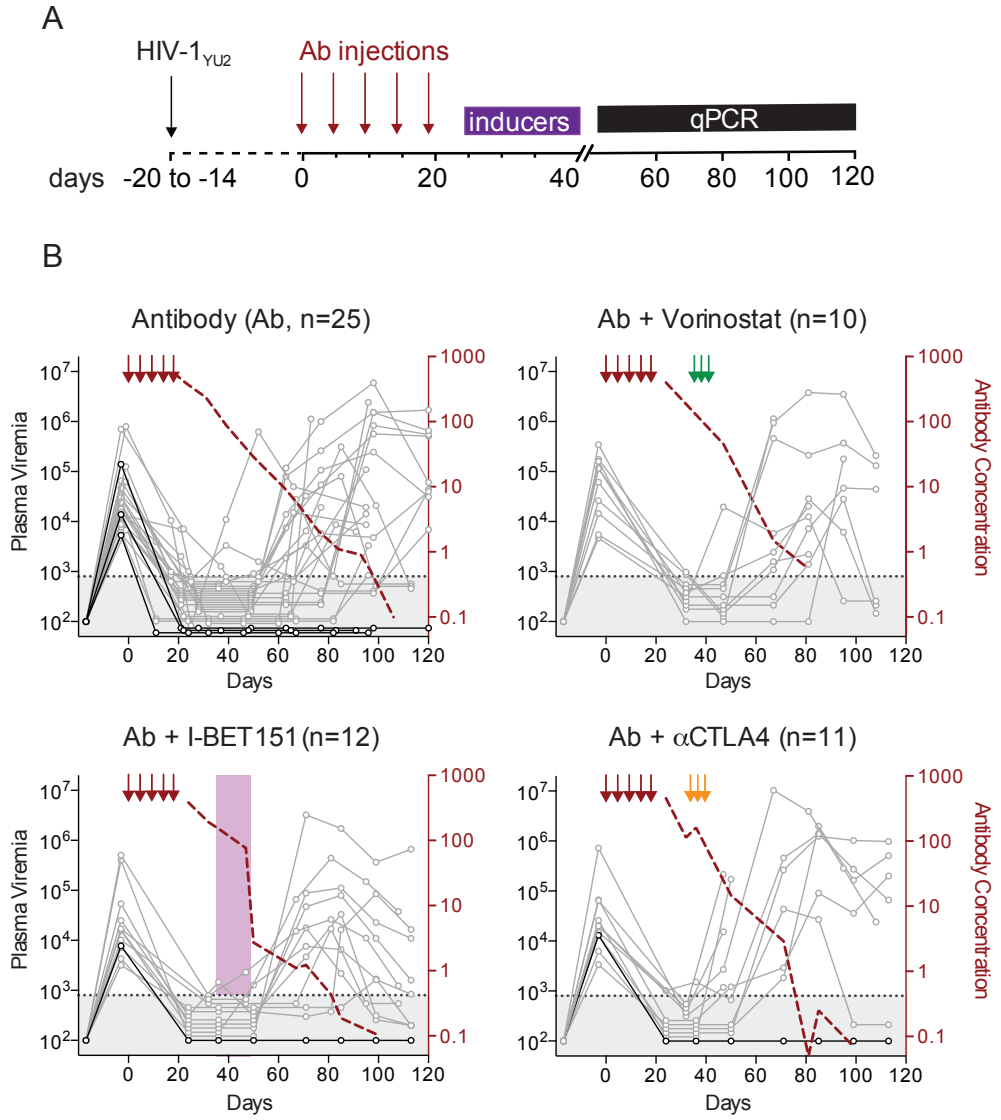

Figure 13. No difference in rebound frequency for antibodies plus a single inducer. Mice were suppressed with combination antibodies, then administered one of three different viral inducers while antibodies were still present, and monitored for viral rebound. (A) Experimental schematic (B) Plasma viremias from mice treated with antibodies alone, or antibodies plus a single inducer. Each line represents an individual mouse. Gray indicates mice that rebound. Black indicates mice that do not rebound by the terminal point. Antibody injections indicated in red. Geometric mean antibody concentration across all mice in the group shown by dashed red line. Green arrows indicate vorinostat administrations (1.5 mg oral gavage). Purple shading indicates I-BET151 administration (30 mg/kg injections daily i.p. for 14 days). Orange arrows indicate αCTLA4 injections (100 μg, i.p.).

To determine whether a combination of inducers might be more effective than a single inducer, I administered all three inducers simultaneously. In the absence of antibody therapy, the combination of all three inducers did not abort or noticeably alter active infection (Fig. 14A). Additionally, the human graft did not differ between untreated mice and mice that received combination of inducers (Fig. 14B). Twenty-three mice that initially suppressed viremia on antibody therapy were treated with the inducers combination and followed for 62-105 days after the last antibody injection (Fig. 15). Only 10 of the 23 mice (43%) showed viral rebound, while the remaining 57% of mice failed to rebound, a significant decrease in rebound frequency compared to antibody alone (p = 0.0018, Fisher's Exact Test), or antibody plus a single inducer (p = 0.0001, Fisher's Exact Test).

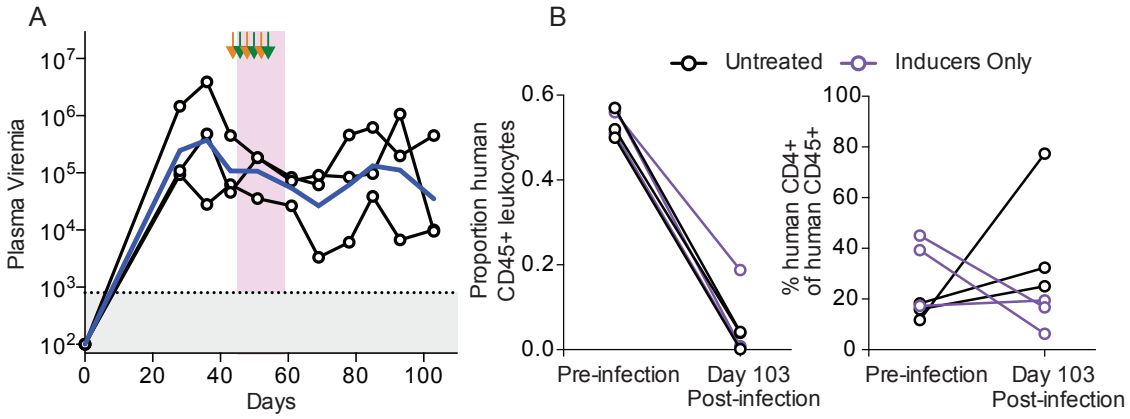

Figure 14. Graft and viremia unaltered by combination inducers alone. (A) Plasma viremia in mice receiving combination inducers alone. Blue line shows geometric mean viremia across the three mice. Arrows and shading as in figure 13. (B) Human graft as determined by flow cytometry from PBMCs.

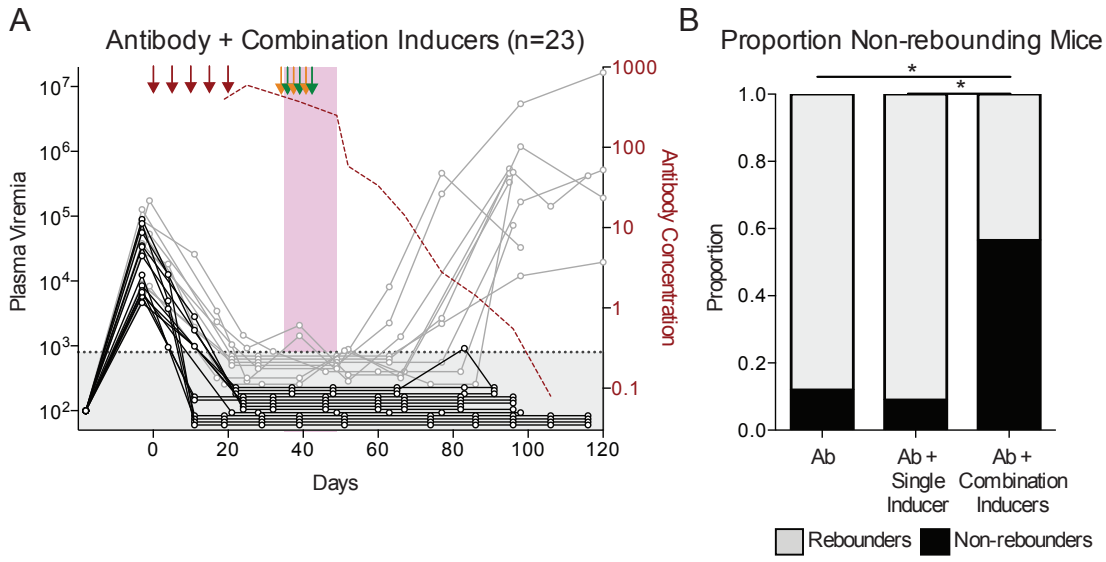

Figure 15. Antibody plus combination inducers reduce frequency of viral rebound. (A) Plasma viremia from mice administered combination inducers in the presence of antibodies. Graph coloring and shading as in figure 14. (B) Comparison of proportion of mice showing viral rebound by the terminal point in mice receiving antibody alone, antibody plus any one of the three inducers, and antibody plus the combination of all three inducers. *, $p < 0.05$, Fisher's exact test.

Importantly, when compared to antibody alone, neither single inducers nor combination inducers measurably altered the frequency of $CD4^+$ T cells remaining at the end of the experiment, which correlated with absolute $CD4^+$ T cell levels (Fig. 16). Additionally, cell-associated viral RNA measured in splenic T-cells at the terminal point supported the results from the plasma viremia levels, with mice that failed to show viral rebound in the plasma also having undetectable cell-associated viral RNA (Fig. 17).

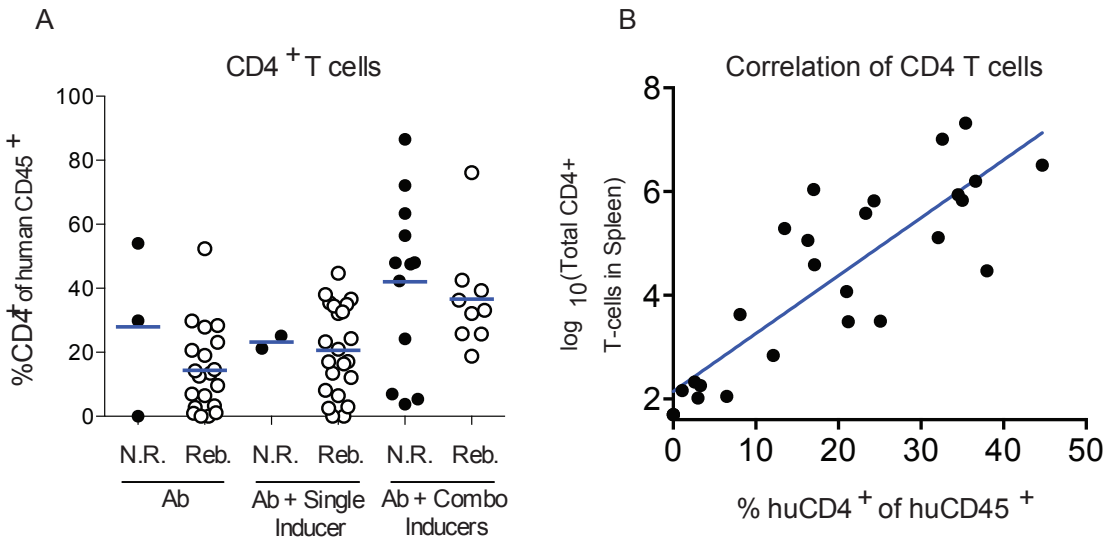

Figure 16. No difference in CD4$^+$ T cell levels between rebounding and non-rebounding mice. (A) The % of human CD4$^+$ T cells among all human CD45$^+$ cells in the spleen of mice at the terminal sac, shown by treatment group and rebound status, N.R. = non-rebounder (solid circles), Reb. = rebounder (open circles). There was no statistically significant difference between any of the groups, Kruskal-Wallis test. (B) correlation between the % human CD4$^+$ T cells among human CD45$^+$ cells and the total number of CD4$^+$ T cells in the spleen by absolute count.

I measured cell-associated viral DNA as an imperfect surrogate of the HIV-1 reservoir. HIV-1 DNA is thought to overestimate the reservoir because it fails to exclude damaged or incomplete viral sequences that cannot be reactivated(Ho et al., 2013). In addition, the overall number of cells assayed in mice is limited and therefore the assay is not very sensitive. Nevertheless, I could not detect viral DNA at the terminal point in the majority of mice that did not rebound, whereas the majority of mice that did rebound had detectable HIV-1 DNA, with an average of 0.09 copies per T cell (Fig. 17).

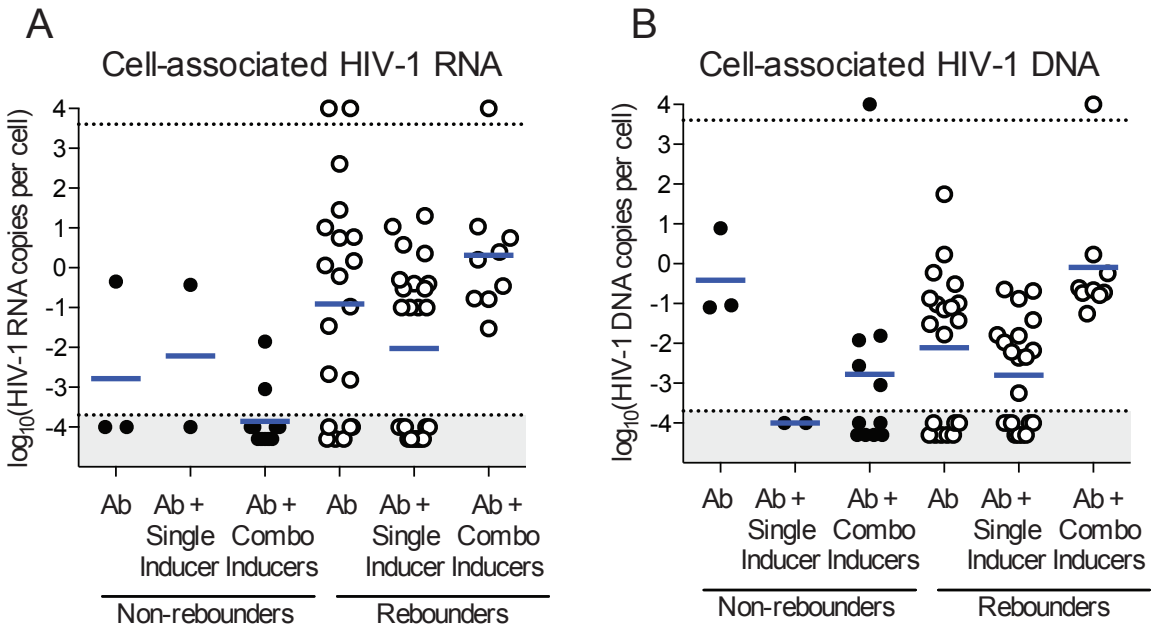

Figure 17. Cell-associated HIV-1 RNA and DNA from splenic T cells reflects rebound status. (A) Cell-associated HIV-1 RNA measured in splenocytes at terminal sac, expressed per cell equivalent as determined by CCR5 DNA copies. Closed circles indicate non-rebounding mice, open circles indicate rebounding mice. Gray shading indicates beneath detection limit. Samples above dotted line indicate detectable HIV-1 RNA, but unreliable detection of CCR5 DNA (B) Cell-associated HIV-1 DNA. Shading and markings as in A.

When compared to controls, mice that failed to rebound after combination antibody and inducer therapy showed similar initial plasma viremias to mice that rebounded across all experimental groups (Fig. 18). Therefore, neither initial viremia levels, nor $CD4^+$ T cell levels can account for the differences between the experimental groups.

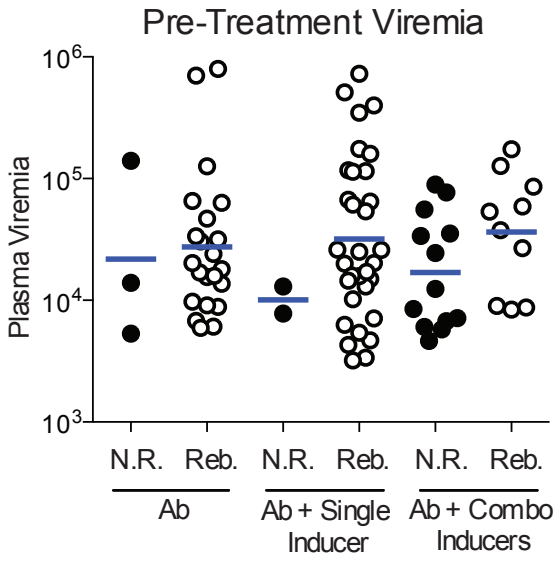

Figure 18. Pre-treatment viremia does not determine rebound status. Pre-treatment viremias shown for all mice, grouped by treatment group and rebound status. There was no statistical difference between any of the groups, Kruskal-Wallis test.

To determine if antibody persistence accounted for differing viral rebound outcomes, I calculated antibody levels at the time of rebound for rebounding mice, and antibody levels at the terminal point for non-rebounding mice. The average plasma antibody concentration at the time of viral rebound was 2.97 µg/ml, which I termed the rebound threshold (Fig. 19). Of the 18 non-rebounding mice, the average antibody concentration at the terminal point was 0.44 µg/ml, with 15 out of 18 mice having antibody concentrations less than 2.97 µg/ml. From this, I conclude that non-rebounding mice did not have residual antibody levels that would prevent rebound.

Since antibody levels decayed to the rebound threshold at different rates within individual mice and the rebound threshold represents a population

average, I calculated the number of days that elapsed from when each individual mouse's antibody levels reached the rebound threshold to when the mouse actually showed rebound viremia. Fifty of 59 mice rebounded within 10 days, indicating consistent timing of rebound kinetics (Fig. 19). In non-rebounding mice, an average of 20.2 days elapsed from the time antibody concentrations reached 2.97 µg/ml to termination (Fig. 19). Thus, failure to rebound cannot be attributed to premature termination. In total, I conclude that combining vorinostat, I-BET151 and αCTLA4 with combination antibodies decreases the frequency of viral rebound in humanized mice.

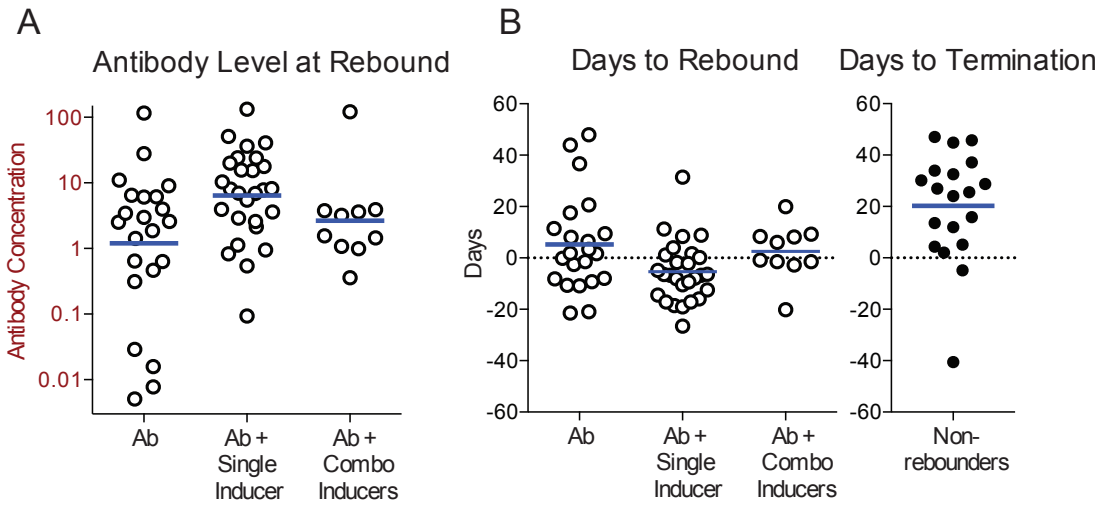

Figure 19. Persistent antibody levels at terminal point cannot explain lack of viral rebound. (A) Antibody level at the time of rebound are shown for all rebounding mice, divided by treatment group. Geometric mean of 2.97 µg/ml is termed the rebound threshold (B) For rebounding mice, number of days that elapsed from when each mouse's antibody levels dropped beneath 2.97 µg/m to when the mouse had rebound viremia (C) For non-rebounders, number of days that elapsed from when each mouse's antibody levels dropped beneath 2.97 µg/ml to when the mouse was sacrificed.

2.7 ART and inducers

While the importance of combination inducers is evident from the 53 of 58 mice that rebound when not administered combination inducers, I sought to determine if combination inducers in the presence of ART was equally efficacious at preventing rebound, or if bNAbs played a unique role. I repeated the experiments testing for viral rebound, except that viremia was suppressed using ART (raltegravir, emtricitabine, tenofovir) rather than bNAbs. Of 9 mice that survived the entire experiment, 6 showed viral rebound, a 67% rebound frequency (Fig. 20). Although this is a higher rebound frequency than the 43% observed for bNAbs plus combination inducers, it is statistically indistinguishable due to limited numbers of mice (p = 0.43, Fisher's Exact Test). To determine the relative importance of bNAbs compared to ART, I adopted a different experimental approach.

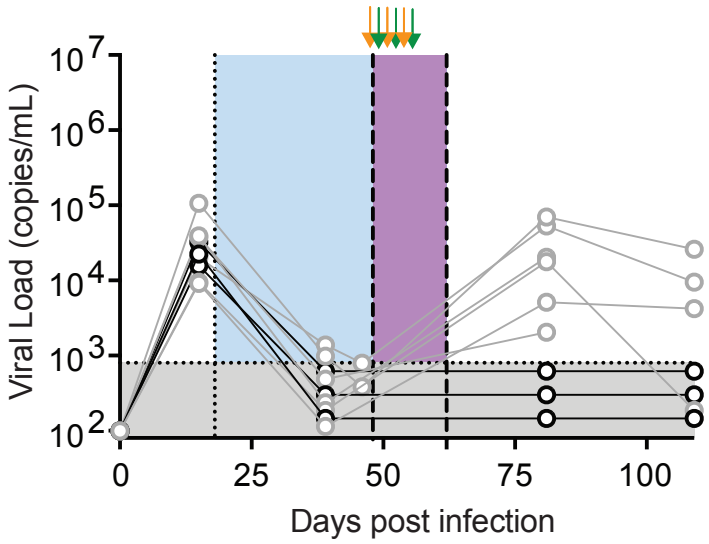

Figure 20. ART plus combination inducers. Plasma viremias from mice receiving ART plus combination inducers. ART administration shown in blue shading, otherwise, coloring and shading as in figure 15.

2.8 bNAbs as post-exposure prophylaxis

Mice were exposed to HIV-1_{YU2} and treated with either ART or a tri-mix of bNAbs 96 hours later, whether or not plasma viremia was detectable. Mice for this experiment were selected with very stringent humanization criteria, and 14 of 15 untreated mice became viremic (Fig. 21). When non-humanized NRG mice were exposed to identical amounts of HIV-1, virus was undetectable in the plasma by 48 hours (Fig. 21). To estimate the total number of productively infected cells within the spleen of a mouse just prior to therapy initiation, a separate group of mice that had similar levels of human reconstitution were exposed to HIV-1, then 96 hours later, plasma was collected and the mouse was sacrificed. Plasma viremia was measured by qPCR, and the total number of

human $CD3^{+}CD8^{-}p24^{+}$ cells within each spleen was determined by flow cytometry (Fig. 21).

In the experimental groups of mice receiving treatment, ART was administered in the food for up to 40 days. Antibodies were administered subcutaneously with an initial dose of 3 mg per mouse, and 3-5 subsequent doses of 1.5 mg each, spaced 3-4 days apart, so that antibody levels were maintained above 10 μg/ml for approximately 40 days (Fig. 21). Although plasma viremia was suppressed beneath the detection limit in all 22 ART-treated mice and cell-associated RNA was undetectable in 15 of 16 mice measured during therapy, 18 mice showed rebound viremia after ART termination (Fig. 21). The rebounding mice even included 5 mice that did not have detectable plasma viremia before ART was initiated (measured ~90 hours following viral exposure). Among the 18 viremic mice, viremia was first detected 28 to 84 days after ART termination (Fig. 22). From this, I conclud that a pool of infected cells capable of producing rebound viremia forms very early after exposure and persists throughout therapy, indicating that ART is relatively ineffective at preventing reservoir establishment in humanized mice when administered 4 days after infection, consistent with human and macaque studies(Landovitz and Curry, 2009; Whitney et al., 2014).

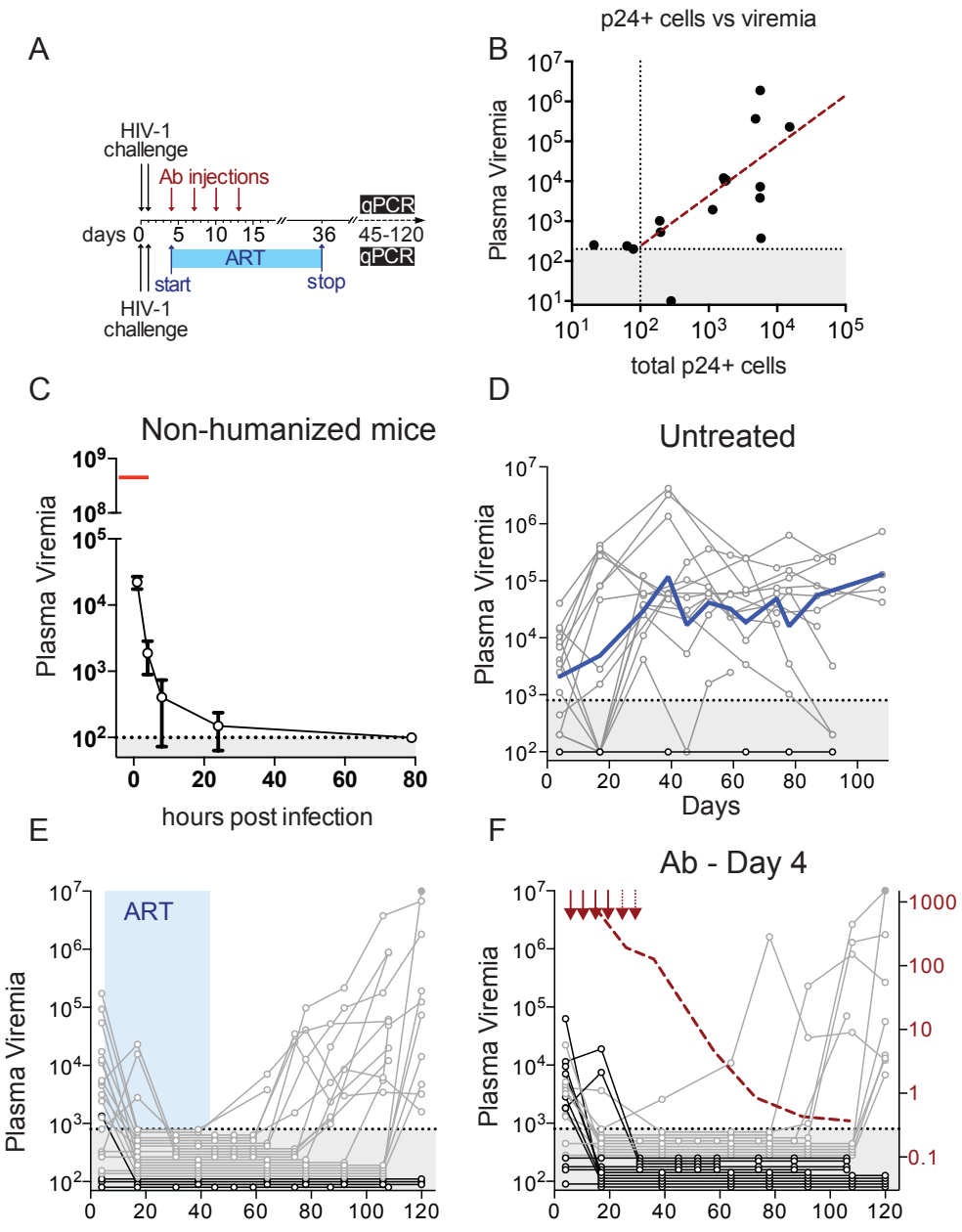

Figure 21. bNAbs and ART as PEP in humanized mice. (A) Experimental schematic for post-exposure prophylaxis experiments (B) Absolute numbers of human $CD3^{+}CD8^{-}p24^{+}$ cells purified from the spleens of infected mice 4 days after viral exposure (C) Clearance of cell-free plasma viremia in non-humanized NRG mice. Red tick indicates copy number of virus stock injected i.p. (D) plasma viremia in untreated mice. Geometric mean viremia shown in blue. (E) Plasma viremia for mice treated with ART food. Gray lines indicate mice that become viremic. Black lines indicate mice that do not become viremic by terminal point. (F) Plasma viremia for bNAb-treated mice. Coloring as in figure 13.

In contrast, only 10 of 21 (48%) mice treated with antibodies 4 days after infection showed viremia by the terminal point, a statistically significant decrease compared to ART (p = 0.027). For 9 of these 10 viremic mice, the first detectable viremia occurred 74 or more days after the last antibody injection. The delay in viral rebound observed for mice treated with antibody at day 4 was statistically significant compared to ART-treated mice (Fig. 22). The mice that rebounded showed a geometric mean antibody concentration at rebound of 0.46 µg/ml. However, sustained inhibitory antibody levels did not account for the 11 mice that did not rebound, all of which had antibody levels ≤0.50 µg/ml by termination (Fig. 23).

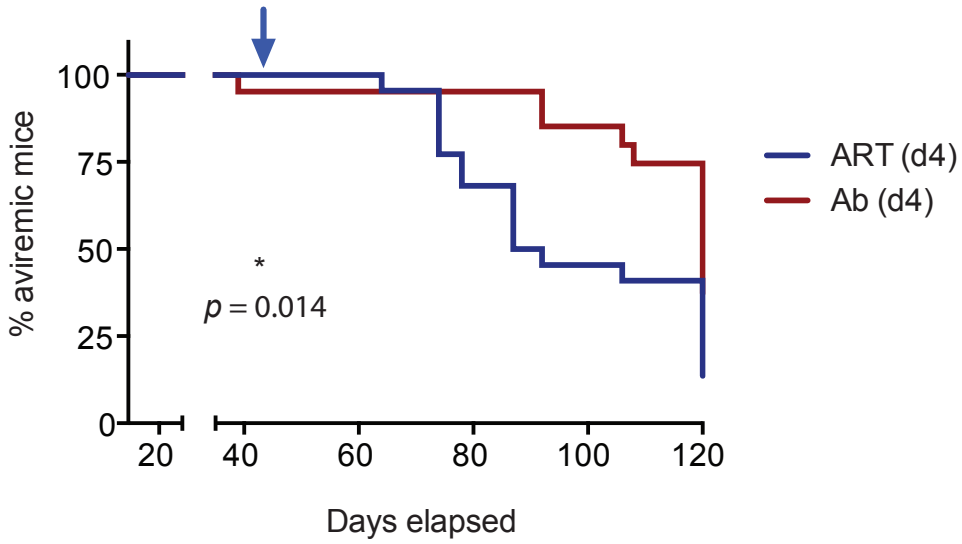

Figure 22. Delay in viral rebound for bNAb-treated mice relative to ART-treated mice. Survival curve showing the proportion of mice that are aviremic over time following discontinuation of therapy. Blue arrow indicates discontinuation of ART food.

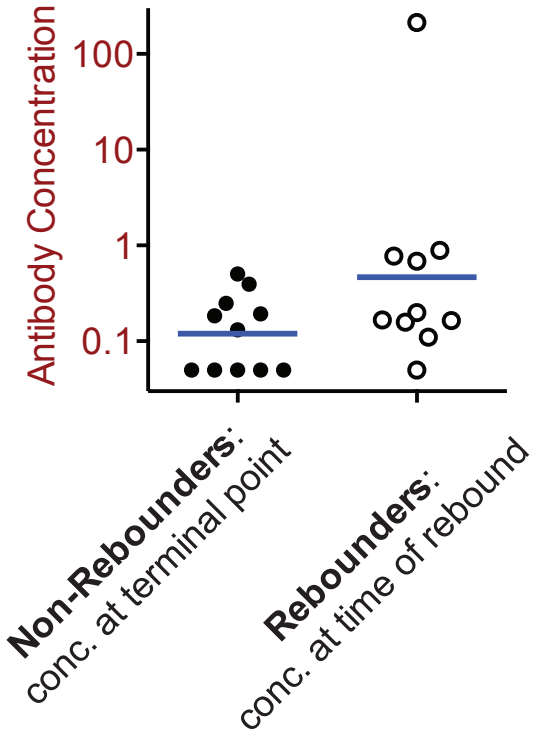

Figure 23. Antibody concentration at time of rebound or terminal point in PEP mice. Antibody concentration at the terminal point is shown for non-rebounding mice (left, black as shown in 21E), and antibody concentration at the time of rebound viremia for rebounding mice (right, gray as shown in 21E)

Mice in the early treatment group that failed to show detectable plasma viremia were further examined for the presence of human $CD4^+$ T cells and cell-associated HIV-1 RNA and DNA in the spleen. I found that mice that failed to develop sustained plasma viremia had similar percentages of $CD4^+$ T cells relative to infected controls (Fig. 24). Therefore, differences in $CD4^+$ T cell levels are unlikely to account for the observed differences between viremic and aviremic mice. Moreover, T cell-associated HIV-1 RNA levels were consistent with plasma viral loads, with mice that remained aviremic having either undetectable or lower cell-associated HIV-1 RNA than mice that developed sustained viremia (Fig. 25A). HIV-1 DNA measurements were also consistent with each mouse's rebound status (Fig. 25B). I conclude that bNAbs can interfere with the establishment of the HIV-1 reservoir in humanized mice as determined by the significant delay in viral rebound.

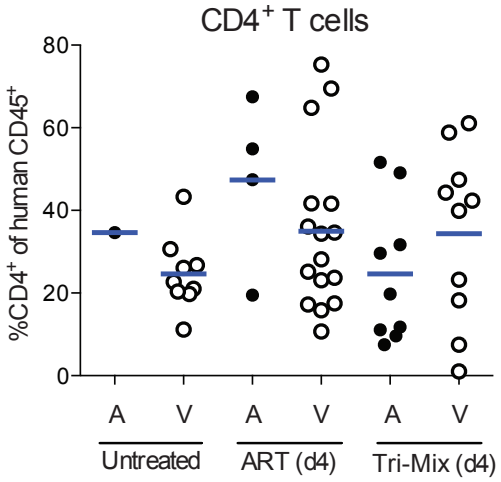

Figure 24. $CD4^+$ T cell levels in the spleen do not differ across treatment groups or viremia status. % human $CD4^+$ T cells among human $CD45^+$ cells as measured by flow cytometry of splenocytes at the terminal point, grouped by treatment and viremia status. Mice that never became viremic (A), closed circles. Mice that became viremic (V), open circles. There is no statistical difference across the groups (Kruskal-Wallis test).

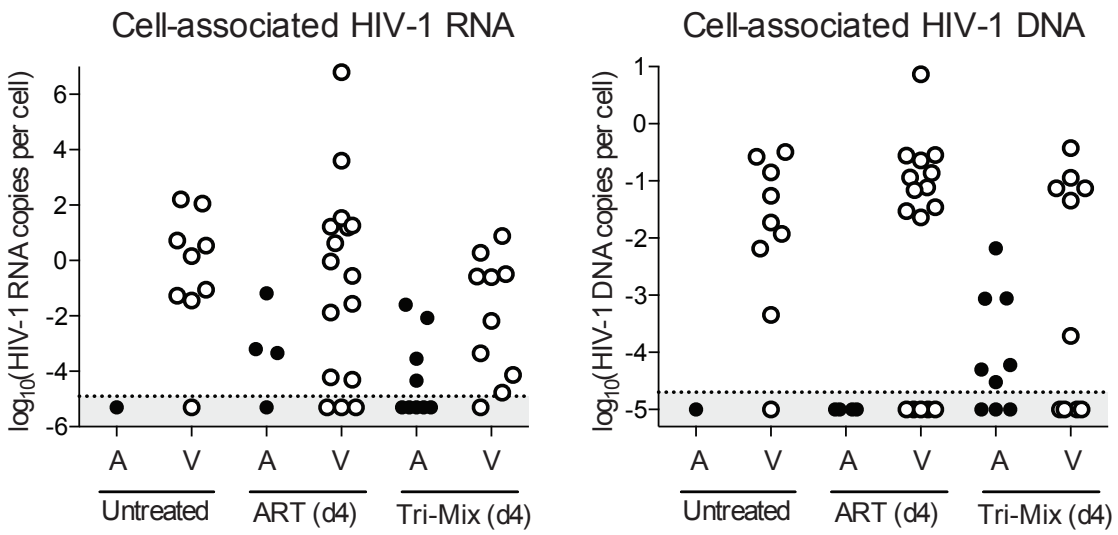

Figure 25. Cell-associated HIV-1 RNA and DNA in spleen of PEP mice. Cell-associated RNA (left) and DNA (right), expressed per cell equivalent, as determined by CCR5 DNA copies. Gray shading shows beneath detection limit. Circles and abbreviations as in figure 24.

To determine if bNAbs' ability to prevent viral rebound could be improved by initiating therapy earlier, I administered the same tri-mix of bNAbs 72 hours after viral exposure. Only 2 of the 7 mice tested (29%) showed viremia by the terminal point, when antibody levels were undetectable in the plasma (Fig. 26). Although the observed rebound frequency was less than the 48% observed when bNAbs were initiated 96 hours after exposure, there were too few mice to show a significant difference. To see if bNAbs' ability to prevent rebound viremia extended beyond 3-4 days post-exposure, I administered the same tri-mix of bNAbs 8 days after viral exposure. Ten of the 11 treated mice showed viral rebound 44-58 days after the last antibody injection (Fig. 27). In total, the results

show that bNAbs can interfere with the establishment of the viral reservoir, but the efficacy is very time sensitive.

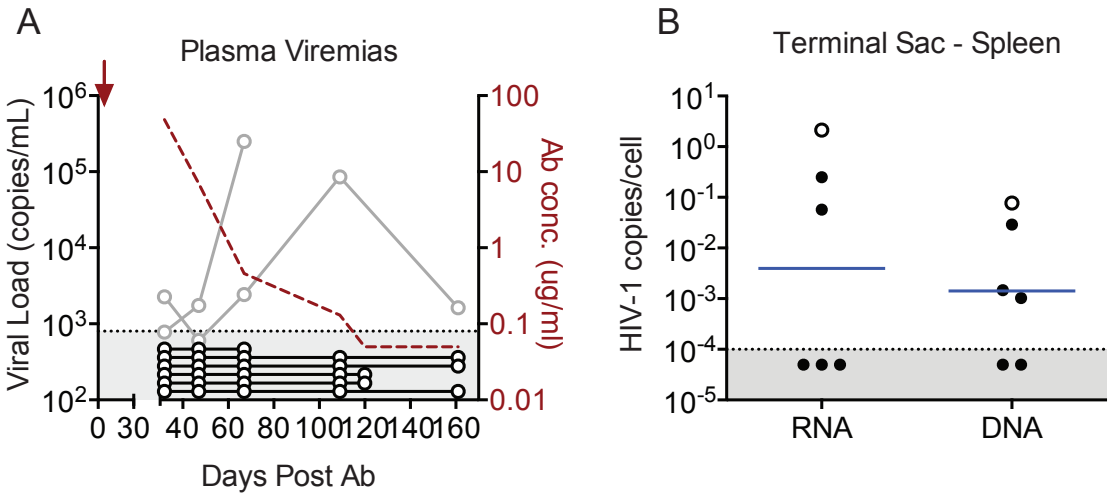

Figure 26. Antibody PEP initiated at 72 hours following viral exposure. (A) Plasma viremias for mice given a single injection of tri-mix bNAbs 72 hours after viral exposure. Lines and coloring as in figure 21E. (B) HIV-1 copies per cell, taken from the spleen at the terminal point. Open circles indicate mice that became viremic, closed circles indicate mice that never became viremic. Of note, one mouse that became viremic died before spleen could be harvested and so is excluded in (B).

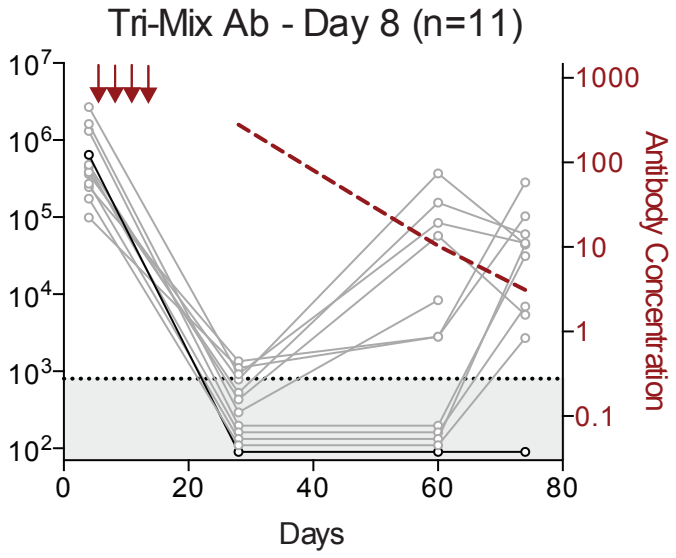

Figure 27. Antibody PEP initiated at day 8. Plasma viremias for mice initiated with tri-mix bNAbs 8 days following viral exposure. Coloring and lines as in figure 21E

Because of the time sensitivity of therapy initiation and the different routes of administration for bNAbs (subcutaneous injection) and ART (orally in food) in these experiments, it was possible that the observed difference in the ART-treated and bNAb-treated mice was due to different pharmacokinetics of the two treatments. Specifically, the bNAbs were administered as a high-dose bolus injection, whereas ART might have taken additional time to reach therapeutic levels. However, measuring concentrations of anti-retroviral drugs in humanized mice is difficult, so I used post-exposure prophylaxis treatments to indirectly address this issue.

ART has been shown to be completely protective when administered subcutaneously 24 hours after intravenous viral exposure and maintained for 28 days in macaques, but incompletely protective when initiated 48 hours after exposure(Tsai et al., 1995; 1998). Thus any lack of protection when ART is administered 24 hours after exposure via food suggests slower time to reach therapeutic levels. Of 10 mice that were exposed to HIV-1 and given ART food 24 hours later for 30 days, all 10 remained aviremic for 92-131 days following ART cessation (Fig. 28). There was no detectable cell-associated viral RNA in the spleens of all mice tested (Fig. 28). From this, I conclude that ART administered in the food within 24 hours of exposure can protect against viral acquisition. By extension, the difference in efficacy of bNAbs and ART started at 4 days following exposure is not solely due to pharmacokinetics.

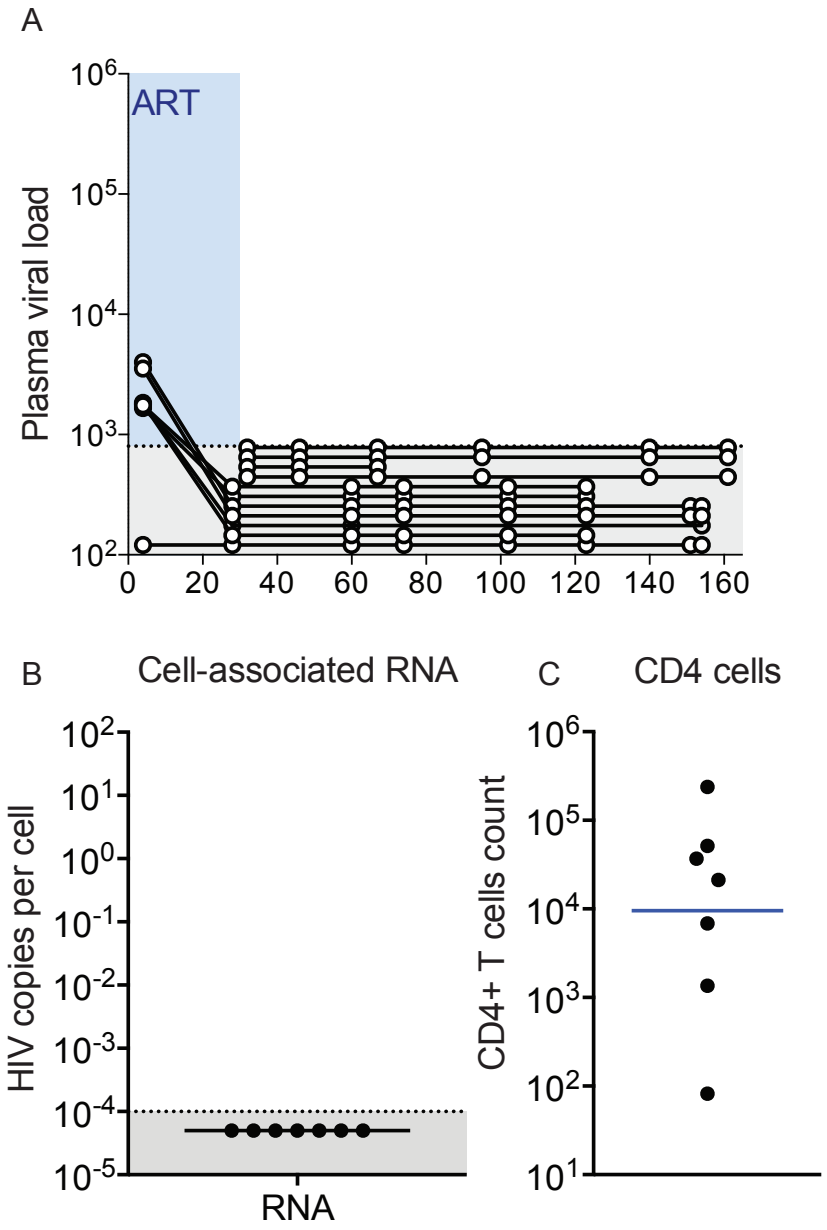

Figure 28. ART as PEP within 24 hours. (A) Plasma viremias from mice initiated on ART food 24 hours after viral exposure. (B) Cell-associated HIV-1 RNA taken from splenocytes at the terminal point, expressed per cell equivalent, as determined by CCR5 DNA copies. (C) absolute count of total $CD4^+$ T cells within the spleen at the terminal point.

2.9 Importance of Fc Receptor Binding for bNAb Activity

Because pharmacokinetics could not entirely explain the observed differences in preventing viremia between ART and bNAbs, I asked if bNAbs' unique ability to engage components of the immune system through their Fc domains played a role. I repeated the day 4 post-exposure prophylaxis experiments using the same tri-mix of bNAbs, except the Fc region in each of the component bNAbs carried mutations that abrogate both human and mouse Fc-receptor binding (G236R/L328R; GRLR, herein referred to as FcR^{null}(Horton et al., 2010). Despite equivalent neutralizing activity in TZM-bl assays(Pietzsch et al., 2012), FcR^{null} antibodies were far less potent than controls *in vivo* (Fig. 29). Mice treated with FcR^{null} tri-mix initially suppressed viremia at the same rate as the wild type antibody-treated mice. However 9 of 15 mice receiving post exposure prophylaxis with the FcR^{null} tri-mix showed viral rebound by 44 days after the last antibody injection. In contrast, 44 days after the last injection of control antibodies, only 1 of 21 mice showed rebound viremia ($p = 0.0004$). Not only was the delay in viral rebound significantly reduced for FcR^{null} antibodies, but the antibody levels at the time of viral rebound were ~50-fold higher for mice receiving FcR^{null} tri-mix compared to wild-type tri-mix ($p = 0.0014$, Fig. 29). This suggests FcR^{null} antibodies have reduced activity *in vivo*, and thus Fc function enhances antibody activity but is not an absolute requirement.

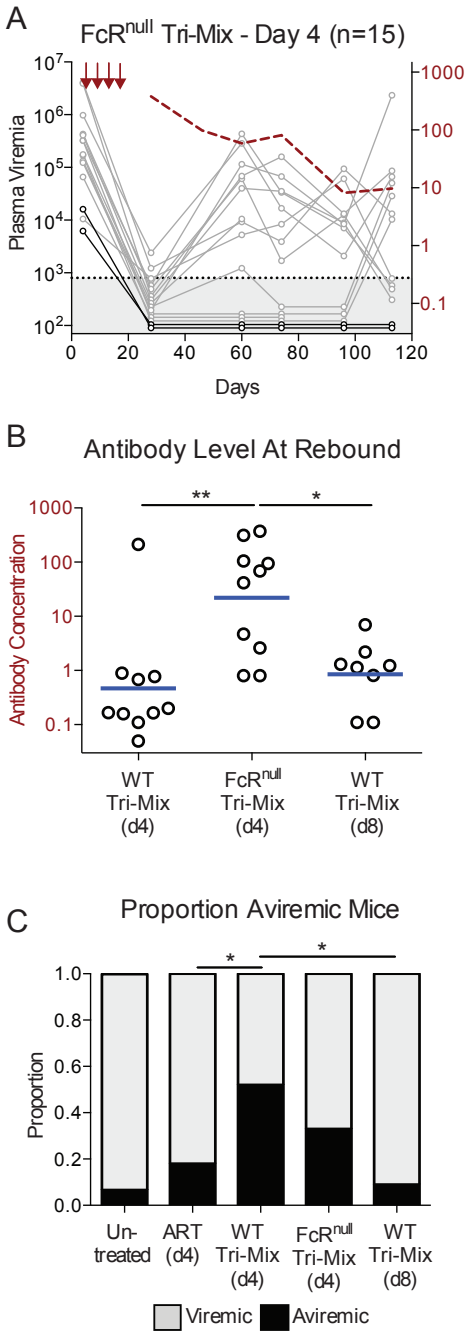

Figure 29. FcR^{null} antibodies less effective than wild-type antibodies at day 4. (A) plasma viremias shown for mice treated with tri-mix of FcR^{null} antibodies beginning 4 days after viral exposure. Coloring as in figure 21E. (B) Antibody concentration at the time of viral rebound, shown by treatment group. *, $p < 0.05$, **, $p < 0.01$, Mann-Whitney U Test (C) Proportion of mice that become viremic, by treatment group. *, $p < 0.05$, Fisher's exact test.

Because mice receiving FcR^{null} tri-mix showed viral rebound in the presence of antibody concentrations far higher than the therapeutic threshold for wild-type antibodies, we cloned and sequenced gp120 from the 9 mice that rebounded by day 44 to examine the mechanism for viral breakthrough in the presence of FcR^{null} tri-mix (Fig. 30). As a control, gp120 clones from mice treated with wild-type antibodies at day 8 were also sequenced. Among all 40 clones sequenced from FcR^{null} tri-mix treated mice, not a single clone had the triple combination of signature mutations that confer escape to the antibody-tri-mix. I conclude that viral rebound in FcR^{null} tri-mix treated mice is not attributable to antibody escape, but rather reduced antibody potency. Thus, FcR^{null} mutant antibodies, which cannot engage Fc receptors, are less active in suppressing infection than their wild type counterparts, and optimal post-exposure prophylaxis by bNAbs requires engagement of Fc-receptors.

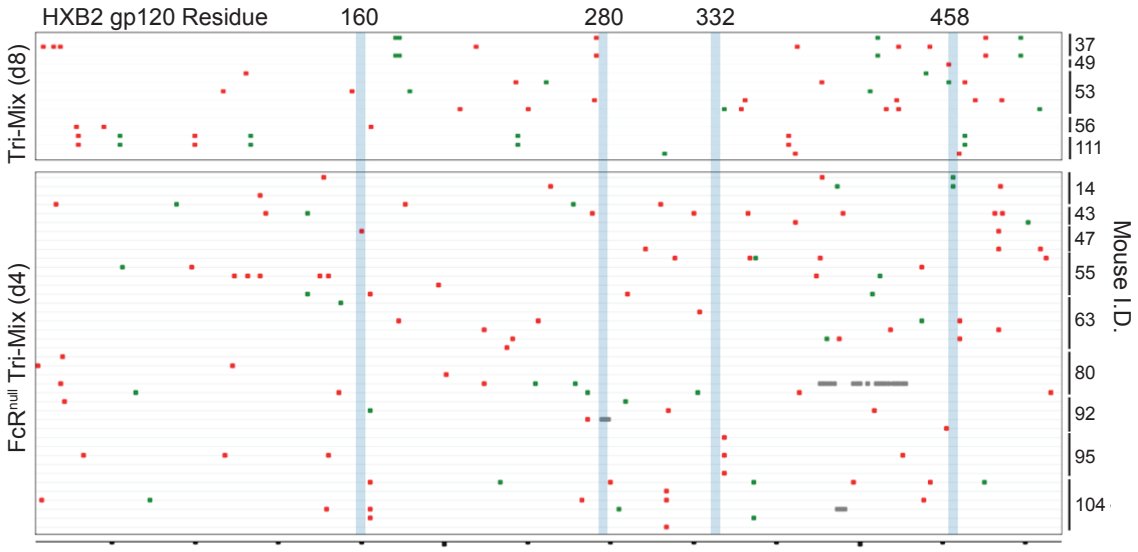

Figure 30. Gp120 sequences of viral breakthrough clones show no signature escapes. Gp120 sequences shown as in Figure 7.

CHAPTER 3:

DISCUSSION

3.1 bNAb discovery

Prior to 2009, there were no known naturally occurring, potent, broadly neutralizing antibodies against HIV-1. Advances in single cell cloning techniques that allowed comprehensive probing of HIV-1-specific B-cells uncovered a “next-generation” of bNAbs with remarkable breadth and potency(Mouquet et al., 2012; Scheid et al., 2011; Walker et al., 2009; 2011; Wilson and Andrews, 2012; Wu et al., 2010). Although the best bNAbs come from rare patients that are carefully selected, their discovery revealed the capacity of the human B-cell response to target HIV-1 is far more impressive in some cases than previously recognized. Additionally, structural, biochemical, and genetic characterization of bNAbs and the viruses they neutralize revealed new sites of vulnerability on the virus. Most importantly, these bNAbs provide a blueprint for a vaccine since passive transfer of bNAbs prior to HIV-1 challenge can prevent viral acquisition(Hessell et al., 2009; Mascola et al., 1999; Moldt et al., 2012; Shingai et al., 2013a).

However, within the patients whom these bNAbs come from, there has been no definitive evidence showing bNAb-mediated viral control. In fact, these patients appear to have circulating virus that is resistant to their own bNAbs(Wu et al., 2012), likely owing to the kinetics of HIV-1 diversification and the B-cell response. By the time the B-cell response can potently target HIV-1, the virus

has already generated sufficient diversity to produce escape variants, giving rise to a chase in which the virus is always a step ahead(Liao et al., 2013; Wei et al., 2003). Because of the immense viral diversity and previous failed attempts to use antibodies as therapeutic agents(Poignard et al., 1999; Trkola et al., 2005), the therapeutic value of next-generation bNAbs was not immediately considered following their discovery.

3.2 First demonstration of bNAb therapy

While the monoclonal antibodies ibalizumab and PRO140, which target the human host receptors CD4 and CCR5, respectively, have been shown to reduce viral loads in patients and may prove to be useful therapeutics, these antibodies are not directly antiviral(Jacobson et al., 2009; 2010a; 2008; 2010b; Kuritzkes et al., 2004). Our experiments demonstrated the efficacy of viral-binding bNAbs as therapy *in vivo* for the first time. Our data suggest that rapid escape can occur to both single and double bNAbs, but combinations of three or more bNAbs can fully suppress viremia. The most striking aspect of these experiments was the restricted escape routes observed in the virus for single or double bNAb-therapy. While previous analyses of antibody-mediated escape found a wide-range of viral escape options, often involving addition and removal of N-linked glycosylation sites across many residues in gp120(Frost et al., 2005; Wei et al., 2003), I found that escapes to the bNAbs tested were limited to just 1-3 sites shared across multiple mice. For 10-1074, the restriction was particularly

impressive, with only a single amino acid substitution at a single residue dominating the viral quasi-species. An important caveat is that humanized mice in our experiments were infected with monoclonal HIV-1_{YU2}, a clade B primary isolate, and viral escape routes with other virus strains should be tested to be more comprehensive.

Our data suggest that the *in vivo* success of the next-generation bNAbs we tested compared to the failures of previous antibodies tested is attributable to the exceptional potencies and restricted escapes. The geometric mean inhibitory concentration to block 50% infection (IC_{50}) as tested by in vitro TZM.bl assays of the four efficacious bNAbs is 0.07 μg/ml, whereas it is ~1.5 logs lower at 2.63 μg/ml for 2G12, 2F5 and b12—the 3 antibodies tested in a humanized mouse system previously. The lone “next-generation” antibody we tested that did not have any therapeutic effect *in vivo*, 3BC176, has an IC_{50} resembling the ineffective antibodies at 1.87 μg/ml. Additionally, 10-1074, the antibody that produced the largest transient drop in viremia of 1.5 logs had the most restricted *in vivo* escapes detected.

Despite the transient drops in viral load and emergence of limited escape mutations, there was no evidence of a fitness cost imposed by these mutations. The viral loads quickly returned to pre-therapy levels, and the virus maintained the mutations even when therapy was stopped. Additionally, the escape mutations to the various antibodies did not appear incompatible in any way when they were all present in the same virus. Rather, the escape mutations we saw in single-bNAb treated mice were the same as those seen in mice that escaped

from a combination of two efficacious bNAbs. Additionally, a virus engineered to contain escapes to all four of the efficacious bNAbs we tested was shown to be highly infectious in humanized mice. Together, this shows that escape to bNAbs is additive. Furthermore, it is possible that pre-existing viral clones within a patient's quasi-species contain escapes to all bNAbs in a cocktail, in which case the cocktail will be ineffective. This issue can likely be overcome by choosing bNAb cocktails that have rare, restricted escapes unlikely to be present within the same virus simultaneously by pre-screening patients and databases of viruses within the population. In all, these studies demonstrated sufficiently broad and potent bNAbs could lead to sustained viral suppression *in vivo* for the first time.

3.3 Antibodies as PEP

Because antibodies have the potential for Fc-mediated cell killing while ART can only block new rounds of replication, I employed a post-exposure prophylaxis model to test the role of cell killing. By comparing the PEP efficacy of antibodies versus ART, I can infer therapeutic roles that extend beyond blocking new rounds of replication. I found that cell-free virus injected intraperitoneally into non-humanized NRG mice is undetectable in plasma by 48 hours. Thus plasma viremia detectable after 48 hours in humanized mice must come from productively infected cells. If therapy is initiated 48-96 hours after exposure, and assuming therapy completely blocks viral spread, it can be inferred that viral rebound occurring after therapy cessation comes from the earliest infected cells.

Conversely, if there is no viral rebound upon therapy cessation, then either the early-infected cells were cleared, or they remained in a silent state without virus production. While this experimental setup requires many assumptions to indirectly conclude that antibodies kill infected cells, there is no alternative model to prove this *in vivo*. This is complicated by the fact that productively infected cells die very quickly, so any role for antibody-mediated killing is likely to be supplemental.

Nevertheless, my experiments show that bNAbs were significantly more effective than ART at preventing viral rebound in the PEP model. However, the enhanced efficacy of bNAbs is abrogated when their ability to bind Fc receptors is removed. Identifying which Fc-expressing cells are most important for Fc-mediated effects of bNAbs remains an open question. It is particularly difficult to address in the humanized mouse model because of the incomplete human reconstitution. While bNAbs were administered by subcutaneous injection and ART was administered orally in the food, the difference in efficacy between antibodies and drugs is unlikely to be solely due to pharmacokinetics. When orally administered ART was initiated at 24 hours following viral exposure, no mice showed viremia by the terminal point, in agreement with results in NHPs(Tsai et al., 1995). In NHPs, low-potency neutralizing IgG was tested for PEP and shown to be effective only when initiated within 6 hours(Nishimura et al., 2003). The extended window of opportunity for next-generation bNAbs needs to be tested in the NHP model, but the results suggest a role for enhanced killing or viral containment with bNAbs. If bNAbs as PEP show similar beneficial effects

in NHPs, there is a strong case to include them in early treatment regimens. Additionally, they can be added to ART as a superior PEP for occupational exposures.

3.4 Model for Latency Purging Regimens

The possibility of antibody-mediated killing stimulated me to test the effects of bNAbs in clearing latent cells. However, there is no established small animal model to test this. From our experiments testing bNAbs as therapy, I noticed the majority of mice that were suppressed showed viral rebound when antibody levels dropped beneath the therapeutic threshold. There were no signature escape mutations contained within the rebounding virus, and it remained sensitive to antibody neutralization, implying the persistence of a silent pool of infected cells capable of producing viral rebound. By purifying resting $CD4^+$ T cells from suppressed mice and detecting HIV p24+ in the supernatant following culture in T-cell stimulatory conditions, I was able to confirm the existence of replication-competent virus within this cell subset. Although I have not proven that this cell subset is responsible for the rebounding virus observed in humanized mice, I demonstrated that it exists, in agreement with findings from bone marrow-liver-thymus (BLT) humanized mice(Denton et al., 2012; Marsden et al., 2012). Given that resting memory $CD4^+$ T cells with replication-competent provirus are regarded as the biggest barriers to reservoir eradication, the model gave me the opportunity to study viral purging strategies *in vivo*.

I carefully designed our viral purging experiments to work within the constraints of the humanized mouse model. Because the duration of the human graft is variable and limiting, I planned the entire course of treatment to fit within 4 months, a time frame well within the empirically determined graft duration of the model. I suppressed viremia in mice, administered the experimental therapies, then stopped therapy and assayed for viral rebound in the plasma. I used viral rebound since it is considered the gold standard for evaluating viral eradication strategies. Additionally, it has an easy to interpret binary outcome, represents the most important clinical parameter, and avoids the problems associated with reservoir size measurements.

3.4.1 Limitations of the model

Despite the unique experimental opportunities provided by the humanized mouse model, using it for viral purging strategies comes with many caveats. The main caveats related to the experiments discussed are: (1) incomplete reconstitution of human cells, (2) lack of proper lymph node architecture (3) limited duration of the human graft, (4) significantly reduced absolute cell numbers, and (5) non-physiological environment of mixed human and mouse cells.

The incomplete human reconstitution manifests as a very narrow range of human immune cells populating each mouse. Although, mice that have clear populations of human $CD4^+$ T cells are selectively chosen for the experiments, it has never been verified that these $CD4^+$ T cells are capable of differentiating into

the full range of $CD4^+$ T cell subtypes. Additionally, there are very few innate immune human cells in these mice, such as macrophages, and natural killer cells(Brehm et al., 2010). Considering some of these innate cells have been implicated as being susceptible to HIV infection, and may contribute to the HIV reservoir in some cases, humanized mice have a significantly reduced pool of cells capable of forming the reservoir. Therefore it must be tested whether targeting strategies that eliminate reservoirs in humanized mice translate to the more diverse, complex reservoirs in humans.

The humanized mice used in these experiments also lack proper lymph node architecture, as well as lymphoid tissues that are relevant for HIV infection, such as gut associated lymphoid tissue (GALT) and mucosa associated lymhphoid tissue (MALT) (Li et al., 2005; Moir et al., 2011). Given the high levels of viral replication and relatively high frequencies of HIV-infected cells in these tissues, the absence of these tissues from hu-mice may make the bar to purging virus far lower than in animal models that have these features.

The limited duration of the human graft poses one of the greatest caveats to the model. Following infection, plasma viremia is stable for ~3-6 months in humanized mice, with gradual depletion of $CD4^+$ T cells(Baenziger et al., 2006). Eventually, the human graft's proliferative capacity cannot keep pace with cell loss, and both human immune cells and plasma virus become undetectable—limiting the study duration of HIV therapeutics. In clinical trials of latency purging strategies, patients who receive the experimental intervention have usually been chronically infected with HIV for many years then suppressed on ART drugs for 6

months or longer. The purpose of this minimal suppression time is usually attributed to the presence of labile, unintegrated forms of HIV that are able to persist in the presence of ART for up to 6 months(Blankson et al., 2000). However, these more labile forms of HIV are not believed to represent the stable reservoir and so they are excluded from tests of purging efficacy. It is not possible to use the same stringent time constraints in tests with humanized mice. Rather, mice are suppressed following just weeks of infection—a time frame considered acute for humans—and the experimental intervention is initiated after just weeks of suppression. As a result, it is unknown if clearance of latent reservoirs in mice will translate to clearance of human latent reservoirs.

Additionally, many latency purging pharmacologic regimens tested in clinical trials use multiple weekly drug cycles extending over many months(Archin et al., 2014; MD et al., 2014). It is believed that a single short-course administration of latency reversal agents is not sufficient to reactivate enough of the silent reservoir to make a difference. However, it is not possible to test multiple cycles of treatment in mice because the total experimental window is too short.

The total number of human $CD4^+$ T cells within each humanized mouse is orders of magnitude less than in a human. While I demonstrated that the frequency of latently infected resting $CD4^+$ T cells is comparable to that seen in humans, the total number of latently infected cells is likely orders of magnitude less. Given the total number of ~1 to 10 million human $CD4^+$ T cells in each mouse—and on the order of 10^4 p24+ cells during active infection—there are

likely only 1-10 latently infected resting $CD4^+$ T cells within each mouse. This is in contrast to the 10^4-10^7 estimated latently infected resting $CD4^+$ T cells that exist in an infected human(Chun et al., 1997a; Zhang et al., 1999a). While the precise number of latently infected cells that can remain without causing virological relapse is unknown, it is generally appreciated that even very few numbers of latently infected cells can lead to virological relapse(Henrich et al., 2014). As a result, the very few numbers of latently infected cells within a humanized mouse make the possibility of viral eradication significantly easier.

The environment of mixed mouse and human cells that are free to interact within the humanized mouse model is another potential shortcoming for studying latency in the humanized mouse model. The main concern is that mouse cells provide continual allogeneic stimulation to the human immune cells, which precludes a true resting state. Considering that HIV latency is most stable within resting $CD4^+$ T cells that do not express activation markers such as CD25, CD69, or HLA-DR, the mixing of mouse and human cells may make the environment significantly different from that which latent cells in a human are exposed to. However, this concern remains speculative and there has been no clear evidence suggesting that human cells cannot exist within a resting state within an NRG mouse. To the contrary, I was able to identify resting $CD4^+$ T cells that were $CD25^-CD69^-$HLA-DR^-. However, additional comparisons between silent, persistently infected cells from humanized mice and latently infected human $CD4^+$ T cells, such as integration site analyses and gene expression analyses will have to be done to address this issue directly.

3.5 Importance of combinations for latency reversal

Although combination antibody therapy appeared to work similarly to ART in that triple combinations were required, the unique potential for Fc-mediated effects that can directly kill infected cells led me to test the “shock and kill” approach. I tested three candidate inducers of viral transcription (aka LRAs) based on their abilities to reverse latency *in vitro*, target different mechanisms of transcriptional silencing, and toxicities. I found that combining a bNAb cocktail that could suppress viremia with a single inducer had no impact on the frequency of viral rebound in humanized mice. However, a combination of all three inducers significantly reduced the frequency of viral rebound. This is the first demonstration of a therapy regimen other than irradiation and stem cell transplant with HIV-resistant donor cells that reduced viral rebound *in vivo*.

This study demonstrates that current LRAs are unlikely to have a significant impact on the latent reservoir when administered as single agents. This is supported by studies investigating vorinostat and panobinostat as single agents(Archin et al., 2014; Elliott et al., 2014; MD et al., 2014). It suggests that future studies should focus on optimizing the best inducer combinations, rather than relying on single agents. Of note, I did not optimize my inducer regimen, and ~40% of treated mice still showed viral rebound, underscoring room for improvement. However, I attribute the improved success of the LRA combination to synergy in targeting different mechanisms of reactivation. This is likely related

to the multiple mechanisms regulating HIV transcriptional silencing. No single agent is likely to target all these mechanisms, so there is probably a population of unperturbed latent cells capable of producing rebound viremia when single agents are used. This is supported by *in vitro* findings that show a very small fraction of proviruses are activated by single LRAs(Cillo et al., 2014). Additionally, single agents may induce viral transcription, but there is no evidence that single agents robustly reverse latency to induce viral protein expression, which is likely required for immune-mediated killing.

3.6 Testing for latency reversal

Rather than testing for cell-associated viral RNA, the more relevant test is for viral protein expression, including cell surface-HIV Env, in reactivated cells. Not only do broad, potent bNAbs exhibit clinical promise, but they can be used in the laboratory as agents to identify infected cells expressing surface Env. This has the potential to offer a more relevant assay for detecting cells that were reactivated sufficiently for bNAb-mediated killing.

Although I tested for changes in cell-associated viral RNA during the inducers treatment, I was unable to detect any in both the single inducers treated mice and combination-inducers treated mice. While this differs from the ~3-5 fold increases observed in vorinostat and panobinostat trials(Archin et al., 2012; Elliott et al., 2014; MD et al., 2014), it could simply be due to a lower sensitivity in this model due to fewer cells assayed. But more importantly, the lack of cell-

associated RNA detection did not predict lack of viral rebound, which suggests an updated readout should be used for clinical trials that test latency reversal. In total, my experiments make clear that current LRA strategies are likely limited by incomplete reactivation and major effort should go toward improving this, as well as assays to detect reactivated cells that can be killed.

Given the challenges in improving latency reversal and infected-cell killing, it is critical to have an *in vivo* model amenable to testing many strategies. Prior to this work, only *in vitro* models consisting of transformed cell lines or PBMCs isolated from ART-suppressed patients existed for testing “shock and kill” strategies pre-clinically. While these models allow high-throughput screening, they lose physiologic relevance. Prior to this work, LRAs could not even be tested in NHPs because there were no fully-suppressive ART regimens available. This issue has now been resolved, but there are still significant advantages of using humanized mice.

For one, humanized mice involve HIV infection of human cells. In contrast, restriction factors limit the tropism of HIV, so NHPs have to be infected with either simian immunodeficiency virus (SIV) or an SIV/HIV hybrid virus termed SHIV. It is unclear how SIV or SHIV viruses differ from HIV for latency and eradication strategies and it is unclear how LRAs will interact with simian cells since LRAs are generally discovered based on activity in human cells. Additionally, humanized mice are less costly and more high-throughput than NHPs.

However, humanized mice also have some disadvantages. For one, they are immune-compromised so it is difficult to study the role of the immune system in viral clearance and eradication. NHPs offer the advantage of a fully competent immune system. Also, studies of latency in humanized mice are limited by human graft duration and composition. Most studies of candidate LRAs in humans involve patients who are suppressed on ART for >6 months to avoid effects from labile forms of unintegrated HIV. This is not possible in humanized mice unless an alternative approach is adopted. To further the model for latency testing, it will be important to characterize the forms of integrated and unintegrated forms of HIV in humanized mice and compare them to ART-suppressed patients. The limited graft duration also limits the duration of reactivation treatment that can be tested, making it impossible to optimize dosing schedules.

Nevertheless, I established an *in vivo* system to test LRAs in conjunction with both ART and antibodies. I was also able to test Fc-mediated effects by manipulating the Fc region of the antibody. However, my studies come with the caveat that innate human immune cells expressing Fc receptors, such as monocytes and Natural Killer cells, are rare in my model so it is impossible to assess the full extent of Fc-FcR interactions. I believe that improved humanized mouse systems that partially restore innate immune function will further our understanding of Fc-FcR mediated effects on infected cells *in vivo*(Rongvaux et al., 2014).

However, the duration of the human graft is reported to be much shorter than 4 months in these improved humanized mouse systems, so they seem more

amenable to studying short-term cell-killing. Alternatively, an adapted model for studying LRAs and antibodies could be used in these mice by adoptively transferring resting memory $CD4^+$ T cells known to harbor integrated provirus, either from patients or other mice. This eliminates the first two months where the mouse is infected then suppressed, allowing the experimental regimen to be administered and viral rebound to be monitored within the duration of the human graft. Additionally, this approach could be adopted in our current humanized NRG mouse model to allow time for multiple rounds of LRA administration. In my recent studies, multiple rounds were not permitted within the experimental time frame.

3.7 Translation to humans

Ultimately though, the concepts and most promising treatment regimens need to be tested in humans. Traditionally, the pipeline to reach human clinical trials involves testing in the NHP model. During the course of this work, passive antibody therapy was shown to be effective at sustainably suppressing viral loads in NHPs(Barouch et al., 2013; Shingai et al., 2013b).

While rapid escape to single bNAbs may occur, it remains unclear what combinations of bNAbs will be required to suppress viremia in an immune competent individual that can mount both B-cell and T-cell responses. The viral diversity within patients, as well as the immune responses mounted by patients are both likely to be important variables. Evidence from NHPs suggest that a

single bNAb is sufficient in some cases, and work in humanized mice suggests this is because of endogenously produced V3-loop antibodies that complement the passively administered bNAb to prevent escape(Klein et al., 2014).

Alternatively, we showed that reducing viral loads in humanized mice with ART prior to bNAb administration—presumably reducing viral diversity as well—enabled a single bNAb to sustainably suppress viremia without escape(Horwitz et al., 2013). In light of our results in mice, and the extension to NHPs, bNAb therapy has progressed to clinical trials (clinicaltrials.gov NCT02018510, NCT02165267, and NCT02256631). While these first studies are testing safety, pharmacokinetics, and therapeutic efficacy of monocloncal antibodies in humans, I expect my data demonstrating the ability of bNAbs to interfere with reservoir establishment and maintenance in humanized mice will inspire additional human studies examining the impact on the latent reservoir.

Human studies of LRAs combined with antibodies are also likely to advance to clinical trials in light of my work. However, the “shock and kill” approach requires many more advances until it carries the same promise that bNAb-therapy possesses. For one, LRA combinations and a dosing schedule should be optimized. Both of these remain major questions in the field. LRAs have predominantly focused on HDAC inhibitors, and it is likely that other candidate LRAs will be needed to reverse latency more robustly.

Regardless of the findings from the initial clinical trials, it is important to note that there are many potential improvements for bNAbs. One, half-life can be significantly increased with select mutations in the Fc region that impact binding

to Fc neonatal receptor (FcRn) and endosomal recycling(Ko et al., 2014). Two, bNAbs can be engineered to have different Fc-mediated properties depending on the relative affinities for various Fc receptors. And three, bNAbs can be rationally designed to enhance breadth and/or potency(Diskin et al., 2011). Ultimately, the studies conducted and reported here offer promise for the future of bNAbs in treating HIV-1, but many important advances are required to achieve the very difficult goal of viral eradication.

CHAPTER 4:

METHODS

4.1 Humanized Mice

4.1.1 Mice.

NOD Rag1$^{-/-}$Il2rg^{NULL} (NOD.Cg-*Rag1^{tm1Mom} Il2rg^{tm1Wjl}*/SzJ, NRG) mice were purchased from The Jackson Laboratory. All mice were and bred and maintained at the Comparative Bioscience Center of The Rockefeller University according to guidelines established by the Institutional Animal Committee. All experiments were performed with authorization from the Institutional Review Board and the IACUC at The Rockefeller University.

4.1.2 Hematopoietic Stem Cell Purifications.

Human fetal livers (gestational age 16-22 weeks) were obtained from Advanced Bioscience Resources (ABR). Fetal livers were homogenized and incubated in Hank's Balanced Salt Solution (HBSS) media with 0.1% collagenase IV (Sigma-Aldrich), 40 mM HEPES, 2 mM $CaCl_2$ and 2 U ml^{-1} DNAase I (Roche) for 30 minutes at 37° C. Human CD34+ HSCs were isolated from digested liver using CD34^{+} HSC isolation kit (Stem Cell Technologies) according to manufacturere's protocol. Neonatal NRG mice (1-5 days old) were sublethally irradiated with 100-400 cGy and injected intrahepatically with 2×10^5 human CD34+ HSCs 6 hours after irradiation.

4.1.3 Humanized Mouse screening.

Eight or more weeks after HSC injection, mice were screened for the presence of human lymphocytes in peripheral blood by flow cytometry. 200 µl whole blood was collected by facial vein bleed and peripheral blood mononuclear cells (PBMCs) were isolated by density gradient centrifugation using Ficoll-Paque Plus (GE Healthcare Life Sciences). PBMCs were stained with antibodies to mouse CD45-PECy7, human CD45-Pacific Orange, human CD3-Pacific Blue, human CD19-APC, human CD4-PE, human CD8-FITC, and human CD16-Alexa700 for 25 min at 4°C. Cells were washed and fixed using Cytofix/Cytoperm (BD Biosciences). Flow cytometry analysis was performed with a LSRFortessa (BD) and FlowJo software (Tree Star). For each mouse, the percentage of human lymphocytes [(100 x human $CD45^+$) / (human $CD45^+$ + mouse $CD45^+$)], termed $huCD45^+$ %, and the percentage of human $CD4^+$ T cells (100 x human $CD45^+CD3^+CD4^+$ / human $CD45^+$), termed $huCD4^+$ %, was calculated. Mice with at least 10% $huCD45^+$ and 10% $huCD4^+$ were selected for post-exposure prophylaxis experiments, and infected with two doses of HIV-1_{YU2} (150 ng p24) by i.p. injections, 24 hours apart. Pre-treatment viremia was measured at 72-96 hours following the first HIV-1_{YU2} injection, and treatment was initiated 4 days following the first injection. For experiments assessing the effects of bNAbs and inducers on established infections, mice with measurable human $CD4^+$ cells by FACS were injected with two doses of HIV-1_{YU2} (150 ng p24), and pre-treatment viremia was measured 14-18 days after the first injection. Mice with plasma viral loads >3000 RNA copies/ml were selected to receive antibody therapy. After five

subcutaneous antibody injections (see below), post-treatment viremias were measured. Only mice with completely suppressed plasma viremias were selected for further analysis and to receive viral inducers.

4.2 HIV-1_{YU2} virus production

HIV-1_{YU2} used for mouse infections was produced in 293T cells. 25 µg plasmid was mixed into 1.3 ml Opti-MEM (Life Technologies) and 75 µl Xtreme Gene 9 (Roche) was added to form DNA mixture. DNA mixture was then added dropwise to 293T cells in reduced serum media (RPMI plus 3% Fetal calf serum). Media was replaced 6 hours later with reduced serum media. Viral supernatant was harvested at 24 hours and 48 hours after transfection. Supernatant was passed through 0.22 µm filter and viral concentration was measured by p24 AlphaLISA (PerkinElmer) according to manufacturer's instructions.

4.3 Generation of HIV-1_{YU2} envelope mutants

Single, double and triple mutations were introduced into wild-type HIV-1YU2 envelope by site-directed mutagenesis using the QuikChange site-directed mutagenesis kit (Agilent Technologies) according to the manufacturer's specifications.

4.4 Plasma viral load measurements

300-500 µl of whole blood was collected from mice at each time point by facial vein bleed. Whole blood was spun at 300*g* for 10 minutes to separate plasma from the cellular fraction. Total RNA was extracted from 100 µl plasma using QIAmp MinElute Virus Spin Kit (Qiagen) in combination with RNase-free DNase (Qiagen), eluted in a 50 µl volume. HIV-1 RNA was quantified by qRT-PCR. The reaction mixture was prepared using TaqMan RNA-to-Ct 1-Step kit (Applied Biosystems), with 20 µl of eluted RNA, and a sequence specific probe targeting a conserved region of the HIV-1 *pol* gene (/HEX/5'-CCCACCAACARGCRGCCTTAACTG-3'/ZenDQ, HXB2 nt 4603 to 4626) (Integrated DNA Technologies). Forward and reverse primer sequences were 5'-TAATGGCAGCAATTTCACCA-3' (HXB2 nt 4577-4596) and 5'-GAATGCCAAATTCCTGCTTGA-3' (HXB2 nt 4633 to 4653), respectively. Reaction mixtures included 450 nM forward and reverse primers and 125 nM probe. Cycle threshold (Ct) values were calibrated using standard samples with known amounts of absolute viral RNA copies. The quantitation limit was determined to be 800 copies/ml.

4.5 Cell-associated HIV-1 RNA

The cellular fraction of whole blood was resuspended in 400 µl PBS and PBMCs were isolated by density gradient centrifugation as described above.

Lymphocytes were split into two samples, one for cell-associated HIV-1 RNA measurements, and one for cell-associated HIV-1 DNA measurements. Cell-associated RNA was extracted and quantified by the same procedures as described above for plasma viral RNA. The lower limit of detection was determined to be 10 copies viral RNA per qRT-PCR reaction. Cell-associated HIV-1 RNA is reported as the ratio of HIV-1 RNA copies per sample to CCR5 genomic DNA copies per equivalent sample measured in DNA extract. For terminal point measurements, spleen tissue was isolated, homogenized, and filtered through 40 μm mesh. Splenocytes were used to isolate HIV-1 RNA as described above.

4.6 Cell-associated HIV-1 DNA

PBMCs were isolated from whole blood as described above. Splenocytes were isolated from spleen as described above. Total DNA was extracted using QIAmp DNA Blood Mini Kit (Qiagen) and eluted in 80 μl volume. Purified DNA was quantified for HIV-1 DNA by qPCR using the primers and probe for HIV-1 RNA quantification mentioned above. Genomic human CCR5 DNA was quantified with primers 5'-GTTGGACCAAGCTATGCAGGT-3' (forward) and 5'-AGAAGCGTTTGGCAATGTGC-3' (reverse), and the sequence-specific probe /HEX/5'-TTGGGATGACGCACTGCTGCATCAACCCCA-3'/ZenDQ. All qPCR reactions contained 25 μl AmpliTaq Gold PCR master mix (Applied Biosystems), in 50 μl reaction volume. Reaction mixtures were 150 nM forward and reverse

primers with 41.5 nM CCR5 probe. HIV-1 DNA is reported as copies per sample to CCR5 genomic copies per equivalent sample.

4.7 Gp120 Sequencing

4.7.1 Gp120 cloning

All PCR amplifications were performed in ThermoGrid 96-well plates (Denville Scientific). cDNA was synthesized from viral RNA using SuperScript III reverse transcriptase (Invitrogen Life Technologies). cDNA was amplified with either Expand High Fidelity PCR System (Roche) or Clontech Advantage 2 PCR System (BD). Primers for the first round of PCR were 5'-GGCTTAGGCATCTCCTATGGCAGGAAGAA-3' and 5'-GGTGTGTAGTTCTGCCAATCAGGGAAGWAGCCTTGTG-3'. Primers for the second round of PCR were 5'-TAGAAAGAGCAGAAGACAGTGGCAATGA-3' and 5'-TCATCAATGGTGGTGATGATGATGTTTTTCTCTCTGCACCACTCTTCT-3'.

Cycling parameters for first round PCR were 94° C for 2 min followed by 40 cycles of 94° C for 30 s, annealing temperature of 55–65° C for 45 s, 68° C for 4 min, and a final extension at 68° C for 10 min, where the annealing temperature was 65° C for the first 3 cycles, 60° C for the next 11 cycles, and 55° C for the final 26 cycles. 3 ml of product from the first round was used as the template for the second round of PCR. Cycling conditions for the second round PCR were 94° C for 2 min followed by 40 cycles of 94° C for 30 s, annealing

temperature of 53–55° C for 45 s, 68° C for 2 min and 30 s, and a final extension at 68° C for 10 min, where annealing temperature was 53° C for the first 9 cycles and 55° C for the next 31 cycles. After the second-round PCR amplification, 0.5 µl Taq polymerase was added to each 50 µl reaction and an additional 72° C extension for 15 min was performed to add 3' A overhangs for use in cloning. Gel-purified PCR amplicons were ligated into pCR4-TOPO (Invitrogen) and transformed into One Shot TOP10 cells. Individual colonies were sequenced using M13F and M13R primers.

4.7.2 Sequence alignments and mutation analysis

Forward and reverse sequence reads from individual samples were assembled using Geneious Pro software version 5.5.6 (Biomatters Ltd) and aligned to gp120 $_{YU2}$ (accession number M93258). *Env* sequences containing frameshift mutations or large deletions were excluded from further analysis. All sequences were analyzed for mutations relative to gp120 $_{YU2}$ using the Los Alamos Highlighter tool (http://www.hiv.lanl.gov/content/sequence/HIGHLIGHT/HIGHLIGHT_XYPLOT/highlighter.html), and mutations were numbered using HXBc2 numbering as determined by the Los Alamos Sequence Locator tool (http://www.hiv.lanl.gov/content/sequence/LOCATE/locate.html)

4.8 Terminal Graft

The presence of human lymphocytes at the terminal point was quantified from the spleen and PBMCs by flow cytometry. Isolation of PBMCs and splenocytes were as described above. Staining procedures were the same as described for humanized mice screening.

4.9 Measuring Antibody Levels

Plasma levels of passively administered antibodies were quantified by two independent methods. The first method was gp120 specific ELISA. Costar 96-Well EIA/RIA Stripwell plates were coated overnight with $gp120^{YU2}$ protein at 50 µg/ml, in 50 µl volume per well. Plates were washed 3× with distilled water plus 0.05% Tween and blocked for 2 h with PBS containing 0.1% Tween-20, 2% Bovine Serum Albumin and 1 mM EDTA. After washing the plate, mouse plasma was applied in 1:3 serial dilutions with a 1:20 starting dilution. 3BNC117 and 10-1074 of known concentration were used as standard antibodies for each plate to quantify gp120-specific IgGs. Starting concentration of 3BNC117 and 10-1074 standards were 12 µg/ml, and diluted in 1:3 serial dilutions identical to the serum samples. The plate was then incubated for 1 h at 37° C, followed by washing the plate and 1 h incubation with peroxidase-conjugated goat anti-human IgG (Jackson ImmunoResearch), 1:1000 dilution, 50 µl per well. Plates were washed and developed using ABTS single solution (Invitrogen). Optical density was

measured at 405 nm and IgG concentration determined by correlation to the standard curve of the reference antibodies. The detection limit was 0.05 μg/ml. Because PG16 does not bind gp120, and endogenously produced gp120-reactive antibodies could confound the ELISA measurement, plasma antibody levels were also quantified by TZM-bl neutralization using the Tier 2 envelopes 3301.v1.c24 and YU2. Because we have never observed Tier 2 neutralizing activity endogenously produced from a humanized mouse, this measurement is more stringent for detecting the passively administered antibodies. Mouse plasma samples were serially diluted 1:5 down to a final dilution of 1:~4×10^6, starting at 1:50 dilution. Each dilution was tested on TZM.bl assay for neutralization of the pseudoviruses mentioned above to give an IC_{50} neutralizing titer. A mixture with known amounts of 3BNC117, 10-1074, and PG16 was used as standard. The IC_{50} neutralizing titer of the serum samples was compared to the IC_{50} concentrations of the antibody standard mix to determine antibody concentrations from the serum samples.

4.10 Day of viral rebound and antibody level at rebound

Plasma viremias immediately preceding and following viral rebound were plotted on a semi-log-y-axis versus days post initial antibody injection (x-axis) for each individual mouse. The linear portion of viremia was fit to a line by least-squares linear regression. The day that viremia crossed the 800 copies/ml quantitation limit, termed rebound day, was calculated from the viremia fit. The antibody

concentrations (as determined by TZM-bl neutralization) spanning before and after viral rebound were plotted on a semi-log-y-axis versus days post initial antibody injection. The linear portion of antibody concentrations was fit to a line by least-squares linear regression, and the antibody concentration on the rebound day was calculated from the fit.

4.11 Anti-retroviral therapy

Individual tablets of tenofovir disproxil-fumarate (TDF; Gilead Sciences), emtricitabine (FTC; Gilead Sciences), and raltegravir (RAL; Merck) were crushed into fine powder and manufactured with TestDiet 5B1Q feed (Modified LabDiet 5058 with 0.12% amoxicillin) into ½" irradiated pellets. Final concentrations of ART drugs in the food were 720 mg/kg TFV, 520 mg/kg FTC, and 4800 mg/kg RAL. Doses were chosen based on suppression of viremia in humanized mice as previously published(Denton et al., 2012; Nischang et al., 2012), and by pharmacokinetic analysis of these drugs in humanized mice (unpublished, Speck Laboratory). To test potential toxicity, or reduced preference for drug-supplemented food, mice were weighed daily on normal diet, then switched to ART feed and weighed daily. There were no visible signs of toxicity and mice maintained their weights. On average, each mouse consumed 4.7 g of food per day, consistent with reports for typical mouse consumption.

4.12 Antibody therapy

Plasmids encoding 10-1074 or PG16 heavy- and light- chain Ig genes were transfected into HEK 293E cells. Antibodies were isolated from tissue-culture supernatant using Protein G Sepharose 4 Fast-Flow (GE Healthcare). Antibodies were then buffer-exchanged into PBS and sterile-filtered using Ultrafree-CL centrifugal filters (0.22μm; Millipore). Endotoxin was removed from antibody preparations using Triton X-114 (Sigma-Aldrich). Antibody suspensions were mixed with 10% Triton-X114 in a 15 ml falcon tube, vortexed, placed on ice for 15 min, vortexed again, placed in 42° C water bath for 15 min, then centrifuged at 3000 rpm for 5 minutes without brake. The top phase containing the endotoxin-removed antibody was kept and concentrated to 10 mg/ml. Sterile, endotoxin-free 3BNC117 (20 mg/ml) was obtained from CellDex Therapeutics. All antibodies were injected subcutaneously as described.

4.13 Inducers

Vorinostat (Selleckchem) was suspended in sterile water or sterile water plus 0.5% methylcellulose, 0.1% Tween (v/v) and administered by oral gavage at doses of 60 mg/kg. For each mouse, three total doses were administered, spaced 48 hours apart. 100 μg doses of αCTLA4 were injected intraperitoneally (i.p.). Three total doses were administered, spaced 48 hours apart. I-BET151

was obtained from GlaxoSmithKline and dissolved in 10% beta-cyclodextrin, 5% DMSO in 0.9% saline and injected daily for 14 days at doses of 30 mg/kg.

4.14 Viral outgrowth assay

Mice were sacrificed and spleen and lymph nodes were homogenized into single cell suspension through 40 μm filter. To isolate resting human $CD4^+$ T cells for culture, a three-step process was used. First, mouse cells were depleted using the Mouse Cell Depletion Kit (Miltenyi) according to manufacturer's instructions. Second, human $CD4^+$ T cells were enriched by negative selection using human $CD4^+$ T cell isolation kit (Miltenyi). Third, activated $CD4^+$ T cells were depleted using CD69, HLA-DR, and CD25 microbeads, leaving untouched, human resting $CD4^+$ T cells of >90% purity. In total, 1.6×10^7 cells were isolated from 16 mice. Based on treatment, suppression status, and fetal liver donor used for human reconstitution, the samples were combined into 10 independent groups for culturing. The isolated resting $CD4^+$ T cells were plated with MOLT4/CCR5 target cells as previously described(Laird et al., 2013) and kept in culture for 28 days. P24 from culture supernatant was measured by ELISA at days 14, 21, and 28.

4.15 p24 stain and viral cell quantification

To determine the number of productively infected cells, mice were sacrificed and the spleen was homogenized into a single cell suspension. Human $CD45^+$ cells

were positively selected by staining with human CD45-PE (20 µl per spleen), then incubating with anti-PE microbeads, and binding to a magnetic column. Immediately following collection of cells from the magnetic column, cells were counted using AccuCheck Counting Beads (Invitrogen). Cells were stained with anti-human CD45-PE, anti-mouse CD45-A780, anti-human CD3-Pacific Blue, anti-human CD4-APC, anti-human CD8-A700, anti-human CD69-PE/Cy7, anti-human HLA-DR-BV605, followed by fixation/permeabilization, and stain with anti-p24-FITC (1:100). Flow cytometry analysis was performed with a LSRFortessa (BD) and FlowJo software (Tree Star).

CHAPTER 5:

REFERENCES

Archin, N.M., Bateson, R., Tripathy, M.K., Crooks, A.M., Yang, K.H., Dahl, N.P., Kearney, M.F., Anderson, E.M., Coffin, J.M., Strain, M.C., et al. (2014). HIV-1 Expression within Resting CD4 T-Cells Following Multiple Doses of Vorinostat. J. Infect. Dis. *210*, 728–735.

Archin, N.M., Liberty, A.L., Kashuba, A.D., Choudhary, S.K., Kuruc, J.D., Crooks, A.M., Parker, D.C., Anderson, E.M., Kearney, M.F., Strain, M.C., et al. (2012). Administration of vorinostat disrupts HIV-1 latency in patients on antiretroviral therapy. Nature *487*, 482–485.

Archin, N.M., Keedy, K.S., Espeseth, A., Dang, H., Hazuda, D.J., and Margolis, D.M. (2009). Expression of latent human immunodeficiency type 1 is induced by novel and selective histone deacetylase inhibitors. Aids *23*, 1799–1806.

Baenziger, S., Tussiwand, R., Schlaepfer, E., Mazzucchelli, L., Heikenwalder, M., Kurrer, M.O., Behnke, S., Frey, J., Oxenius, A., Joller, H., et al. (2006). Disseminated and sustained HIV infection in CD34+ cord blood cell-transplanted Rag2-/-gamma c-/- mice. Proc. Natl. Acad. Sci. U.S.a. *103*, 15951–15956.

Barouch, D.H., Whitney, J.B., Moldt, B., Klein, F., Oliveira, T.Y., Liu, J., Stephenson, K.E., Chang, H.-W., Shekhar, K., Gupta, S., et al. (2013). Therapeutic efficacy of potent neutralizing HIV-1-specific monoclonal antibodies in SHIV-infected rhesus monkeys. Nature *503*, 224–228.

Blankson, J.N., Finzi, D., Pierson, T.C., Sabundayo, B.P., Chadwick, K., Margolick, J.B., Quinn, T.C., and Siliciano, R.F. (2000). Biphasic decay of latently infected CD4+ T cells in acute human immunodeficiency virus type 1 infection. J. Infect. Dis. *182*, 1636–1642.

Boehm, D., Calvanese, V., Dar, R.D., Xing, S., Schroeder, S., Martins, L., Aull, K., Li, P.-C., Planelles, V., Bradner, J.E., et al. (2013). BET bromodomain-targeting compounds reactivate HIV from latency via a Tat-independent mechanism. Cc *12*, 452–462.

Boucher, C.A., Tersmette, M., Lange, J.M., Kellam, P., de Goede, R.E., Mulder, J.W., Darby, G., Goudsmit, J., and Larder, B.A. (1990). Zidovudine sensitivity of human immunodeficiency viruses from high-risk, symptom-free individuals during therapy. Lancet *336*, 585–590.

Brehm, M.A., Cuthbert, A., Yang, C., Miller, D.M., DiIorio, P., Laning, J.,

Burzenski, L., Gott, B., Foreman, O., Kavirayani, A., et al. (2010). Parameters for establishing humanized mouse models to study human immunity: analysis of human hematopoietic stem cell engraftment in three immunodeficient strains of mice bearing the IL2rgamma(null) mutation. Clin. Immunol. *135*, 84–98.

Brenchley, J.M., Hill, B.J., Ambrozak, D.R., Price, D.A., Guenaga, F.J., Casazza, J.P., Kuruppu, J., Yazdani, J., Migueles, S.A., Connors, M., et al. (2004). T-Cell Subsets That Harbor Human Immunodeficiency Virus (HIV) In Vivo: Implications for HIV Pathogenesis. Journal of Virology *78*, 1160–1168.

C, F., Ferguson, N.M., Ghani, A.C., MM, P.J., Lange, J.M., Goudsmit, J., Anderson, R.M., and de Wolf, F. (2000). Reduction of the HIV-1-infected T-cell reservoir by immune activation treatment is dose-dependent and restricted by the potency of antiretroviral drugs. Aids *14*, 659–669.

Chomont, N., El-Far, M., Ancuta, P., Trautmann, L., Procopio, F.A., Yassine-Diab, B., Boucher, G., Boulassel, M.-R., Ghattas, G., Brenchley, J.M., et al. (2009). HIV reservoir size and persistence are driven by T cell survival and homeostatic proliferation. Nature Publishing Group 1–9.

Chun, T.W., Carruth, L., Finzi, D., Shen, X., DiGiuseppe, J.A., Taylor, H., Hermankova, M., Chadwick, K., Margolick, J., Quinn, T.C., et al. (1997a). Quantification of latent tissue reservoirs and total body viral load in HIV-1 infection. Nature *387*, 183–188.

Chun, T.W., Murray, D., Justement, J.S., Blazkova, J., Hallahan, C.W., Fankuchen, O., Gittens, K., Benko, E., Kovacs, C., Moir, S., et al. (2014). Broadly neutralizing antibodies suppress HIV in the persistent viral reservoir. Proceedings of the National Academy of Sciences *111*, 13151–13156.

Chun, T.-W., Stuyver, L., Mizell, S.B., Ehler, L.A., Mican, J.A.M., Baseler, M., Lloyd, A.L., Nowak, M.A., and Fauci, A.S. (1997b). Presence of an inducible HIV-1 latent reservoir during highly active antiretroviral therapy. Proc. Natl. Acad. Sci. U.S.a. *94*, 13193–13197.

Cillo, A.R., Sobolewski, M.D., Bosch, R.J., Fyne, E., Piatak, M., Coffin, J.M., and Mellors, J.W. (2014). Quantification of HIV-1 latency reversal in resting CD4+ T cells from patients on suppressive antiretroviral therapy. Proceedings of the National Academy of Sciences *111*, 7078–7083.

Cohen, M.S., Chen, Y.Q., McCauley, M., Gamble, T., Hosseinipour, M.C., Kumarasamy, N., Hakim, J.G., Kumwenda, J., Grinsztejn, B., Pilotto, J.H.S., et al. (2011). Prevention of HIV-1 Infection with Early Antiretroviral Therapy. N Engl J Med *365*, 493–505.

Contreras, X., Schweneker, M., Chen, C.-S., McCune, J.M., Deeks, S.G., Martin, J., and Peterlin, B.M. (2009). Suberoylanilide hydroxamic acid reactivates HIV from latently infected cells. J. Biol. Chem. *284*, 6782–6789.

Davey, R.T., Bhat, N., Yoder, C., Chun, T.W., Metcalf, J.A., Dewar, R., Natarajan, V., Lempicki, R.A., Adelsberger, J.W., Miller, K.D., et al. (1999). HIV-1 and T cell dynamics after interruption of highly active antiretroviral therapy (HAART) in patients with a history of sustained viral suppression. Proc. Natl. Acad. Sci. U.S.a. *96*, 15109–15114.

Day, C.L., Kaufmann, D.E., Kiepiela, P., Brown, J.A., Moodley, E.S., Reddy, S., Mackey, E.W., Miller, J.D., Leslie, A.J., DePierres, C., et al. (2006). PD-1 expression on HIV-specific T cells is associated with T-cell exhaustion and disease progression. Nature *443*, 350–354.

Deeks, S.G. (2012). HIV: Shock and kill. Nature *487*, 439–440.

Deng, K., Pertea, M., Rongvaux, A., Wang, L., Durand, C.M., Ghiaur, G., Lai, J., McHugh, H.L., Hao, H., Zhang, H., et al. (2015). Broad CTL response is required to clear latent HIV-1 due to dominance of escape mutations. Nature 1–16.

Denton, P.W., Olesen, R., Choudhary, S.K., Archin, N.M., Wahl, A., Swanson, M.D., Chateau, M., Nochi, T., Krisko, J.F., Spagnuolo, R.A., et al. (2012). Generation of HIV latency in humanized BLT mice. Journal of Virology *86*, 630–634.

Dinoso, J.B., Kim, S.Y., Wiegand, A.M., Palmer, S.E., Gange, S.J., Cranmer, L., O'Shea, A., Callender, M., Spivak, A., Brennan, T., et al. (2009). Treatment intensification does not reduce residual HIV-1 viremia in patients on highly active antiretroviral therapy. Proceedings of the National Academy of Sciences *106*, 9403–9408.

Diskin, R., Scheid, J.F., Marcovecchio, P.M., West, A.P., Klein, F., Gao, H., Gnanapragasam, P.N.P., Abadir, A., Seaman, M.S., Nussenzweig, M.C., et al. (2011). Increasing the potency and breadth of an HIV antibody by using structure-based rational design. Science *334*, 1289–1293.

Dybul, M., Hidalgo, B., Chun, T.-W., Belson, M., Migueles, S.A., Justement, J.S., Herpin, B., Perry, C., Hallahan, C.W., Davey, R.T., et al. (2002). Pilot study of the effects of intermittent interleukin-2 on human immunodeficiency virus (HIV)-specific immune responses in patients treated during recently acquired HIV infection. J. Infect. Dis. *185*, 61–68.

Eisele, E., and Siliciano, R.F. (2012). Redefining the Viral Reservoirs that Prevent HIV-1 Eradication. Immunity *37*, 377–388.

Elliott, J.H., Wightman, F., Solomon, A., Ghneim, K., Ahlers, J., Cameron, M.J., Smith, M.Z., Spelman, T., McMahon, J., Velayudham, P., et al. (2014). Activation of HIV Transcription with Short-Course Vorinostat in HIV-Infected Patients on Suppressive Antiretroviral Therapy. PLoS Pathog *10*, e1004473.

Fauci, A.S., and Lane, H.C. (2012). Chapter 189. Human Immunodeficiency

Virus Disease: AIDS and Related Disorders. In Harrison's Principles of Internal Medicine, 18e, D.L. Longo, A.S. Fauci, D.L. Kasper, S.L. Hauser, J.L. Jameson, and J. Loscalzo, eds. (New York, NY: The McGraw-Hill Companies).

Finzi, D., Hermankova, M., Pierson, T., Carruth, L.M., Buck, C., Chaisson, R.E., Quinn, T.C., Chadwick, K., Margolick, J., Brookmeyer, R., et al. (1997). Identification of a reservoir for HIV-1 in patients on highly active antiretroviral therapy. Science *278*, 1295–1300.

Finzi, D., Blankson, J., Siliciano, J.D., Margolick, J.B., Chadwick, K., Pierson, T., Smith, K., Lisziewicz, J., Lori, F., Flexner, C., et al. (1999). Latent infection of CD4+ T cells provides a mechanism of lifelong persistence of HIV-1, even in patients on effective combination therapy. Nature Medicine *5*, 1–6.

Frost, S.D.W., Wrin, T., Smith, D.M., Kosakovsky Pond, S.L., Liu, Y., Paxinos, E., Chappey, C., Galovich, J., Beauchaine, J., Petropoulos, C.J., et al. (2005). Neutralizing antibody responses drive the evolution of human immunodeficiency virus type 1 envelope during recent HIV infection. Proc. Natl. Acad. Sci. U.S.a. *102*, 18514–18519.

Fukazawa, Y., Lum, R., Okoye, A.A., Park, H., Matsuda, K., Bae, J.Y., Hagen, S.I., Shoemaker, R., Deleage, C., Lucero, C., et al. (2015). B cell follicle sanctuary permits persistent productive simian immunodeficiency virus infection in elite controllers. Nature Publishing Group *21*, 132–139.

Gandhi, R.T., Zheng, L., Bosch, R.J., Chan, E.S., Margolis, D.M., Read, S., Kallungal, B., Palmer, S., Medvik, K., Lederman, M.M., et al. (2010). The effect of raltegravir intensification on low-level residual viremia in HIV-infected patients on antiretroviral therapy: a randomized controlled trial. PLoS Med. *7*.

Goonetilleke, N., Liu, M.K.P., Salazar-Gonzalez, J.F., Ferrari, G., Giorgi, E., Ganusov, V.V., Keele, B.F., Learn, G.H., Turnbull, E.L., Salazar, M.G., et al. (2009). The first T cell response to transmitted/founder virus contributes to the control of acute viremia in HIV-1 infection. J. Exp. Med. *206*, 1253–1272.

Gray, E.S., Moore, P.L., Choge, I.A., Decker, J.M., Bibollet-Ruche, F., Li, H., Leseka, N., Treurnicht, F., Mlisana, K., Shaw, G.M., et al. (2007). Neutralizing antibody responses in acute human immunodeficiency virus type 1 subtype C infection. Journal of Virology *81*, 6187–6196.

Haase, A.T. (2010). Targeting early infection to prevent HIV-1 mucosal transmission. Nature *464*, 217–223.

Hammer, S.M., Squires, K.E., Hughes, M.D., Grimes, J.M., Demeter, L.M., Currier, J.S., Eron, J.J., Feinberg, J.E., Balfour, H.H., Deyton, L.R., et al. (1997). A controlled trial of two nucleoside analogues plus indinavir in persons with human immunodeficiency virus infection and CD4 cell counts of 200 per cubic millimeter or less. AIDS Clinical Trials Group 320 Study Team. N Engl J Med

337, 725–733.

Henrich, T.J., Hanhauser, E., Marty, F.M., Sirignano, M.N., Keating, S., Lee, T.-H., Robles, Y.P., Davis, B.T., Li, J.Z., Heisey, A., et al. (2014). Antiretroviral-Free HIV-1 Remission and Viral Rebound After Allogeneic Stem Cell Transplantation. Ann Intern Med *161*, 319.

Hessell, A.J., Poignard, P., Hunter, M., Hangartner, L., Tehrani, D.M., Bleeker, W.K., Parren, P.W.H.I., Marx, P.A., and Burton, D.R. (2009). Effective, low-titer antibody protection against low-dose repeated mucosal SHIV challenge in macaques. Nature Publishing Group 1–5.

Hill, A.L., Rosenbloom, D.I.S., Fu, F., Nowak, M.A., and Siliciano, R.F. (2014). Predicting the outcomes of treatment to eradicate the latent reservoir for HIV-1. Proceedings of the National Academy of Sciences.

Ho, D.D., Neumann, A.U., Perelson, A.S., Chen, W., Leonard, J.M., and Markowitz, M. (1995). Rapid turnover of plasma virions and CD4 lymphocytes in HIV-1 infection. Nature *373*, 123–126.

Ho, Y.-C., Shan, L., Hosmane, N.N., Wang, J., Laskey, S.B., Rosenbloom, D.I.S., Lai, J., Blankson, J.N., Siliciano, J.D., and Siliciano, R.F. (2013). Replication-competent noninduced proviruses in the latent reservoir increase barrier to HIV-1 cure. Cell *155*, 540–551.

Horton, H.M., Bernett, M.J., Peipp, M., Pong, E., Karki, S., Chu, S.Y., Richards, J.O., Chen, H., Repp, R., Desjarlais, J.R., et al. (2010). Fc-engineered anti-CD40 antibody enhances multiple effector functions and exhibits potent in vitro and in vivo antitumor activity against hematologic malignancies. Blood *116*, 3004–3012.

Horwitz, J.A., Halper-Stromberg, A., Mouquet, H., Gitlin, A.D., Tretiakova, A., Eisenreich, T.R., Malbec, M., Gravemann, S., Billerbeck, E., Dorner, M., et al. (2013). HIV-1 suppression and durable control by combining single broadly neutralizing antibodies and antiretroviral drugs in humanized mice. Proceedings of the National Academy of Sciences *110*, 16538–16543.

Hütter, G., Nowak, D., Mossner, M., Ganepola, S., Müssig, A., Allers, K., Schneider, T., Hofmann, J., Kücherer, C., Blau, O., et al. (2009). Long-term control of HIV by CCR5 Delta32/Delta32 stem-cell transplantation. N Engl J Med *360*, 692–698.

Igarashi, T., Brown, C., Azadegan, A., Haigwood, N., Dimitrov, D., Martin, M.A., and Shibata, R. (1999). Human immunodeficiency virus type 1 neutralizing antibodies accelerate clearance of cell-free virions from blood plasma. Nature Medicine *5*, 211–216.

Ince, W.L., Zhang, L., Jiang, Q., Arrildt, K., Su, L., and Swanstrom, R. (2010). Evolution of the HIV-1 env gene in the Rag2-/- gammaC-/- humanized mouse

model. Journal of Virology *84*, 2740–2752.

Jacobson, J.M., Kuritzkes, D.R., Godofsky, E., DeJesus, E., Larson, J.A., Weinheimer, S.P., and Lewis, S.T. (2009). Safety, pharmacokinetics, and antiretroviral activity of multiple doses of ibalizumab (formerly TNX-355), an anti-CD4 monoclonal antibody, in human immunodeficiency virus type 1-infected adults. Antimicrob. Agents Chemother. *53*, 450–457.

Jacobson, J.M., Lalezari, J.P., Thompson, M.A., Fichtenbaum, C.J., Saag, M.S., Zingman, B.S., D'Ambrosio, P., Stambler, N., Rotshteyn, Y., Marozsan, A.J., et al. (2010a). Phase 2a study of the CCR5 monoclonal antibody PRO 140 administered intravenously to HIV-infected adults. Antimicrob. Agents Chemother. *54*, 4137–4142.

Jacobson, J.M., Saag, M.S., Thompson, M.A., Fischl, M.A., Liporace, R., Reichman, R.C., Redfield, R.R., Fichtenbaum, C.J., Zingman, B.S., Patel, M.C., et al. (2008). Antiviral activity of single-dose PRO 140, a CCR5 monoclonal antibody, in HIV-infected adults. J. Infect. Dis. *198*, 1345–1352.

Jacobson, J.M., Thompson, M.A., Lalezari, J.P., Saag, M.S., Zingman, B.S., D'Ambrosio, P., Stambler, N., Rotshteyn, Y., Marozsan, A.J., Maddon, P.J., et al. (2010b). Anti-HIV-1 activity of weekly or biweekly treatment with subcutaneous PRO 140, a CCR5 monoclonal antibody. Journal of Infectious Diseases *201*, 1481–1487.

Jones, R.B., O'Connor, R., Mueller, S., Foley, M., Szeto, G.L., Karel, D., Lichterfeld, M., Kovacs, C., Ostrowski, M.A., Trocha, A., et al. (2014). Histone Deacetylase Inhibitors Impair the Elimination of HIV-Infected Cells by Cytotoxic T-Lymphocytes. PLoS Pathog *10*, e1004287.

Kao, S.Y., Calman, A.F., Luciw, P.A., and Peterlin, B.M. (1987). Anti-termination of transcription within the long terminal repeat of HIV-1 by tat gene product. Nature *330*, 489–493.

Klein, F., Gaebler, C., Mouquet, H., Sather, D.N., Lehmann, C., Scheid, J.F., Kraft, Z., Liu, Y., Pietzsch, J., Hurley, A., et al. (2012). Broad neutralization by a combination of antibodies recognizing the CD4 binding site and a new conformational epitope on the HIV-1 envelope protein. J. Exp. Med. *209*, 1469–1479.

Klein, F., Nogueira, L., Nishimura, Y., Phad, G., West, A.P., Halper-Stromberg, A., Horwitz, J.A., Gazumyan, A., Liu, C., Eisenreich, T.R., et al. (2014). Enhanced HIV-1 immunotherapy by commonly arising antibodies that target virus escape variants. J. Exp. Med. *211*, 2361–2372.

Ko, S.-Y., Pegu, A., Rudicell, R.S., Yang, Z.-Y., Joyce, M.G., Chen, X., Wang, K., Bao, S., Kraemer, T.D., Rath, T., et al. (2014). Enhanced neonatal Fc receptor function improves protection against primate SHIV infection. Nature *514*, 642–

645.

Kuritzkes, D.R., Jacobson, J., Powderly, W.G., Godofsky, E., DeJesus, E., Haas, F., Reimann, K.A., Larson, J.L., Yarbough, P.O., Curt, V., et al. (2004). Antiretroviral activity of the anti-CD4 monoclonal antibody TNX-355 in patients infected with HIV type 1. J. Infect. Dis. *189*, 286–291.

Laird, G.M., Eisele, E.E., Rabi, S.A., Lai, J., Chioma, S., Blankson, J.N., Siliciano, J.D., and Siliciano, R.F. (2013). Rapid Quantification of the Latent Reservoir for HIV-1 Using a Viral Outgrowth Assay. PLoS Pathog *9*, e1003398.

Laird, G.M., Rosenbloom, D.I.S., Siliciano, R.F., and Siliciano, J.D. Measuring the frequency of latent HIV-1 in resting CD4+ T cells using a limiting dilution co-culture assay. In HIV Protocols.

Landovitz, R., and Curry, J. (2009). Postexposure Prophylaxis for HIV Infection. N Engl J Med 1–8.

Lane, H.C., Masur, H., Edgar, L.C., Whalen, G., Rook, A.H., and Fauci, A.S. (1983). Abnormalities of B-cell activation and immunoregulation in patients with the acquired immunodeficiency syndrome. N Engl J Med *309*, 453–458.

Lehrman, G., Hogue, I.B., Palmer, S., Jennings, C., Spina, C.A., Wiegand, A., Landay, A.L., Coombs, R.W., Richman, D.D., Mellors, J.W., et al. (2005). Depletion of latent HIV-1 infection in vivo: a proof-of-concept study. Lancet *366*, 549–555.

Li, Q., Duan, L., Estes, J.D., Ma, Z.-M., Rourke, T., Wang, Y., Reilly, C., Carlis, J., Miller, C.J., and Haase, A.T. (2005). Peak SIV replication in resting memory CD4+ T cells depletes gut lamina propria CD4+ T cells. Nature *434*, 1148–1152.

Li, Z., Guo, J., Wu, Y., and Zhou, Q. (2012). The BET bromodomain inhibitor JQ1 activates HIV latency through antagonizing Brd4 inhibition of Tat-transactivation. Nucleic Acids Res. *41*, 277–287.

Liao, H.-X., Lynch, R., Zhou, T., Gao, F., MunirAlam, S., Boyd, S.D., Fire, A.Z., Roskin, K.M., Schramm, C.A., Zhang, Z., et al. (2013). Co-evolution of a broadly neutralizing HIV-1 antibody and founder virus. Nature *496*, 469–476.

Mansky, L.M., and Temin, H.M. (1995). Lower in vivo mutation rate of human immunodeficiency virus type 1 than that predicted from the fidelity of purified reverse transcriptase. Journal of Virology *69*, 5087–5094.

Markowitz, M., Louie, M., Hurley, A., Sun, E., Di Mascio, M., Perelson, A.S., and Ho, D.D. (2003). A Novel Antiviral Intervention Results in More Accurate Assessment of Human Immunodeficiency Virus Type 1 Replication Dynamics and T-Cell Decay In Vivo. Journal of Virology *77*, 5037–5038.

Marsden, M.D., Kovochich, M., Suree, N., Shimizu, S., Mehta, R., Cortado, R., Bristol, G., An, D.S., and Zack, J.A. (2012). HIV latency in the humanized BLT mouse. Journal of Virology *86*, 339–347.

Mascola, J.R., Lewis, M.G., Stiegler, G., Harris, D., VanCott, T.C., Hayes, D., Louder, M.K., Brown, C.R., Sapan, C.V., Frankel, S.S., et al. (1999). Protection of Macaques against pathogenic simian/human immunodeficiency virus 89.6PD by passive transfer of neutralizing antibodies. Journal of Virology *73*, 4009–4018.

McMichael, A.J., Borrow, P., Tomaras, G.D., Goonetilleke, N., and Haynes, B.F. (2009). The immune response during acute HIV-1 infection: clues for vaccine development. Nat. Rev. Immunol. *10*, 11–23.

MD, D.T.A.R., PhD, M.T., PhD, C.R.B., PhD, R.O., MD, C.E., Solomon, A., Winckelmann, A., PhD, S.P., MD, P.C.D., PhD, M.B., et al. (2014). ArticlesPanobinostat, a histone deacetylase inhibitor, for latent- virus reactivation in HIV-infected patients on suppressive antiretroviral therapy: a phase 1/2, single group, clinical trial. The Lancet HIV *1*, e13–e21.

Mellors, J.W., Rinaldo, C.R., Gupta, P., White, R.M., Todd, J.A., and Kingsley, L.A. (1996). Prognosis in HIV-1 infection predicted by the quantity of virus in plasma. Science *272*, 1167–1170.

Moir, S., Chun, T.-W., and Fauci, A.S. (2011). Pathogenic Mechanisms of HIV Disease *. Annu. Rev. Pathol. Mech. Dis. *6*, 223–248.

Moldt, B., Rakasz, E.G., Schultz, N., Chan-Hui, P.Y., Swiderek, K., Weisgrau, K.L., Piaskowski, S.M., Bergman, Z., Watkins, D.I., Poignard, P., et al. (2012). Highly potent HIV-specific antibody neutralization in vitro translates into effective protection against mucosal SHIV challenge in vivo. Proceedings of the National Academy of Sciences *109*, 18921–18925.

Mouquet, H., Scharf, L., Euler, Z., Liu, Y., Eden, C., Scheid, J.F., Halper-Stromberg, A., Gnanapragasam, P.N.P., Spencer, D.I.R., Seaman, M.S., et al. (2012). Complex-type N-glycan recognition by potent broadly neutralizing HIV antibodies. Proceedings of the National Academy of Sciences.

Nishimura, Y., Igarashi, T., Haigwood, N.L., Sadjadpour, R., Donau, O.K., Buckler, C., Plishka, R.J., Buckler-White, A., and Martin, M.A. (2003). Transfer of neutralizing IgG to macaques 6 h but not 24 h after SHIV infection confers sterilizing protection: implications for HIV-1 vaccine development. Proc. Natl. Acad. Sci. U.S.a. *100*, 15131–15136.

Otten, R.A., Smith, D.K., Adams, D.R., Pullium, J.K., Jackson, E., Kim, C.N., Jaffe, H., Janssen, R., Butera, S., and Folks, T.M. (2000). Efficacy of postexposure prophylaxis after intravaginal exposure of pig-tailed macaques to a human-derived retrovirus (human immunodeficiency virus type 2). Journal of Virology *74*, 9771–9775.

Pantaleo, G., Graziosi, C., and Fauci, A.S. (1993). New concepts in the immunopathogenesis of human immunodeficiency virus infection. N Engl J Med *328*, 327–335.

Perelson, A.S., Essunger, P., Cao, Y., Vesanen, M., Hurley, A., Saksela, K., Markowitz, M., and Ho, D.D. (1997). Decay characteristics of HIV-1-infected compartments during combination therapy. Nature *387*, 188–191.

Pierson, T.C., Zhou, Y., Kieffer, T.L., Ruff, C.T., Buck, C., and Siliciano, R.F. (2002). Molecular characterization of preintegration latency in human immunodeficiency virus type 1 infection. Journal of Virology *76*, 8518–8531.

Pietzsch, J., Gruell, H., Bournazos, S., Donovan, B.M., Klein, F., Diskin, R., Seaman, M.S., Bjorkman, P.J., Ravetch, J.V., Ploss, A., et al. (2012). A mouse model for HIV-1 entry. Proceedings of the National Academy of Sciences *109*, 15859–15864.

Poignard, P., Sabbe, R., Picchio, G.R., Wang, M., Gulizia, R.J., Katinger, H., Parren, P.W., Mosier, D.E., and Burton, D.R. (1999). Neutralizing antibodies have limited effects on the control of established HIV-1 infection in vivo. Immunity *10*, 431–438.

Ramratnam, B., Mittler, J.E., Zhang, L., Boden, D., Hurley, A., Fang, F., Macken, C.A., Perelson, A.S., Markowitz, M., and Ho, D.D. (2000). The decay of the latent reservoir of replication-competent HIV-1 is inversely correlated with the extent of residual viral replication during prolonged anti-retroviral therapy. Nature Medicine *6*, 82–85.

Ramratnam, B., Ribeiro, R., He, T., Chung, C., Simon, V., Vanderhoeven, J., Hurley, A., Zhang, L., Perelson, A.S., Ho, D.D., et al. (2004). Intensification of antiretroviral therapy accelerates the decay of the HIV-1 latent reservoir and decreases, but does not eliminate, ongoing virus replication. J. Acquir. Immune Defic. Syndr. *35*, 33–37.

Razooky, B.S., Pai, A., Aull, K., Rouzine, I.M., and Weinberger, L.S. (2015). A Hardwired HIV Latency Program. Cell *160*, 990–1001.

Richman, D.D., Wrin, T., Little, S.J., and Petropoulos, C.J. (2003). Rapid evolution of the neutralizing antibody response to HIV type 1 infection. Proceedings of the National Academy of Sciences *100*, 4144–4149.

Rongvaux, A., Willinger, T., Martinek, J., Strowig, T., Gearty, S.V., Teichmann, L.L., Saito, Y., Marches, F., Halene, S., Palucka, A.K., et al. (2014). Development and function of human innate immune cells in a humanized mouse model. Nat Biotechnol.

Ruelas, D.S., and Greene, W.C. (2013). An integrated overview of HIV-1 latency. Cell *155*, 519–529.

Sagot-Lerolle, N., Lamine, A., Chaix, M.-L., Boufassa, F., Aboulker, J.-P., Costagliola, D., Goujard, C., Pallier, C., Paller, C., Delfraissy, J.-F., et al. (2008). Prolonged valproic acid treatment does not reduce the size of latent HIV reservoir. Aids *22*, 1125–1129.

Saravolatz, L.D., Winslow, D.L., Collins, G., Hodges, J.S., Pettinelli, C., Stein, D.S., Markowitz, N., Reves, R., Loveless, M.O., Crane, L., et al. (1996). Zidovudine alone or in combination with didanosine or zalcitabine in HIV-infected patients with the acquired immunodeficiency syndrome or fewer than 200 CD4 cells per cubic millimeter. Investigators for the Terry Beirn Community Programs for Clinical Research on AIDS. N Engl J Med *335*, 1099–1106.

Scheid, J.F., Mouquet, H., Ueberheide, B., Diskin, R., Klein, F., Oliveira, T.Y.K., Pietzsch, J., Fenyo, D., Abadir, A., Velinzon, K., et al. (2011). Sequence and structural convergence of broad and potent HIV antibodies that mimic CD4 binding. Science *333*, 1633–1637.

Shan, L., Deng, K., Shroff, N.S., Durand, C.M., Rabi, S.A., Yang, H.-C., Zhang, H., Margolick, J.B., Blankson, J.N., and Siliciano, R.F. (2012). Stimulation of HIV-1-Specific Cytolytic T Lymphocytes Facilitates Elimination of Latent Viral Reservoir after Virus Reactivation. Immunity *36*, 491–501.

Sharkey, M., Triques, K., Kuritzkes, D.R., and Stevenson, M. (2005). In vivo evidence for instability of episomal human immunodeficiency virus type 1 cDNA. Journal of Virology *79*, 5203–5210.

Shingai, M., Donau, O.K., Plishka, R.J., Buckler-White, A., Mascola, J.R., Nabel, G.J., Nason, M.C., Montefiori, D., Moldt, B., Poignard, P., et al. (2013a). Passive transfer of modest titers of potent and broadly neutralizing anti-HIV monoclonal antibodies block SHIV infection in macaques. J. Exp. Med. *210*, 1235–1249.

Shingai, M., Nishimura, Y., Klein, F., Mouquet, H., Donau, O.K., Plishka, R., Buckler-White, A., Seaman, M., Piatak, M., Lifson, J.D., et al. (2013b). Antibody-mediated immunotherapy of macaques chronically infected with SHIV suppresses viraemia. Nature *503*, 277–280.

Shirakawa, K., Chavez, L., Hakre, S., Calvanese, V., and Verdin, E. (2013). Reactivation of latent HIV by histone deacetylase inhibitors. Trends in Microbiology *21*, 277–285.

Sigal, A., and Baltimore, D. (2012). As Good As It Gets? The Problem of HIV Persistence despite Antiretroviral Drugs. Cell Host and Microbe *12*, 132–138.

Sigal, A., Kim, J.T., Balazs, A.B., Dekel, E., Mayo, A., Milo, R., and Baltimore, D. (2011). Cell-to-cell spread of HIV permits ongoing replication despite antiretroviral therapy. Nature *477*, 95–98.

Siliciano, J.D., Kajdas, J., Finzi, D., Quinn, T.C., Chadwick, K., Margolick, J.B.,

Kovacs, C., Gange, S.J., and Siliciano, R.F. (2003). Long-term follow-up studies confirm the stability of the latent reservoir for HIV-1 in resting CD4+ T cells. Nature Medicine *9*, 727–728.

Siliciano, J.D., Lai, J., Callender, M., Pitt, E., Zhang, H., Margolick, J.B., Gallant, J.E., Cofrancesco, J., Jr, Moore, R.D., Gange, S.J., et al. (2007). Stability of the latent reservoir for HIV-1 in patients receiving valproic acid. J. Infect. Dis. *195*, 833–836.

Siliciano, R.F., and Greene, W.C. (2011). HIV Latency. Cold Spring Harbor Perspectives in Medicine *1*, a007096–a007096.

Sloan, D., Irrinki, A., Kaur, J., Murry, J., Cihlar, T., Lalezari, J. “TLR7 Agonist GS-9620 Activates HIV-1 in PBMCs From HIV-Infected Patients on cART”. 2015 CROI.

Spivak, A.M., Andrade, A., Eisele, E., Hoh, R., Bacchetti, P., Bumpus, N.N., Emad, F., Buckheit, R., McCance-Katz, E.F., Lai, J., et al. (2014). A Pilot Study Assessing the Safety and Latency-Reversing Activity of Disulfiram in HIV-1-Infected Adults on Antiretroviral Therapy. Clinical Infectious Diseases *58*, 883–890.

Stellbrink, H.-J., Lunzen, J.V., Westby, M., O'Sullivan, E., Schneider, C., Adam, A., Weitner, L., Kuhlmann, B., Hoffman, C., Fenske, S., et al. (2002). Effects of interleukin-2 plus highly active antiretroviral therapy on HIV-1 replication and proviral DNA (COSMIC trial). Aids 1479–1487.

Todd, J., Glynn, J.R., Marston, M., Lutalo, T., Biraro, S., Mwita, W., Suriyanon, V., Rangsin, R., Nelson, K.E., Sonnenberg, P., et al. (2007). Time from HIV seroconversion to death: a collaborative analysis of eight studies in six low and middle-income countries before highly active antiretroviral therapy. Aids *21 Suppl 6*, S55–S63.

Traggiai, E., Chicha, L., Mazzucchelli, L., Bronz, L., Piffaretti, J.-C., Lanzavecchia, A., and Manz, M.G. (2004). Development of a human adaptive immune system in cord blood cell-transplanted mice. Science *304*, 104–107.

Trkola, A., Kuster, H., Rusert, P., Joos, B., Fischer, M., Leemann, C., Manrique, A., Huber, M., Rehr, M., Oxenius, A., et al. (2005). Delay of HIV-1 rebound after cessation of antiretroviral therapy through passive transfer of human neutralizing antibodies. Nature Medicine *11*, 615–622.

Tsai, C.-C., Emau, P., Follis, K., Beck, T., Benveniste, R., Bischofberger, N., Lifson, J., and Morton, W. (1998). Effectiveness of Postinoculation (R)-9-(2-Phosphonylmethoxypropyl)Adenine Treatment for Prevention of Persistent Simian Immunodeficiency Virus SIV Infection Depends Critically on Timing of Initiation and Duration of Treatment. Journal of Virology 4265.

Tsai, C.-C., Follis, K., Sabo, A., Beck, T., Grant, R., Bischofberger, N., Benveniste, R., and Black, R. (1995). Prevention of SIV Infection in Macaques by (R)-9-(2-Phosphonylmethoxypropyl)adenine. Science 1–3.

Turnbull, E.L., Wong, M., Wang, S., Wei, X., Jones, N.A., Conrod, K.E., Aldam, D., Turner, J., Pellegrino, P., Keele, B.F., et al. (2009). Kinetics of Expansion of Epitope-Specific T Cell Responses during Primary HIV-1 Infection. The Journal of Immunology *182*, 7131–7145.

UNAIDS (2007). 2007_epiupdate_en. 1–60.

Van Praag, R., MM, P.J., Roos, M.T., and Schellekens, P. (2001). OKT3 and IL-2 Treatment for Purging of the Latent HIV-1 Reservoir in vivo results in selective long-lasting CD4+ T cell depletion. 1–9.

Walker, L.M., Huber, M., Doores, K.J., Falkowska, E., Pejchal, R., Julien, J.-P., Wang, S.-K., Ramos, A., Chan-Hui, P.-Y., Moyle, M., et al. (2011). Broad neutralization coverage of HIV by multiple highly potent antibodies. Nature *477*, 466–470.

Walker, L.M., Phogat, S.K., Chan-Hui, P.-Y., Wagner, D., Phung, P., Goss, J.L., Wrin, T., Simek, M.D., Fling, S., Mitcham, J.L., et al. (2009). Broad and potent neutralizing antibodies from an African donor reveal a new HIV-1 vaccine target. Science *326*, 285–289.

Wei, D.G., Chiang, V., Fyne, E., Balakrishnan, M., Barnes, T., Graupe, M., Hesselgesser, J., Irrinki, A., Murry, J.P., Stepan, G., et al. (2014). Histone Deacetylase Inhibitor Romidepsin Induces HIV Expression in CD4 T Cells from Patients on Suppressive Antiretroviral Therapy at Concentrations Achieved by Clinical Dosing. PLoS Pathog *10*, e1004071.

Wei, X., Decker, J.M., Wang, S., Hui, H., Kappes, J.C., Wu, X., Salazar-Gonzalez, J.F., Salazar, M.G., Kilby, J.M., Saag, M.S., et al. (2003). Antibody neutralization and escape by HIV-1. Nature *422*, 307–312.

Whitney, J.B., Hill, A.L., Sanisetty, S., Penaloza-MacMaster, P., Liu, J., Shetty, M., Parenteau, L., Cabral, C., Shields, J., Blackmore, S., et al. (2014). Rapid seeding of the viral reservoir prior to SIV viraemia in rhesus monkeys. Nature 1–15.

Wilson, P.C., and Andrews, S.F. (2012). Tools to therapeutically harness the human antibody response. Nat. Rev. Immunol. *12*, 709–719.

Wong, J.K., Hezareh, M., Günthard, H.F., Havlir, D.V., Ignacio, C.C., Spina, C.A., and Richman, D.D. (1997). Recovery of replication-competent HIV despite prolonged suppression of plasma viremia. Science *278*, 1291–1295.

Wu, X., Wang, C., O'Dell, S., Li, Y., Keele, B.F., Yang, Z., Imamichi, H., Doria-

Rose, N., Hoxie, J.A., Connors, M., et al. (2012). Selection Pressure on HIV-1 Envelope by Broadly Neutralizing Antibodies to the Conserved CD4-Binding Site. Journal of Virology *86*, 5844–5856.

Wu, X., Yang, Z.-Y., Li, Y., Hogerkorp, C.-M., Schief, W.R., Seaman, M.S., Zhou, T., Schmidt, S.D., Wu, L., Xu, L., et al. (2010). Rational design of envelope identifies broadly neutralizing human monoclonal antibodies to HIV-1. Science *329*, 856–861.

Zhang, L., Ramratnam, B., Tenner-Racz, K., He, Y., Vesanen, M., Lewin, S., Talal, A., Racz, P., Perelson, A.S., Korber, B.T., et al. (1999a). Quantifying residual HIV-1 replication in patients receiving combination antiretroviral therapy. N Engl J Med *340*, 1605–1613.

Zhang, Z., Schuler, T., Zupancic, M., Wietgrefe, S., Staskus, K.A., Reimann, K.A., Reinhart, T.A., Rogan, M., Cavert, W., Miller, C.J., et al. (1999b). Sexual transmission and propagation of SIV and HIV in resting and activated CD4+ T cells. Science *286*, 1353–1357.

Zhu, J., Gaiha, G.D., John, S.P., Pertel, T., Chin, C.R., Gao, G., Qu, H., Walker, B.D., Elledge, S.J., and Brass, A.L. (2012). Reactivation of Latent HIV-1 by Inhibition of BRD4. Cell Rep *2*, 807–816.

TLR7 Agonist GS-9620 Activates HIV-1 in PBMCs From HIV-Infected Patients on cART (CROI).